

Aus dem Zentrum für Orthopädie und Unfallchirurgie
der Universitätsmedizin der Johannes Gutenberg-Universität Mainz

**„Evaluation of the Effect of Bone Sialoprotein on the Easy Graft and
Collagen Cell Carrier“**

**„Evaluation des Effekts von Bone Sialoprotein auf die Materialien Easy
Graft und Collagen Cell Carrier“**

Inauguraldissertation
zur Erlangung des Doktorgrades der Medizin
der Universitätsmedizin
der Johannes Gutenberg-Universität Mainz

Vorgelegt von

Cornelia Möröy
aus Marburg, Hessen

Mainz, 2021

Tag der Promotion:

12. Juli 2022

Für meinen Vater

Zusammenfassung

In der Orthopädie und Unfallchirurgie ist noch keine ideale Lösung für die Überbrückung komplexer Frakturen und Pseudarthrosen. Daher werden für eine optimierte Knochenbildung und -mineralisation neue Biomaterialien und bioaktive Proteine dringend benötigt. Das sogenannte „Bone Sialoprotein“ (BSP) ist dabei ins Zentrum des Interesses gerückt, da es als Komponente der extrazellulären Knochenmatrix ein wichtiger Faktor in der Knochenbildung sowie -mineralisation ist, und somit die Lebensfähigkeit von Knochenzellen auf verschiedenen Biomaterialien verbessern könnte.

In dieser Arbeit wurde daher der Frage nachgegangen, ob immobilisiertes BSP auf Trägermaterialien das Wachstum von Knochen- oder Endothelzellen fördern kann. In die experimentelle Untersuchung wurden eine Kollagenmatrix („CCC“) und ein Tricalciumphosphat-Granulat („Easy Graft“) aufgenommen, die mit zwei unterschiedlichen Methoden („BSP“ und „BSP coat“) mit BSP beschichtet wurden. Osteosarkom-Zellen (MG-63 oder SaOS-2) oder Endothelzellen (HUVECs) wurden dann auf diesen Trägern mit oder ohne BSP Beschichtung über bestimmte Zeiträume kultiviert und auf Viabilität sowie die Expression osteogener Marker hin getestet. Ziel war es zu zeigen, ob sich diese BSP beschichteten Träger als osteogene Kochenersatzmaterialien eignen.

Für das Granulat „Easy Graft“ konnte in diesen Untersuchungen durch BSP Beschichtung ein Vorteil in der Viabilität von Osteosarkom-Zellen in den ersten Tagen erreicht werden, jedoch ist dieser Effekt minimal, da die Zellen insgesamt keine verbesserte Lebensfähigkeit auf dem Granulat zeigen. Außerdem konnte keine dauerhafte Beschichtung „Easy Graft“ mit BSP erreicht werden. Im Gegensatz hierzu zeigte die BSP Beschichtung der CCC Kollagenmatrix innerhalb bestimmter Kultivierungszeiten einen positiven Effekt auf die Lebensfähigkeit von MG-63 und SaOS2 Zellen, der nahe an eine statistische Signifikanz heranreichte. Darüber hinaus wurde eine signifikante Induktion der Expression mehrere osteogener Marker (*ALP*, *RUNX2*, *COII*) durch BSP beobachtet. Dieser Befund und die Tatsache, dass die BSP Beschichtung auf der CCC Matrix über 24h bei Raumtemperatur stabil blieb, weist auf eine Eignung als Trägermaterial hin.

Die vorliegende Studie erbrachte Hinweise, dass BSP Beschichtung auf bestimmten Materialien sich vorteilhaft auf osteogenes Wachstum von Knochenzellen auswirken kann. Dabei konnte eine klare Überlegenheit der Kollagenmatrix CCC gegenüber dem „Easy Graft“ Granulat festgestellt werden. Diese Resultate müssen in weiteren Studien bestätigt und vertieft werden, stellen aber vielversprechende erste Hinweise für die Einsatzfähigkeit von BSP beschichteten Materialien in der Klinik dar.

Contents

List of Figures	1
Charts	4
Abbreviations	5
1. Introduction	6
2. Literature Research.....	7
2.1. Bone Structure	7
2.1.1. Bone compounds (proteins, organic and inorganic matter).....	9
2.1.2. Collagen:.....	10
2.1.3. Bone Cells:	11
2.2. Bone formation (Ossification):	12
2.2.1. Intramembranous ossification	12
2.2.2. Endochondral Ossification	13
2.2.3. Bone remodeling	14
2.2.4. Fracture Healing	15
2.2.5. Challenges of Complex Fracture Healing	16
2.3. Bone Signaling Pathways	17
2.3.1. Bone Sialoprotein:	20
2.4. Biomaterials:	21
2.4.1. Synthetic Collagen.....	24
2.4.2. Calcium Phosphate	25
2.4.3. BMP in Clinical use.....	25
2.4.4. Aim of this Work.....	26
3. Material and Methods	27
3.1. Collagen Cell Carriers.....	27
3.2. Easy Graft	27
3.3. Bone sialoprotein (BSP)	28
3.4. Working Conditions.....	28
3.4.1. Laminar Air Flow	28
3.5. Coating Procedures	28
3.5.1. Preparing the CCC.....	28
3.5.2. Coating	29
3.5.3. Coating Easy Graft	29
3.6. Cells	31
3.6.1. Cell passaging.....	31
3.6.2. Preservation (freezing of cells).....	32
3.6.3. Cell counting	32
3.6.4. Fluorescence Microscopy	32
3.7. Colour and Cell Labeling.....	33
3.7.1. Hoechst cell staining.....	33
3.7.2. Immunofluorescence	33
3.7.3. AlamarBlue®.....	34
3.7.4. Lightning Link.....	36
3.7.5. Cytotoxicity	36

3.7.6.	BSP Release Measurement.....	37
3.8.	Gene expression.....	38
3.8.1.	Housekeeping Gene.....	40
3.9.	Statistics	41
4.	Results.....	42
4.1.	Characterizing Cell Lines	42
4.1.2.	Immunofluorescence of the HUVECs cell line	43
4.2.	Collagen Cell Carrier Membranes (CCC).....	45
4.3.	Cell Carrier Viability	46
4.3.2.	CCC Gene Expression.....	53
4.4.	Easy Graft	54
4.4.1.	BSP coating and release experiment	55
4.4.2.	AlamarBlue® Viability Easy Graft	56
4.4.3.	Easy Graft Cytotoxicity.....	61
5.	Discussion	64
5.1.	Cell Lines.....	64
5.2.	Collagen Cell Carrier – Viability Assay of Bone Cell Lines.....	65
5.2.1.	Viability Assay of Primary Human Osteoblasts (hOBs).....	65
5.2.2.	Viability of Cells from the Bone Osteosarcoma cell line MG-63	66
5.2.3.	Viability Assay of cell line SaOS-2.....	67
5.3.	HUVECs	67
5.3.1.	Validation of HUVECs as the cellular model	67
5.3.2.	Viability Assay of HUVEC cell line	68
5.4.	BSP Coating Stability on the CCC	70
5.5.	Gene Expression	71
5.5.1.	Collagen 1 and ALP as Markers of Ossification	72
5.5.2.	Interaction of RUNX2 and SP7 with BSP.....	72
5.5.3.	Expression Levels of SPARC.....	73
5.5.4.	Osteoblast Differentiation and OPN.....	74
5.6.	Easy Graft	76
5.6.1.	Cell viability on Easy Graft.....	77
5.6.2.	Easy Graft cytotoxicity.....	79
5.6.3.	Chemically Inertia and Stability.....	79
5.6.4.	Sound Engineering Design	80
5.6.5.	Economic Aspects	81
6.	Conclusion	82
6.1.	Collagen Cell Carrier in Clinical Use.....	82
6.2.	Easy Graft in Clinical Use	82
6.3.	Advances with BSP.....	83
7.	Bibliography.....	84
8.	Appendix.....	92

List of Figures

FIGURE 1: ILLUSTRATION OF COMPACT BONE: A) THE CROSS SECTION OF COMPACT BONE WITH ITS BONE UNITS: OSTEONS AS WELL AS THE PERIOSTEUM. BELOW A MICROGRAPHIC VERSION B). HERE THE LAMELLAE AS WELL AS THE CANALICULI ARE SHOWN, SPECKED WITH DARK SPOTS, THE OSTEOCLASTS WHICH RESIDE INSIDE THE LACUNAE. 9

FIGURE 2: SCHEMATIC DEPICTION OF THE ROLE OF RUNX2 IN OSTEOCYTE DIFFERENTIATION FROM MESENCHYMAL STEM CELLS ACCORDING TO (31) 18

FIGURE 3: PICTURE A DEPICTS SEVERAL DIFFERENT SIZES OF COLLAGEN CELL CARRIER MEMBRANES (CCC) ON THE LEFT AS WELL AS CCCS IN A 24-WELL TISSUE PLATE IN B. (ILLUSTRATION A WAS KINDLY PROVIDED BY VISCOFAN-BIOENGINEERING (67)). 27

FIGURE 4: EASY GRAFT SYRINGE: A PREPACKAGED SYRINGE CONTAINING 0.4ML DRY GRANULES..... 28

FIGURE 5: WELL-DRAFT: A SINGLE WELL CONTAINING PBS AND A LAYER OF CCC ON TOP OF THE PBS.PBS IS THE BUFFER UTILIZED TO EQUILIBRATE THE MEMBRANE. DEPENDING ON THE TREATMENT IT WAS MIXED WITH BSP OR LEFT PLAIN RESPECTIVELY. 29

FIGURE 6: EASY GRAFT EXPERIMENT: A SHOWS A CLOSE UP OF A 24-WELL CELL INSIDE WHICH THE 3D PLA MOLD CONTAINING EASY GRAFT IS PLACED. B SHOWS AN IMAGE OF EASY GRAFT CUT INTO SHAPE WITH A SCALPEL..... 30

FIGURE 7: EXPERIMENT EASY GRAFT. NK: NEGATIVE CONTROL WITH NO SCAFFOLD SEEN IN ROW A, EG: SCAFFOLD WITHOUT BSP SEEN IN ROW B, BSP1: SCAFFOLD COATED WITH 5 μ G BSP IN ROW C. CELLS SEEDED ONTO AN ULTRA-LOW ATTACHMENT PLATE WITHOUT A SCAFFOLD (CELLS). 35

FIGURE 8: THIS IMAGE SHOWS HOW CYTOTOXICITY CAN BE MEASURED BY MONITORING LUMINESCENCE. WHENEVER CELLS ARE DESTROYED LDH IS RELEASED. THIS ENZYME CAN CATALYZE LACTATE TO PYRUVATE WITH THE COENZYME NAD. NAD IS CREATED FROM NADH BY THE REDUCTASE ACTIVITY FROM LDH-GLO. THE AMOUNT OF REDUCTASE THAT WAS USED TO REDUCE THE SUBSTRATE TO LUCIFERIN AND CREATE A MEASURABLE FLUORESCENCE IS EQUIVALENT TO THE AMOUNT OF LDH RELEASED BY THE CELLS. 37

FIGURE 9: PHOTOMICROGRAPH OF CULTURED CELLS FROM THE FOLLOWING LINES A: HUVECS B: HOBs C: MG-63 CELLS D: SAOS-2 CELLS, MAGNIFICATION IS 10x. THE SCALE BAR INDICATES 400 μ M. 43

FIGURE 10: IMMUNOFLUORESCENCE STAINING OF HUVECS FOR THE PRESENCE OF CD31. A) IMMUNOFLUORESCENCE STAINING OF CD31, B) HOECHST STAINING OF THE NUCLEUS. C) OVERLAY OF HOECHST AND THE CD31 STAINING. THE SCALE BAR INDICATES 100 μ M..... 44

FIGURE 11: THE IMAGE ABOVE SHOWS AN IMMUNOFLUORESCENCE STAINING OF VEGFA IN A, AS WELL AS A HOECHST STAINING OF THE NUCLEUS IN B AND AN OVERLAY OF HOECHST AND THE IMMUNOFLUORESCENCE IN C. THE SCALE BAR INDICATES 100 μ M. 44

FIGURE 12: IN THIS IMAGE, THE IMMUNOFLUORESCENCE STAINING OF VWF IS SHOWN IN GREEN IN PICTURE B AND C. THE HOECHST STAINING OF THE NUCLEUS IN BLUE IS DEPICTED IN A. C IS AN OVERLAY OF HOECHST AND THE IMMUNOFLUORESCENCE. THE WHITE MARKER INDICATES 100 μ M..... 45

FIGURE 13: THESE IMAGES INDICATE THE PROBLEMS DURING THE SET-UP OF THE CCC. THE MEMBRANES WOULD START TO CURL AWAY FROM THE TISSUE PLATE. ON THESE MEMBRANES, NO MEASUREMENTS WERE POSSIBLE DUE TO THE CURLED-UP STRUCTURE OF THE MEMBRANE. 46

FIGURE 14: TESTING THE VIABILITY OF HUMAN OSTEOBLASTS USING ALAMARBLUE[®]. RESULTS ARE EXPRESSED AS MEDIAN AND QUARTILES. HUMAN OSTEOBLASTS WERE SEEDED ONTO COLLAGEN CELL CARRIERS. THE GRAPH SHOWS THE RESULTS OF FOUR DIFFERENT TREATMENTS: A POSITIVE CONTROL, WHERE HUMAN OSTEOBLASTS WERE SEEDED ONTO A REGULAR TISSUE PLATE

(PC, n=24), THE COLLAGEN CELL CARRIER ALONE (CCC, n=21), THE COLLAGEN CELL CARRIER COATED WITH BSP, USING METHOD 1 (BSP, n=24), COLLAGEN CELL CARRIER COATED WITH BSP USING METHOD 2 (BSP COAT., n=18). THE BOXPLOT REPRESENTS THE FLUORESCENCE MEASUREMENTS TAKEN ON DAYS 1, 4 AND 7 WHICH HAVE BEEN NORMALIZED OVER THE NEGATIVE CONTROL (ONLY MEDIUM) OF EACH DAY. A SIGNIFICANT DIFFERENCE BETWEEN TWO VARIABLES IS MARKED WITH AN AND A BRACKET CONNECTING THE TWO VARIABLES. ($p < 0.008$). THE SCALING FACTOR ON THE Y-AXIS IS 10000..... 47

FIGURE 15: MG-63 VIABILITY ASSAY USING ALAMARBLUE® OVER A SEVEN-DAY PERIOD. RESULTS ARE EXPRESSED AS MEDIAN AND QUARTILES. MG-63 CELLS WERE SEEDED ONTO COLLAGEN CELL CARRIERS. THE GRAPH DESCRIBES FOUR DIFFERENT TREATMENTS: A POSITIVE CONTROL, WHERE MG-63 WERE SEEDED ONTO A REGULAR TISSUE PLATE (PC, n=18), THE PLAIN COLLAGEN CELL CARRIER (CCC, n=18), THE COLLAGEN CELL CARRIER COATED WITH BSP COATING, METHOD 1 (BSP, n=15), COLLAGEN CELL CARRIER COATED WITH BSP USING METHOD 2 (BSP COAT., n=18). THE BOXPLOT REPRESENTS THE FLUORESCENCE MEASUREMENTS TAKEN ON DAY 1, 4 AND 7 WHICH HAVE BEEN NORMALIZED ACCORDING TO THE NEGATIVE CONTROL (ONLY MEDIUM) OF EACH DAY. IF A SIGNIFICANT DIFFERENCE BETWEEN TWO VARIABLES WAS DETECTED IT IS MARKED WITH A AND A BRACKET CONNECTING THE TWO VARIABLES ($p < 0.008$). SCALING FACTOR ON THE Y-AXIS IS 100000. 48

FIGURE 16: SAOS-2 VIABILITY ASSAY USING ALAMARBLUE® OVER A SEVEN-DAY PERIOD. RESULTS ARE EXPRESSED AS MEDIAN AND QUARTILES. SAOS-2 WERE SEEDED ONTO COLLAGEN CELL CARRIERS. THE GRAPH DESCRIBES FOUR DIFFERENT TREATMENTS: A POSITIVE CONTROL (PC, n=9), THE COLLAGEN CELL CARRIER (CCC, n=3), THE COLLAGEN CELL CARRIER COATED WITH BSP METHOD 1 (BSP, n=6), COLLAGEN CELL CARRIER COATED WITH BSP USING METHOD 2 (BSP COAT., n=6). THE BOXPLOT REPRESENTS THE FLUORESCENCE MEASUREMENTS TAKEN ON DAY 1, 4 AND 7 WHICH HAVE BEEN NORMALIZED ACCORDING TO THE NEGATIVE CONTROL (ONLY MEDIUM) OF EACH DAY. SCALING FACTOR ON THE Y-AXIS IS 10000..... 50

FIGURE 17: HUVEC VIABILITY ASSAY NUMBER 1 USING ALAMARBLUE® OVER A SEVEN-DAY PERIOD. RESULTS ARE EXPRESSED AS MEDIAN AND QUARTILES. HUVECS WERE SEEDED ONTO COLLAGEN CELL CARRIERS. THE GRAPH DESCRIBES FOUR DIFFERENT TREATMENTS: A POSITIVE CONTROL (PC, n=6), THE COLLAGEN CELL CARRIER PLAIN (CCC, n=6), THE COLLAGEN CELL CARRIER COATED WITH BSP METHOD 1 (BSP, n=6), COLLAGEN CELL CARRIER COATED WITH BSP USING METHOD 2 (BSP COAT., n=6). THE BOXPLOT REPRESENTS THE FLUORESCENCE MEASUREMENTS TAKEN ON DAY 1, 4 AND 7, WHICH HAVE BEEN NORMALIZED ACCORDING TO THE NEGATIVE CONTROL (ONLY MEDIUM) OF EACH DAY. SCALING FACTOR ON THE Y-AXIS IS 10000..... 51

FIGURE 18: HUVEC VIABILITY ASSAY NUMBER 1 USING ALAMARBLUE® OVER A SEVEN-DAY PERIOD. RESULTS ARE EXPRESSED AS MEDIAN AND QUARTILES. HUVECS WERE SEEDED ONTO COLLAGEN CELL CARRIERS. THE GRAPH DESCRIBES FOUR DIFFERENT TREATMENTS: A POSITIVE CONTROL, WHERE HUVECS WERE SEEDED ONTO A TISSUE PLATE (PC, n=9), THE COLLAGEN CELL CARRIER PLAIN (CCC, n=9), THE COLLAGEN CELL CARRIER COATED WITH BSP METHOD 1 (BSP, n=9), COLLAGEN CELL CARRIER COATED WITH BSP USING METHOD 2 (BSP COAT., n=9). THE BOXPLOT REPRESENTS THE FLUORESCENCE MEASUREMENTS TAKEN ON DAY 1, 4 AND 7 WHICH HAVE BEEN NORMALIZED ACCORDING TO THE NEGATIVE CONTROL (ONLY MEDIUM) OF EACH DAY. SCALING FACTOR ON THE Y-AXIS IS 10000. 52

FIGURE 19: SAOS-2 CELLS SEEDED ONTO CCCs TO ANALYZE THE EFFECT OF BSP ON THE GENE FOLD INCREASE OF SP7, RUNX2, SPARC, ALP AND COLLAGEN1 OVER THE CONTROL. THE CONTROL IS UNTREATED CELLS ON AN UNTREATED CCC. THE GRAPH SHOWS GENE EXPRESSIONS OF ALL THE GENES AS MENTIONED ABOVE IN TWO DIFFERENT ENVIRONMENTS, DEPICTED ON THE X-AXIS: THE GENE EXPRESSION OF THE CELLS ON A CCC TREATED WITH BSP, COATING METHOD1 (BSP, n=4) AND THE GENE EXPRESSION OF THE CELLS ON A CCC TREATED WITH BSP COATING METHOD 2 (BSP COAT, n=4). THE CONTROL IS SAOS-2 CELLS SEEDED ONTO PLAIN CCCs (WITHOUT BSP), FOR WHICH THE LEVEL OF GENE EXPRESSION WAS SET TO 1. RESULTS ARE

SHOWN WITH MEDIANS AND QUARTILES. IF A SIGNIFICANT DIFFERENCE BETWEEN THE EXPRESSING GENE AND THE CONTROL WAS DETECTED IT IS MARKED WITH A ($p < 0.05$).....	53
FIGURE 20: LEFT: SCAFFOLD IN PLA MOLD SURROUNDED BY MEDIUM. RIGHT: SCAFFOLDS TAKEN OUT OF THE PLA MOLD. MOST SCAFFOLDS ARE COMPLETELY BROKEN OR CONSIDERABLY DAMAGED.	55
FIGURE 21: STANDARD FLUORESCENCE CURVE USING FLUORESCHEIN-LINKED BSP. THE GRAPH DEPICTS THE AMOUNT OF BSP IN μG IN CORRESPONDENCE TO THE FLORESCENCE IT GENERATES. A LINEAR REGRESSION WAS COMPUTED WITH THE CORRESPONDING EQUATION SHOWN IN THE UPPER RIGHT CORNER AS WELL AS R^2	55
FIGURE 22: A SCAFFOLD OF EASY GRAFT WAS COATED WITH BSP. THE AMOUNT OF BSP RELEASED FROM THE SCAFFOLD INTO ITS SURROUNDING MEDIUM WAS MEASURED VIA THE FLUORESCENCE MEASURED INSIDE THE MEDIUM FOR 24 HOURS. THE AMOUNT OF BSP FOUND IN THE MEDIUM AND THEREFORE SECRETED FROM THE SCAFFOLD IS EXPRESSED IN PERCENTAGE.	56
FIGURE 23: : ATTACHMENT OF CELLS TO EASY GRAFT. A) RESIDUE OF THE PC: MEDIUM AND CELLS 24HOURS AFTER SEEDING ONTO A 96-WELL TISSUE PLATE. B) RESIDUE OF MEDIUM AND CELLS 24HOURS AFTER SEEDING ONTO AN ULTRA-LOW ATTACHMENT PLATE WITHOUT A SCAFFOLD. C) RESIDUE OF MEDIUM AND CELLS 24HOURS AFTER SEEDING ONTO A SCAFFOLD WITH BSP, D) RESIDUE OF MEDIUM AND CELLS 24HOURS AFTER SEEDING ONTO A SCAFFOLD WITHOUT BSP. THE WHITE SCALE BAR INDICATES 1000 μM	57
FIGURE 24: SAOS-2 VIABILITY ASSAY USING ALAMARBLUE [®] OVER A SEVEN-DAY PERIOD. RESULTS ARE EXPRESSED AS MEDIAN AND QUARTILES. SAOS-2 WERE SEEDED ONTO SCAFFOLDS OF EASY GRAFT. THE GRAPH DEPICTS FIVE TREATMENTS GROUPS: A POSITIVE CONTROL (PC, N=14), THE EASY GRAFT SCAFFOLD (SC, N=14), THE EASY GRAFT SCAFFOLD COATED WITH BSP (BSP, N=14), CELLS ON THE ULTRA-LOW ATTACHMENT PLATE (CELLS ONLY N=14) AND A NEGATIVE CONTROL WHICH IS ONLY MEDIUM (NK=14). THE BOXPLOT REPRESENTS THE FLUORESCENCE MEASUREMENTS TAKEN ON DAY 1, 4 AND 7.	59
FIGURE 25: SAOS-2 VIABILITY ASSAY USING ALAMARBLUE [®] OVER A SEVEN-DAY PERIOD WITHOUT THE DATA OBTAINED WITH THE POSITIVE CONTROL. RESULTS ARE EXPRESSED AS MEDIAN AND QUARTILES. SAOS-2 WERE SEEDED ONTO SCAFFOLDS OF EASY GRAFT. THE GRAPH DEPICTS FOUR TREATMENT GROUPS: THE EASY GRAFT SCAFFOLD (SC, N=14), THE EASY GRAFT SCAFFOLD COATED WITH BSP (BSP, N=14), CELLS ON THE ULTRA-LOW ATTACHMENT PLATE (CELLS ONLY N=12) AND A NEGATIVE CONTROL WHICH IS ONLY MEDIUM (NK=14). THE BOXPLOT REPRESENTS THE FLUORESCENCE MEASUREMENTS TAKEN ON DAY 1,4 AND 7. A SIGNIFICANT DIFFERENCE BETWEEN TWO VARIABLES IS MARKED WITH A ($p < 0.008$). SCALING FACTOR ON THE Y-AXIS IS 1000.	60
FIGURE 26: THE CYTOTOXICITY OF EASY GRAFT AND EASY GRAFT IN COMBINATION WITH BSP WAS MEASURED OVER 72 HOURS. THE TOXICITY LIMIT WAS MEASURED USING SAOS-2 CELLS SEEDED ON AN ULTRA-LOW ATTACHMENT PLATE (N=6). THE POSITIVE CONTROL (CELLS, N=6) ARE SAOS-2 CELLS SEEDED ON A TISSUE PLATE (DRAWN IN RED). THE OTHER TREATMENT GROUPS ARE EASY GRAFT PLAIN (EG, N=6) AND THE SCAFFOLD COATED WITH BSP (BSP, N=6). THE SCALING FACTOR OF THE LUMINESCENCE WAS 10^6	62

Charts

TABLE 1: DESCRIPTION OF THE PROPERTIES OF BONE GRAFT SUBSTITUTES WITH EXAMPLES (60). DBM: DEMINERALIZED BONE MATRIX;
BMP: BONE MORPHOGENETIC PROTEINS..... 24

TABLE 2: LIST OF TREATMENT GROUPS EXPLAINING THE TREATMENT SET-UP..... 45

Abbreviations

ALP	Alkaline Phosphatase
BMP	Bone Morphogenetic Proteins
BSA	Bovine Serum Albumin
BSP	Bone Sialoprotein
cAp	Carbonated hydroxyapatite
CCC	Collagen Cell Carrier
Col1	Collagen 1
DMEM/F-12	Dulbecco's Modified Eagle Medium/Nutrient Mixture F-12
DMP-1	Dentin matrixprotein-1
DMSO	Dimethyl sulfoxide
DSPP	Dentin sialophosphoprotein
EBM	Endothelial cell basal medium
ECM	Extracellular matrix
FCS	Fetal calf serum
GAPDH	Glyceraldehyde-3-phosphate dehydrogenase
GMPs	Granulocyte monocyte precursors
hOB	Human osteoblast
HUVEC	Human umbilical vein endothelial cell
ILs	Interleukins
LDH	Lactate dehydrogenase
MEPE	Matrix extracellular phosphoglycoprotein
MSC	Mesenchymal stem cell
NAD	Nicotinamide adenine dinucleotide
NCP	Non collagenous protein
OPN	Osteopontin
PBS	Phosphate-buffered saline
PECAM	Platelet endothelial cell adhesion molecule 1
PFA	Paraformaldehyde
PLA	Poly lactic acid
PLGA	Poly(lactic-co-glycolic) acid
RANK	Receptor activator of nuclear factor kB
rpm	Rotations per minute
RUNX2	Runt-related transcription factor 2
qPCR	Real-time quantitative polymerase chain reaction
SIBLING	Small integrin-binding ligand N-linked glycoprotein
SPARC	Osteonectin
SP7	Osterix
TCP	Tricalcium phosphate
TGF-beta	Transforming growth factors
TNF	Tumor necrosis factor
ULAP	Ultra-low-attachment plate
VEGF	Vascular endothelial growth factor
vWF	von Willebrand factor

1. Introduction

Until this day, complicated bone fractures or gaps caused by bone cysts are treated with the current gold standard - a graft of human bone. This is because no suitable biomaterial has yet been created that can fully replace or reproduce its consistency or its properties.

It has been stated by Skripitz and colleges that “A critical bone defect is defined by the fact, that immobilization alone will not lead to sufficient bone healing (1)” and there is still a need to provide a suitable solution for these defects. Today, there are three possibilities for bone grafts: autogenic, allogenic and xenogenic grafts (2). Autogenic bone grafts have the advantage of a conductive durable structure, which can also induce bone maturation owing to the osteoblasts and stem cells inside the cancellous bone material. Even though this material offers so many positive properties, it has some limitations, in particular because it leaves a new bone defect in the place out of which it was harvested. A new concept to replace human bone grafts are biomaterials, which need to be durable, yet porous to enable new cells to enter this structure and allow new bone to form. In addition, the material has to be compatible with the patient’s immune system and should provide an ideal environment for bone growth, -formation and -vascularization. To find such a material, which shows all these characteristics, still remains a serious challenge. An alternative approach to promote bone formation, is the use of growth factors, proteins or hormones that can induce bone growth. Examples are the bone morphogenetic proteins -2 (BMP-2) and -7(BMP-7); both growth factors already used in vertebra surgeries or in the treatment of open tibia fractures. A new approach is the use of bone sialoprotein (BSP).

Bone material consists of 80% collagen type 1 and non-collagenous proteins. BSP is one of the non-collagenous proteins that belongs to the SIBLING (Small Integrin-Binding Ligand N-linked Glycoprotein) proteins (3). It has been shown to “enhance osteoblast differentiation and new bone deposition” (4). This led to the hypothesis that the addition of BSP to any given biomaterial could enhance the growth and the mineralization of bone. In this thesis it was examined whether additional coating of biomaterials with BSP has benefits on bone growth and vascularization. Experiments were performed with two specific materials were tested: a “Cell Carrier Membrane” made from collagen type 1 fibrils and “Easy Graft”, which consists of calcium phosphate granules coated with a polylactide, which can be molded into shape and will later harden in situ. It was investigated whether i) these two biomaterials are fit for the use in modern orthopedic surgery and, ii) if the presence of BSP can induce a positive effect on bone formation and bone growth in either of these materials.

2. Literature Research

The most durable component of the human body is the skeleton and the elements it is made of the bones. In addition to ensure stability of the body, bones enable locomotion and provide physical protection. Since bone also yield an attachment site for tendons and muscles, they are the basis for the ability of movement. Finally, bones are the biggest metabolic reservoir inside the human body, especially for calcium (5).

2.1. Bone Structure

The morphology of bone tissue can vary depending on the location of the bone in the skeleton and its main functions. It is also contingent on the mechanical pressure and strength required of the bone, forcing it to adapt accordingly. The following types of bone have to be distinguished: compact bone or cortical bone, which makes up the outer, dense layer of calcified bone mass (7), cancellous or spongy (trabecular) bone, which is porous and filled with haematopoietic tissue and subchondral bone, which is typically found underlying certain joint types (6). Cortical and trabecular bone are made up of the same bone structure, yet due to their mechanical characteristics they have different stability and serve different purposes. Trabecular bone is only around 20% calcified, porous and arranged in a spongy way to allow blood cells and haematopoietic precursor cells to pass through, whereas compact bone is nearly 85% calcified, dense and serves as an outer shield. Trabecular bone has foremost a metabolic function whereas compact bone plays a major role in the stability and durability of the skeleton (7).

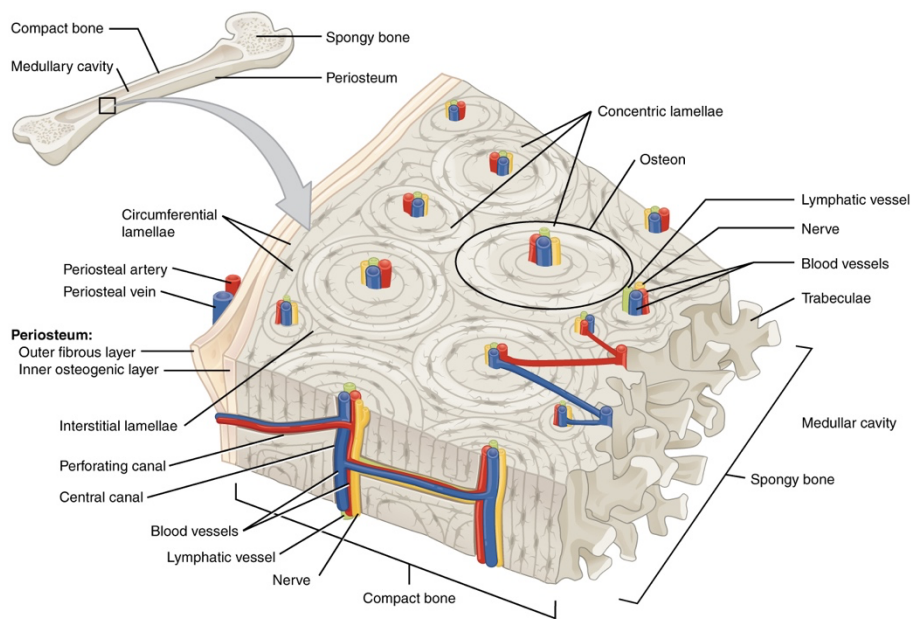
The typical long bone is divided into three zones: the epiphysis, metaphysis (transition zone) and diaphysis, which is the long shaft of the bone that has a joint on both ends. The end of the long bone transitions from the shaft into the metaphysis and ends at its outer part at the epiphysis. The epiphysis and metaphysis are separated by a line of hyaline cartilage, which continually mineralizes and introduces longitudinal growth until the end of the growth period. This is referred to as the epiphyseal plate or growth plate. In the diaphysis lies the medullar cavity with the trabecular bone structure and haematopoietic bone marrow. Trabecular bone can simply be nourished by the multitude of blood vessels surrounding and penetrating their structures. This is not the case with compact bone, consisting of compact units called the Haversian system (see below) which subdivides the bone into units with their own blood supply.

The bone structure is differentiated into lamellar bone (mature/adult bone) and woven bone (immature bone). Lamellar bone is arranged in thick sheets consisting out of parallel

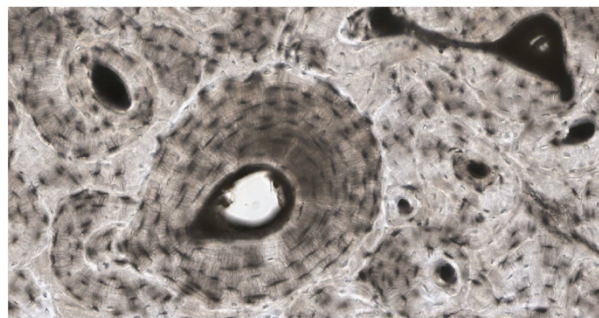
collagen fibers, whereas the collagen in the woven bone is unorganized, creating a mechanically weaker material (5). Woven bone is created during new bone formation for instance during fetal development or during the regeneration after a trauma and is later remodelled into lamellar bone. All three bone structures (compact, trabecular and subchondral) are made of lamellar bone in an adult human skeleton (8). Lamellar bone is either made of basic units, the osteons, which are layers of lamellar bone that are formed around a blood vesicle in a concentric order or is organised in long bones into large scale lamellae that coat the perimeter of the bone shaft.

An Osteon or Haversian system is a cylindrical bond of calcified lamellar bone. In the beginning osteoclasts carve out large tunnel-like cavities, which are then filled with bone in a cylindrical shape layer by layer. The process is complete when the structure is almost completely filled with mineralized, lamellar bone except for an inner canal, which provides the space for a blood vessel to run through the osteon. This canal is called the Haversian canal and also includes nerves and lymph flow (6, 8-11). Cross sections illustrate well the circular layers of lamellar bone around one blood vessel that create the Haversian system (as seen in figure 1), which resembles the cross section of a tree trunk. The layers of the lamellar bone are oriented in alternating direction, creating a strong structure. These Haversian canals are connected through Volkmann's canals, running through the bone tissue, ensuring constant blood circulation. Each layer contains an osteocyte in a lacunae, which maintain bone mass (8). These are nurtured though the canaliculi radiating from the lacunae.

At its core bone is organized in 7 different hierarchical levels, as described by Weiner and Wagner (9). Level 1 consists of the following components: collagen 1 fibrils, carbonated apatite and water, but also non-collagenous proteins, which can make up to 10% of the bone mass. Level 2 are the mineralized collagen type 1 fibrils, which form fibers that are defined as level 3. Lamellar bone is level 4 whereas the osteon (i.e. Haversian system) can be defined as level 5. Level 6 is the trabecular or compact bone and finally, level 7: is the entire bone. The proportion of collagen, carbonated apatite and water plays a defining role for the purpose of the bone. The relationship between these three components is defined by the ratio of water and mineral content, as the collagen content stays about the same (9). Water is located within the fibrils and gaps of collagenous fibers but also within the bounds of tropocollagen.



(a)



(b)

Figure 1: Illustration of compact bone: a) The cross section of compact bone with its bone units: osteons as well as the periosteum. Below a micrographic version b). Here the lamellae as well as the canaliculi are shown, speckled with dark spots, the osteoclasts which reside inside the lacunae. (Illustration provided by openstax Anatomy and Physiology (12))

2.1.1. Bone compounds (proteins, organic and inorganic matter)

Bone is formed by organic and inorganic matter. The organic component, the matrix, is made up of 95% collagen type 1 fibrils and the inorganic part is mostly composed of carbonated hydroxyapatite (9, 10). The third major component is water. The matrix also contains non-collagenous proteins (NCPs), proteoglycans, glycosaminoglycans and lipids (11). As long as this organic matrix is not yet mineralized it is called the osteoid (5, 13). The mineralization process requires high amounts of calcium and phosphate to form the spindle- or plate-shaped hydroxyapatite ($\text{Ca}_{10}(\text{PO}_4)_6(\text{OH})_2$) crystals that are deposited inside the collagenous fibrils. This process determines the strength and rigidity of the bone being formed. This process of bone mineralization is believed to slowly replace and edge out the proteoglycans of the matrix

of the cartilage. The NCPs are a multitude of proteins interacting with each other and the matrix itself (14). The roles of the non-collagenous proteins and therefore also proteoglycans have not all been defined, but they play a role in the maturation, mineralization and the homeostasis of the entire tissue (15). For example, the production of osteocalcin, a glycoprotein, which can also be considered a non-collagenous protein is regulated by vitamin D in osteoblasts and a number of studies have shown that osteocalcin is required to regulate and limit the bone formation (16). Similarly, overexpression of other proteoglycans has been shown to result in less mineralization. This could also be due to the fact, that proteoglycans attract water and therefore foster hydration. They also attract cations such as calcium which is vital in the process of mineralization (15). The phosphoproteins have the important property of being highly anionic, which enables them to attach to calcium and hydroxyapatite and stabilize the mineral inside the matrix.

2.1.2. Collagen:

On a microscopic level, “bone” describes a vast variety of materials, which at its core is always defined by mineralized collagen fibrils (9). Therefore the organic part of bone, collagen, can be described as the core of bone providing elasticity and structure (6, 17). Many different types of collagen have been found within the human body. The collagen, which is found in bone is primarily collagen type 1 but also type 3 and 5 are present in lower quantities.

Collagens are polypeptide chains of about 1000 amino acid that are bound together through hydrogen bonds in left-handed helices with an average diameter of around 1.5nm. These hydrogen bonds can form because of the repetitive sequence of the amino acids in collagen, which consists of repeats of Glycin-X-Y where X and Y are most often proline and hydroxyproline residues (18). To be able to take its characteristic alpha-helix form, a glycine must be at every third position (17). Three polypeptide chains can be referred to as fibrils or tropocollagen, creating a strong coiled cylindrical shape (9, 19). In secondary bonding tropocollagens arrange in a parallel, yet staggered way. These structures then organize in different, larger alignments and planar orientations, which are never radial. Once the tropocollagens have bound together they are referred to as fibers (9). These are then further stabilized through enzymatic and non-enzymatic cross linking (17). This parallel, staggered orientation of the tropocollagen is called quarter-staggered or is described as an end-overlap organisation. This composition within these long collagen fibers results in gaps or overlap zones, which are assumed to be responsible for the banding pattern seen in transmission electron microscopy and also to provide a holding space for mineral deposition, also known as the

nucleation of calcium apatite crystals. Once deposited they grow parallel to the collagen fibrils (18). The mineralization phase determines how much carbonate apatite is deposited, depending on the stiffness, needed to achieve. Not only carbonate apatite can be deposited between the collagen fibers but also water. Depending on the force, durability and flexibility the bone needs, the amount of water varies.

2.1.3. Bone Cells:

The human bone structure has only four cell types that make up its existence: osteoblasts, osteoclasts, bone lining cells and osteocytes (19). Osteoblasts are defined by their ability to build new bone matter. These cells differentiate from mesenchymal stem cells into osteoprogenitor cells and then into osteoblasts (13). Osteoprogenitor cells reside in the lining of the blood vessels, such as the Haversian canals and are activated during bone formation or bone injury (6). Once surrounded by hard bone mass inside the Haversian system after formation of the bone has finished, the osteoblasts are called osteocytes (8). They are situated in the lacunae of the Haversian system (5). Although they are considered inactive, they still have sensing functions and can communicate with other cells through their dendritic structures and gap junctions. It is thought that osteocytes can sense mechanical pressures and send out stimuli to regulate bone remodeling functions (6, 20, 21).

Osteoblasts are cuboidal or polygonal when active with a particularly large Golgi apparatus, representative for the secretory activity and synthesize osteoid (5, 6). They also dispose of a large rough endoplasmic reticulum; due to the abundance of proteins they produce. Osteoblasts themselves possess vesicles that can be secreted during osteoid formation. These vesicles contain high levels of calcium and phosphate as well as alkaline phosphatase and pyrophosphatase which remove phosphate residues from other molecules (5).

While osteoblasts form new bone, osteoclasts remove, erode and resorb mineralized bone. Osteoclasts are derived from granulocyte monocyte precursors (GMPs) that are formed during early myeloid differentiation by haematopoietic stem- and progenitor cells. Through different stimulators, GMPs generate osteoclast precursors, which circulate in the blood flow and attach to bone surfaces. They fuse with other precursor cells to form multi-nucleated osteoclasts. The surface of osteoclasts is a convoluted membrane which has a ruffled structure. Inside these ruffles, lysosomal enzymes are released, which dissipate the bone membrane. To resolve the mineralized structure of bone, osteoclasts need to create a highly acidic environment. Therefore, they possess H^+ ATPases located in the ruffled cell membrane acting as proton pumps. In addition, a chloride anion exchanger is also located within this ruffled membrane creating a pH

of 4.5. Other enzymes such as acid phosphatase, metalloproteinases, β -glucuronidases and cysteine-proteinases and many others are also released for the process of bone resorption. At this low pH the bone mineral is released from its organic matrix, which is then destroyed through the lysosomal protease cathepsin K. (5, 20, 22).

Bone lining cells are sometimes referred to as flattened mesenchymal cells or endosteal lining cells, but they can have a variety of other names. The small line of flattened cells, surrounding and enveloping inactive bone, has been called a functional “membrane” between the bone and other tissues. They are also supporting cells for osteocytes as they have gap junctions and seem to be able to communicate with osteocytes. However, their precise functional role is still under investigation (23).

Since bone is constantly remodeling, all these cells work simultaneously to either form lamellar bone out of woven bone, to produce new osteoid or to resorb old bone matter (6). Cytokines including IL-1 β and IL6 play a major role in osteoclast recruitment and are critical to maintain the communication between cells during bone remodeling. Another important element in osteoclast differentiation and activation is the receptor RANK (Receptor activator of nuclear factor κ B), which belongs to the TNF receptor family and its ligand RANKL. Upon binding to its ligand RANKL, RANK relays signals through its cytoplasmic domain to the nucleus. Osteoprotegerin (OPG) is also called “decoy receptor” for RANKL and can influence and regulate RANK/RANKL signaling (13, 21).

2.2. Bone formation (Ossification):

Bone usually develops from a pre-existing tissue which is replaced and mineralized. This procedure is referred to as endochondral ossification. The other ossification process is called intramembranous ossification and is a direct ossification of mesenchymal cells. Even though these two processes are very different the final product of bone which these two processes produce are not significantly different from each other.

2.2.1. Intramembranous ossification

This ossification process is found in flat bones such as the skull, as well as parts of the cortical bone shafts in long bone such as the clavicle bone. Compared to the endochondral ossification, which has cartilage as its previous processor, intramembranous ossification develops directly through mesenchymal condensation (24, 25). Mesenchymal stem cells develop into osteoprogenitor cells, which continue to develop into osteoblasts, which deposits osteoid in isolated islands which turn into mineralized bone with active remodeling. These

islands start to build trabecular bone, which is later turned into lamellar bone. Even though this direct form (intramembranous) of ossification is different than the indirect (endochondral), the product of lamellar bone is the same. The deciding factors, which ossification process takes place where, are rooted in the embryonic development and are determined by the environmental factors (26). Ossification undergoes three phases: the induction, condensation and differentiation. The induction can be summarized as the phase where mesenchymal cells have to be induced to turn into osteoprogenitor cells to then produce bone matter. Next, the condensation includes a rapid proliferation and migration of cells, which through adhesion play a vital step in the osteogenesis to form the shape and pattern of the final bone. Finally, differentiation occurs which is the conversion into the final bone tissue. The best known example for intramembranous ossification is the skull (5, 24). It should be noted that the ossification right underneath the periosteum, can also be considered intramembranous, as bone is formed directly and without the in-between step of the chondroblasts. This applies only to the subperiosteal compartment, and not to other area of the long bones (27).

2.2.2. Endochondral Ossification

The endochondral ossification is the mineralization of the pre-existing cartilage tissue. Hyaline cartilage is formed from mesenchymal stem cells, which have differentiated into chondroblasts and chondrocytes. During embryonic development almost all of our bones are made out of a hyaline cartilage template, into which bone matter is later deposited (5, 24). Cartilage is flexible, since it contains collagen, but unlike bone it is avascular and obtains its nutrients via diffusion. The ossification is induced through vascularization. Surrounding the initial cartilage is a layer called the perichondrium, which is made up of osteoprogenitor cells and chondroblasts. After osteogenesis is completed this layer will have turned into the periosteum (5, 8). The first step of mineralization starts at the shaft or diaphysis. Osteoblasts form the osteoid, which is mineralized in a layer underneath the perichondrium, creating a compact layer of bone around the diaphysis. Ossification is a constant process, which means that once the deposition of minerals has formed an entire collar around the diaphysis, bone will continue to be added around the outer layer and be resorbed at the most inner layer to widen the bone shaft. This process is called appositional growth and continues during the life of the human as the bone has to adjust to weight and pressure which the skeleton is holding.

The inside of the diaphysis is where later on the haematopoietic bone marrow will form. The ossification in the center is introduced through capillaries which grow through the periosteum. The blood flow ensures that new stem cells and osteoprogenitor cells enter into the

inside of the cartilage. Here osteoblasts produce osteoid and the cartilage is slowly replaced with mineralized bone matter. Through remodeling and reduction, trabecular bone has formed. This formation of bone by replacing cartilage inside the diaphysis is called interstitial growth.

The epiphysis is only mineralized around the time of birth or depending on the part of the skeleton even later. Throughout the early years of childhood into early adulthood, the long bones continue to grow. This is possible with the area between the epiphysis and the diaphysis: an area of active proliferation of cartilage: the epiphysial plate. This cartilage sequentially proceeds from proliferation, maturation and calcification, to turning into trabecular bone and therefore elongating the diaphysis and ensuring the bone to grow in length. The zone of constant cartilage production (epiphysial plate) together with the area of mineralization of cartilage is called the metaphysis (5, 8, 26).

2.2.3. Bone remodeling

Bone is continuously remodeled to adjust to constant changes and new environmental requirements. This remodeling is induced and modified through physical changes, stress and demands, but also changes according to the available calcium and phosphate levels within the body. Over 99% of the body's calcium reservoir is embedded in the skeleton. Therefore, the correlation between the calcium in the blood serum and low levels of calcium due to malnutrition or disease has an impact on the bone mass as well.

Local mechanical stress will lead to new bone deposition to uphold the stability of the skeleton. Old bone is excavated in other areas to keep the balance of the entire bone mass in the body. Therefore the process of remodeling is closely regulated to establish a balance between resorption and bone production (20). The course of action in bone has a specific sequence that occurs at the basic multicellular unit of bone turnover, also known as the bone remodeling unit. Sometimes this unit is referred to as the basic multicellular unit or BMU. Initially, bone resorption is initiated, leading to an activation of osteoclasts, through exposed matrix. The osteoclasts start to dissolve and cleave bone matter leaving an empty space, called the Howship's lacuna (20). The osteoclasts resolve old bone through lysosomal cleavage through the hydrolyzation of collagenous protein and glycosaminoglycans releasing the mineralized slats. To cleave these minerals an acidic environment needs to be created leading to break up the hydroxyapatite into soluble Ca^{2+} and PO_4^- (5).

The process of remodeling takes place in close interaction with the endocrine homeostasis of calcium and phosphate which controlled by parathormone, vitamin D and calcitonin as well as the intestinal absorption of calcium, the kidney's excretion and the mobilization of calcium

and or phosphate from the skeleton (20). Parathormone is produced and secreted by the parathyroid glands and is stimulated by low calcium levels in the blood stream. It increases calcium and decreases phosphate levels through excretion via the kidney. To generate high calcium levels, parathormone can directly stimulate osteoclasts, which will release calcium from the skeleton into the blood stream. Hence the calcium in the blood stream is mainly cleaved out of bone matter. Through different effects in the kidney and intestine parathormone can also heighten the absorption and lessen the loss of calcium. It also increases the 1,25-dihydroxyvitamin D conversion in the kidney.

Calcitonin on the other hand, which is produced by the thyroid C cells, is the antagonist to parathormone. It is secreted when calcium levels are high and can inhibit osteoclasts activation. It also increases the rate of excretion in the kidney and lowers the levels of both calcium and phosphate (5).

Finally, vitamin D is provided through the intestinal uptake and the nutritional diet we ingest. It can also be synthesized through several steps within the skin, liver and kidney. The format in which vitamin D actively regulates calcium levels and bone homeostasis is called 1,25-hydroxyvitamin D. Its role is to stimulate bone resorption and intestinal absorption of calcium, leading to higher free calcium levels within the blood stream. Therefore, the stimulus for 1,25-hydroxyvitamin D are low serum levels of calcium. Parathormone and vitamin D act in a symbiosis leading to higher calcium serum levels (20).

2.2.4. Fracture Healing

Another part of bone remodeling is bone repair after a fracture. This can happen after abnormal stress on the bone, such as a traumatic accident or due to a weakened bone matter which breaks even though a trauma is absent or not adequate to the fracture. This occurs especially in osteoporosis, a disease in which the balance between bone resorption and ossification is perturbed, leading to a weaker bone structure. There are three phases to the process of fracture healing: the inflammatory response, the chondrogenic stage and the osteogenic stage (27). Once a fracture has occurred the local blood vessels are usually affected as well, which causes a local haematoma. Depending on the extent of the fracture, the periost will be disrupted on one or both sides of the bone. Right underneath the periost are the osteogenic layers of osteoblasts which are activated due to the disturbance of the periost. The local haematoma consists of blood cells which have either infiltrated from a peripheral blood vessel or arise from the intramedullar compartment. Mesenchymal stem cells are able to invade

the site of trauma and initiate the formation of chondrogenic tissue and, as a consequence, enchondral bone formation will start (27). This is considered: “indirect fracture healing”.

Initially the body reacts with an inflammatory response to a fracture. This is necessary for cytokines, interleukins and factors of the TNF family to commence the process of cell recruitment and promote angiogenesis. The mesenchymal stem cells differentiate into ontogenetic cells. All this leads to the assembly of a cartilaginous callus, serving as a guide or bridge to correct the fracture. It starts out as connective tissue which is then mineralized within 6 weeks into a primary bony callus. The initial collagen matrix is slowly dissolved, chondrocytes will undergo apoptosis and be replaced by osteoblasts and osteocytes. This is initially woven bone which is consequently turned into lamellar bone. This process can have a very different turnout, depending on the orientation of the fracture, the immobility and the width of the break which has to be overcome. To heal ideally and be replaced with high quality lamellar bone, the fracture needs to be immobilized, yet not completely since the healing process is enhanced by micro-motion and a little bit of weight. Nevertheless, if the fracture is too mobile and under too much pressure this can lead to a non-union and the fracture will never be able to heal. This risk is especially high in fractures with multiple fragments. Therefore, a fracture needs to be correctly immobilized in its initial orientation with either ends of the fracture meeting directly and firmly together for the result to be lamellar bone, which is in no way inferior in quality and strength to the original bone. After years and constant remodeling and excellent conditions of the fracture, there will be little to no remaining evidence of a fracture (8, 28).

This process of indirect fracture healing is the most common and natural process of rebuilding a bony structure. Direct fracture healing is rare and is usually enforced through surgery. In this case the fracture is reduced and aligned rigidly. Any fragments or gaps bigger than 1 mm need to be eliminated. If these conditions are achieved lamellar bone can be produced directly without the in-between stage of a callus.

2.2.5. Challenges of Complex Fracture Healing

A complex fracture is a broad term combining fractures which are peri- or intra-articular as well as consisting out of many fragments or segments. The definition can be further subdivided in the AO definition or the many classifications depending on the bone and the area of the fracture. Yet they all have similar challenges: stabilization and union of fragments, vascularization and overcoming the fracture discontinuation. These challenges are directly related to the outcome, such as the mobility of the joint and limb, with the most dramatic

outcome being a non-union. A non-union is achieved when the fracture does not heal within 6 months of the trauma. In radio imaging this is visualized through persistent fracture lines, as well as sclerosis, and a hypertrophic callus. When the fracture does not heal over a period of 9 months, with an irreconcilable gap between the bone ends it is considered a pseudarthrosis. To address these difficulties, modern surgical techniques make use of implant technologies. To stabilize fractures there is a variety of plates, intramedullar nailing and screws to support the healing process of such a fracture. This is called osteosynthesis. To overcome non-unions or fractures big enough or complex enough to threatening a non-union, orthopedics also makes use of bone grafts. A bone graft can be non-vascularized or vascularized as well as autografts or allografts. If bone grafts are used in combination with internal or external fixation it is called adjunctive bone grafting. This method of transplanting bone tissue either from a donor or from the patient itself is a unique opportunity to overcome the fracture with a material similar to bone matter itself. The advantages of autologous bone grafts, compared to regular osteosynthesis, lie in the osteoconductive framework as well as in the osteogenic potential due to the variety of cells which are implanted, and which create an osteoinductive environment. This is achieved by taking the bone graft from cancellous bone. Bone substitutes or biomaterials which are biocompatible, resorbable as well as structurally durable enough do not offer the same osteoinductivity and lack in structural integrity. Here materials such as ceramics and calcium phosphates are most often used. To this date however, most if not all biomaterials are still inferior in comparison to autologous bone grafts (29).

2.3. Bone Signaling Pathways

Bone development, formation, remodeling and fracture healing are regulated through complex signaling pathways. The bone matter, which is created embryonically and during bone regeneration, is the same on a histological level. This explains the similarities in the pathway in ossification as well as bone reparation. To create a manageable insight into the important pathways only the genes, which are analyzed in this study, are discussed in the following segment.

Bone development is influenced by transforming growth factors (TGF-beta) which include the bone morphogenetic proteins, the BMPs. These factors are vital for the condensation process of bone development as well as for the healing process after a fracture. The BMP family counts 15 known members which all interact with the process of ossification. BMP 2-7,9 and 14 are the ones relevant for osteoinduction. This means they play a vital role in the differentiation of mesenchymal stem cells into chondroblasts and osteoblasts. For the skeletal

homeostasis to stay in balance, different BMPs are activated and deactivated throughout different phases of bone growth. BMPs are produced by mesenchymal progenitor cells, osteoblasts and chondrocytes. The immediate inflammatory response to a bone fracture includes the production of cytokines such as IL-5, IL-6 and TNF- α and causes mesenchymal as well as hematological progenitor cells to infiltrate the area. The healing process includes chondrogenesis and angiogenesis to build bone matter via the endochondral pathway. During the first 24h, the BMP-2 level is at its peak and is the primary initiator for bone healing to take place. This has been substantiated through the observation, that the lack of BMP-2 in mice without any BMP-2 prohibits bone from healing. BMP-2 also plays an essential role in regulating the expression of other BMPs (27).

The RUNX2 (runt-related transcription factor 2) protein is a transcription factor, which directly binds DNA at the promoters of specific target genes, such as osteocalcin, and regulate their expression. RUNX2 is expressed in osteoblasts and chondrocytes and influences the differentiation and maturation of these cells and is therefore vital for the ossification process. This was demonstrated by Komori and Kishimoto in 1998 in a study, where RUNX2 deficient mice were generated that completely lacked bone formation. In early mesenchymal differentiation phases, RUNX2 will first lead to the formation of immature osteoblasts, but then self-regulate their expression through negative feedback and inhibit further differentiation into osteocytes. RUNX2 helps osteoblast differentiation in early stages and inhibits it in later stages and is essential in steering mesenchymal stem cells to the path of osteoblasts differentiation. This also explains why an overexpression of RUNX2 after differentiation is not beneficial, since RUNX2 inhibits the formation of osteocytes therefore hindering further maturation. It has even been observed that the overexpression of RUNX2 in mice over a prolonged period can lead to osteopenia and bone fractures. Another important observation made in RUNX2 $-/-$ mice is the lack of vascular invasion into the cartilage. It is known that vascularisation is important to initiate mineralization, but the exact interaction RUNX2 and vascularization is not yet been understood (30-32).

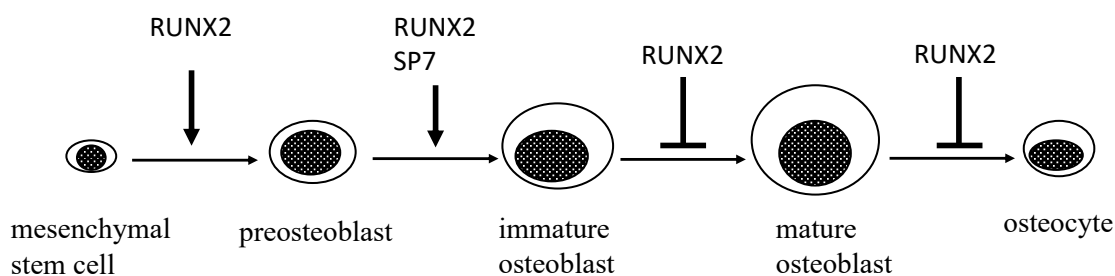


Figure 2: Schematic depiction of the role of RUNX2 in osteocyte differentiation from mesenchymal stem cells according to (31)

RUNX also seems to be regulated through BMPs and TNF- α and upregulates the expression of a number of effector genes, among them collagen type 1 (Coll1), alkaline phosphatase (ALP), bone sialoprotein (BSP), in osteoblasts (13, 31, 32). Osterix (OSX) or specificity protein-7 (SP7) is another transcription factor, which has been shown to be important in the bone formation process, since it's the ablation of either one RUNX2 or SP7 leads to the abolition of skeletal development. This was further supported by the observation that OSX null mice do not have a complete osteoblasts differentiation and therefore are not able to grow bone. This is a phenotype similar to RUNX2 null mice except for the lack of osteonectin, osteopontin, osteocalcin and bone sialoprotein. Furthermore, the expression of collagen type 1 was significantly reduced in OSX deficient mice. The role of OSX in its entirety is still under the investigation, but it is known that OSX is highly expressed during the early stages of bone formation and healing, similarly to RUNX2, by some it is considered to be a downstream molecule of RUNX2 (33, 34), but this has not yet been undisputedly proven. Rather in 2006 Nishio and Dong showed that RUNX2 regulates the promoter and therefore the expression of OSX (35).

Osteonectin also known as secreted protein acidic and rich in cysteine (SPARC) is a non-collagenous extracellular, matrix-associated, glycoprotein of the bone tissue and modulates interaction of cells with extracellular matrix interaction (36). It is therefore important during cell turnover and highly expressed during bone remodeling but also critical, for the differentiation of marrow stromal cells into different bone cells (37). It is secreted by osteoblasts (38) as well as fibroblasts and cells of the endothelial tissue and can bind directly to hydroxyapatite and calcium. During bone remodeling SPARC binds to different types of collagen (1, 3, 4 and 5) and other mediators (36). Through its interaction with collagen and also hydroxyapatite, new mineralization can occur, since SPARC has specific binding sites for both (39). SPARC null mice have shown to produce less collagen 1. Other studies have shown a link between SPARC levels and collagen deposition and assembly. Unfortunately, the exact interaction of collagen, procollagen, transglutaminases which are needed to link collagen and SPARC needs to be further analyzed to be understood completely. As other mediators of bone formation the levels of SPARC rise in immature bone and are relatively low in mature bone. SPARC is critical in bone remodeling and is in correlation with its turnover. This is especially evident in SPARC null mice since these suffer osteopenia and much lower trabecular bone mass (39). Osteopenia is a decreased bone mineral density which can be described as the precursor to osteoporosis. Not only are these mice born with a lower bone density, but this worsens as they grow older. It was shown that after 17 weeks the SPARC null mice had weaker bones, less

trabecular bone volume and decreased numbers in osteoblasts and osteoclast. The final role of SPARC in mineralization and in the modification of the matrix has not yet been completely understood (40).

Osteopontin (OPN) is expressed by osteoblasts, osteocytes and hypertrophic chondrocytes but can also be found in all body fluids and also the extracellular matrix of bone (41, 42). Its role is similar to cytokines as it is also found in inflammatory processes. OPN is a ligand for many integrins and can therefore interact with cells, especially osteoclasts. It has been proposed that OPN facilitates the adhesion of macrophages and stimulates phagocytosis through the interaction with integrins and therefore stimulates bone resorption (41, 43). Studies of OPN null mice have led to the conclusion, that OPN is not necessary for the development of bone per se, as this is completed even in knockout mice. However, when OPN deficient mice are ovariectomized, bone density did not decrease at the same level as in wildtype animals. Furthermore, it has been reported that bisphosphonates repress the function and expression of OPN which could explain the success in treating osteoporosis with bisphosphonates (3, 41, 44). It also plays a role in bone remodeling and the inhibition of bone mineralization. Therefore, it seems to work as an antagonist of bone formation.

To analyze and quantify bone formation there have been several markers found within the literature, for example Collagen 1. During the osteogenic phase of bone formation the expression of Collagen 1 and Osteocalcin start to rise and find peak around day 14 and day 21 post trauma (27). Therefore, Collagen1 has been used as a marker for early ossification as well as bone formation. Another possibility to monitor bone turnover and bone formation is the activity of alkaline phosphatase. ALP is ubiquitously found in the body and exists as several isoenzymes specific for the placenta, liver, intestine or bone. It is intrinsic in plasma membranes and although the specific role has not yet been fully understood, it is part of the vesicular transportation system of cells. Bone ALP (B-ALP) was found in the matrix vesicles derived from the cell membrane of osteoblasts, it is produced by osteoblasts and can be measured in high concentrations during new bone formation. This in direct correlation of osteoblasts activity since whenever osteoblasts “budd” of part of their membrane in the act of sending vesicles, ALP rises. B-ALP is now used to quantify and indicate bone production and osteoblast activity in the clinic (45).

2.3.1. Bone Sialoprotein:

Bone Sialoprotein (BSP) is a non-collagenous, glycoprotein found in the extracellular matrix of bone and belongs to the SIBLING family of proteins. This “Small Integrin-binding

Ligand N-linked Glycoproteins” family consists out of five proteins: BSP, osteopontin (OPN), dentin matrixprotein-1 (DMP-1), dentin sialophosphoprotein (DSPP) and matrix extracellular phosphoglycoprotein (MEPE) (4). BSP has several N- and O- glycosylation sites that are pivotal for the interaction of this protein with cells and the regulation of its activities. A specific binding site for collagen is located in the N-terminal part of BSP. Through the direct binding of BSP to collagen, BSP can be part of the initiation of bone mineralization as well as the process of nucleation. This explains why the initial detection during bone formation of BSP coincides with the beginning of embryonic development or whenever bone is subjected to mechanical stress, highlighting the role BSP plays in bone remodeling (3, 14, 44). BSP also has a so called “RGD” motif, which is made of a sequence of three amino acids: Arginine, Glycine and Aspartic Acid. This region as well as other glutamate rich regions have been proposed to help with the nucleation process of hydroxyapatite as well (46, 47). The RGD sequence also enables other cell interaction, like the one with osteoclasts through the receptor vitronectin, and therefore is part of the process of reabsorption of bone (48). BSP also serves as a regulator of endothelial cells, and promotes endothelial cell migration, attachment and angiogenesis (49). This is achieved through the interaction of the $\alpha_v\beta_3$ integrin with the RGD sequence of BSP as well as ligands such as vitronectin (50).

OPN and BSP can be categorized further into one group as they are both expressed by osteoblasts and osteoclasts but also in hypertrophic chondrocytes which lead to high levels in primary bone (51). These two seem to be working as opposites as BSP is part of the initial mineralization steps and OPN works to inhibit bone formation. During experiments in which BSP was inhibited, osteoblasts differentiation could not take place. BSP null mice were smaller and had a lower weight than the wildtype mice, but not because of malnutrition or altered body fat ratios. The developed bones were smaller and thinner and had a lower bone density. This phenotype was apparent in young mice and disappeared in adult animals, indicating how important BSP is in the initial formation of bone early in life. It also shows that BSP is less important in adult bone formation and underlines that the regulation of mature bone is complex and depends also on a number of other regulators such as OPN. Overall it can be said that BSP serves as cell-attachment and cell-signaling role in new bone formation and supports the nucleation of hydroxyapatite (3, 52).

2.4. Biomaterials:

A biomaterial can be any substance, which can be used to replace or support a function inside the human body safely and physiologically. This includes materials which reside in or

are incorporated within the human body. These materials can include sutures and catheters but also implants or prostheses and are used to support or repair the natural functions of the human body. Therefore, they need to fulfill a number of requirements, such as biocompatibility, stability and a stable and harmless interaction with the surrounding tissue and immune system (53). Here, I will focus on biomaterials that are used in orthopedics, especially supporting, replacing and guiding bones and joints. Park and Lakes list in their book “Biomaterials: An Introduction” eight requirements for biomaterials of a bone plate, which are still valid for any bone material to date.

The first requirement is biocompatibility, which has many different aspects. Any material must be accepted by the human body and therefore must be nontoxic, nonallergic, and must not interact with the immune system of the patients. Most materials can be handled accordingly through sterilization processes. This is an important factor for clinical use, if the material cannot be made sterile through heat, UV or any other treatment, it cannot be used in a clinical setting.

The second requirement asks for materials to be “chemically inert and stable” and refers to the ability to uphold its shape and function over longer periods of time. This element no longer needs to be considered as a requirement when the body is able to naturally degrade the biomaterial over time and replace it with its own tissue. In this case the biomaterial can help as a guide or a temporary support structure. Once the body, which required a biomaterial, starts to heal, and can resume its original function, the biomaterial is no longer needed. This is a new aspect in this field and now a widely accepted goal for new biomaterials. Another demand the material needs to withstand is adequate strength and resistance to fatigue of the biomaterial. This is especially important in orthopedics, as the biomaterial, which is to replace bone, needs to sustain a massive fraction of the body weight. To safely use such a material the forces which it can undertake need to be understood and measured. This goes hand in hand with the density, weight and design of the material, which all have to tie in together in the end. In summary, this aspect can be called sound engineering design.

Another requirement is more of an economic nature and concerns the cost of production, marketing and its adaptability to different patients. A number of different sources are used for biomaterials. Metals such as titanium for example are frequently used in prosthetics and joint replacements, because of their strength and durability. Polymers such as silicone or nylon are not as strong as titanium but are in contrast much more elastic and can adapt into the shape that is needed. Therefore, it is used in a number of implants.

Other properties that are sought after in biomaterials are bioactivity, osteoinductivity or osteoconductivity as well as osseointegration. Bioactivity describes the property of interaction

between the human tissue with the biomaterial or implant. A good bioactivity leads to better cell attachment and cell growth, whereas a bad bioactivity could be an immune reaction or rejection. A biomaterial is osteoconductive if it provides a suitable setting for bone formation, such as cell attachment, as well as enabling bone growth onto or into the graft. Denry et al state that for ideal osteoconduction macropores of 150 to 500 μm in diameter and 60 to 80% interconnected porosity should be strived towards (54). Yet osteoinductivity does not only support bone formation it induces it by changing the cellular structure to differentiate from mesenchymal stem cells into osteoprogenitor cells and then osteoblasts. A scaffold which is osteoconductive provides a surface on which bone can grow, but a scaffold which is also osteoinductive has the ability to provide an environment which attract bone cells, causing bone to grow faster and better (55). Osseointegration describes the interaction between the bone cells and the implant or biomaterial on a histological level (56). It refers to the attachment of the cells on the material. It is hard to define each of these terms on their own as they are all linked to one another. A material which is not osteoconductive cannot be osseointegrative. Osteoinduction is important for both, osteoconduction and osseointegration, since the attachment and growth of the cells on these surfaces, also depend on the differentiation status of the cells. Another desired aspect which should be included in the construction of scaffold is a porous architecture. This facilitates the cell growth onto and throughout the scaffold as well as neovascularization. This aspect is vital as the vascularization is a prerequisite of osteogenesis (57, 58).

Autologous bone grafts are at this moment the only implants which combine all the necessary features listed above: they are osteoinductive as well as osteoconductive and they also inhabit osteogenic cells. They are also biocompatible, sterile and stable, but they are limited in their yield since a new defect needs to be created to harvest this scaffold with a series of risks such as infection or chronic pain (58). Still, they are considered the “gold standard” in bone graft tissue engineering. There are two main groups of bone substitutes: biological materials or synthetic materials. Biological materials are for example natural polymers such as collagen but can also be materials like corals (59). Synthetic materials are a large group of glass ceramics, synthetic polymers and calcium phosphates such as tricalcium phosphates (58).

Properties of Bone Graft Substitutions

Property	Description	Classes
Osteoconduction	Support of direct bone formation through a passive porous scaffold	Calcium Sulphate Ceramics Calcium Phosphates Collagen Synthetic Polymers
Osteoinduction	The differentiation of stem cells is induced into osteogenic cells	DBM BMP Growth Factors Gene Therapy
Osteogenesis Combines	Stem cells with osteogenic potential are combined with one or more of the above mentioned properties.	Bone Marrow Aspirate Composites

Table 1: Description of the properties of bone graft substitutes with examples (60). DBM: demineralized bone matrix; BMP: bone morphogenetic Proteins

2.4.1. Synthetic Collagen

Collagen is a major component of connective tissue inside the human body. Therefore, the notion to recreate a synthetic collagen to replace or augment its functions was an early step in the production of biomaterials. Often collagen membranes are used as wound dressings and surgical repair since collagen has an inherent biocompatibility and easy remodeling structure (61). Another advantage of this material is its degradability. The material could be implanted and later be resorbed and replaced by the original tissue. This idea leads to the use of collagen as a bridging element, to help the body to overcome the time until the original tissue has healed and has replaced the biomaterial. This results in no need for a later operation to remove or replace the initial product. Because the make-up of collagen is understood in such detail, it can be recreated to some extent. In addition, collagen has the important feature not to interfere with the natural immune reaction of a patient. According to the requirements of biomaterials as listed above, collagen responds to most. It has high tensile strength, good cell and immune compatibility, high affinity to water, it is absorbable and can be created in the shapes as needed for a specific purpose. Moreover, some of its properties can be chemically and physically adapted. For example, the water content of collagen, which is an important component to define the flexibility of the material. By introducing various crosslinks and exposing it to irradiation, the water content of collagen can be heightened. This is especially important for soft contact lenses and collagen gels. Collagen can as well be treated with enzymes to further reduce its antigenic properties. This holds especially true for type 1 collagen as type 2 collagen has been shown to induce arthritis and is no longer used as a biomaterial for this reason. The introduction of crosslinks can also determine the absorption rate, which depends on the type of tissue that

collagen is implanted into the body, but also the crosslinks of collagen. Collagen also has a very positive impact on cell adhesion and has shown to be a valuable substrate for cell growth (62).

2.4.2. Calcium Phosphate

Calcium phosphate is already a biomaterial known in orthopedics and is used for bone substitution. Due to its strength and durability, it can withstand the force which is projected daily on our skeleton. There have been many adaptations to calcium phosphates to create a material that is strong, stiff and resorbable and which is also osteoinductive. Ceramic β -tricalcium phosphate seems to be one of the early calcium phosphates used for its good absorbability. They have the advantage of being osteoconductive as well as having a long shelf life. There is no risk of transmitting a disease or a virus through this material (high biocompatibility) and they are available in any shape with a adaptable porosity or composition (63). In 1996 the first calcium phosphate cement was approved by the US Food and Drug Administration to be implanted. It was self-hardening and formed into hydroxy apatite when implanted into bone grafts. After this initial step, a series of new calcium phosphate compounds flooded the market. These products, although different in components always end in hydroxy apatite production, but the hardening times are very different as are the solubility and strength. The way the calcium phosphate cement hardens needs to have strength without being brittle, therefore new biocompatible fibers were included to create more flexibility, this is still an area where constant research is needed to find the balance of toughness and adaptability. In addition, the material is required to offer an adequate environment for cells to reside and grow in. Macropores seemed to facilitate this and needed to be incorporated, without being detrimental to the strength of the material. Therefore, this material can meet the demands of osteoconduction by including porosity within their structure. Another demand which the calcium phosphate biomaterials should meet is to be absorbed and replaced by bone, but at a rate commensurate to the bone growth. Studies have shown, that if this timing is not ideal and the material is resorbed too quickly, a lower quality in bone is obtained. Calcium phosphates as a biomaterial is still a topic of intense investigation, notably to reach a solution that meets all demands and requirements and takes into account all recent advancements (64).

2.4.3. BMP in Clinical use

To find biomaterials suitable for bone substitution a better osteoinductive environment has to be created. To create this, growth factors have been used to facilitate and initiate skeletal formation, most commonly, growth factors such as BMP-2 and BMP-7 have been tested in

experimental and clinical studies and have been found to be osteoinductive. They can be coated onto or placed inside the biomaterials (64). As a member of the transforming growth factor- β family of proteins, BMP-2 and BMP-7 are approved for clinical use in specific bone reconstructive surgeries as drugs, not as biomaterials (55). The method of delivery is still a topic of debate as currently many approaches such as using collagen sponges or syringes are being tested. The approach to coat osteosynthetic implants with growth factors is under investigation as it would drastically facilitate the drug delivery process. There would be no need to expose the fracture or implant other devices and reduce the infection risk by reducing the number of contaminants into the body. These bioactive implants could be the future of orthopedic surgeries (58). At the moment BMP has to be added in supra-physiological dosage to be osteoinductive and even then, the growth rate is still not elevated to a convincing rate of bone formation. The costs of BMP, however, are extravagant and lead to a low use of this drug in the clinical practice. Therefore, the clinical evaluation is still in need of further investigation. This also leads to the need of another product, which can elevate osteoinductivity and be readily available in the modern orthopedics and trauma surgeries (55, 65).

2.4.4. Aim of this Work

The aim of this work was to analyse if the two different materials CCC and Easy Graft can be influenced in the suitability for bone cells with the addition of BSP. The biomaterials in question were “Collagen Cell Carriers” (CCC), which are membranes out of collagen type 1 fibrils and a material called “Easy Graft”, which consists of calcium phosphate granules with a poly lactide coating. These materials were examined with the goal to find a biomaterial applicable in the field of orthopedics and trauma repair surgery, to replace autologous bone grafts with an equal or superior solution. The material needs to be compatible with live bone cells, as active biomolecules such as BSP.

The viability of bone and endothelial cells on CCCs with and without BSP was investigated, as well as the expression rate of osteogenic markers of osteosarcoma cells on the CCC with and without BSP. For the material Easy Graft, the viability was evaluated with the osteosarcoma cell line. The linking of BSP to the material was examined as well as the cytotoxicity of the material itself. To be a suitable biomaterial, the material under evaluation should be able to sustain and promote bone growth. To achieve this the right combination of osteogenic material and active biomolecule coating, still has to be found.

3. Material and Methods

A complete list of all the manufacturers of the materials described below, can be found in the Appendix.

3.1. Collagen Cell Carriers

Collagen Cell Carriers (66) are produced by Viscofan Bio Engineering (Weinheim, Germany). Collagen type 1 fibers are woven together to create a membrane, which is pre sterilized and transferred into sterile conditions. Here, membranes with the size of 14 mm x 20 μ m size which fit to a 24-well plate and of 34 mm x 20 μ m - the size of a 6-well plate – were used. Some example sizes are shown in Fig.2.

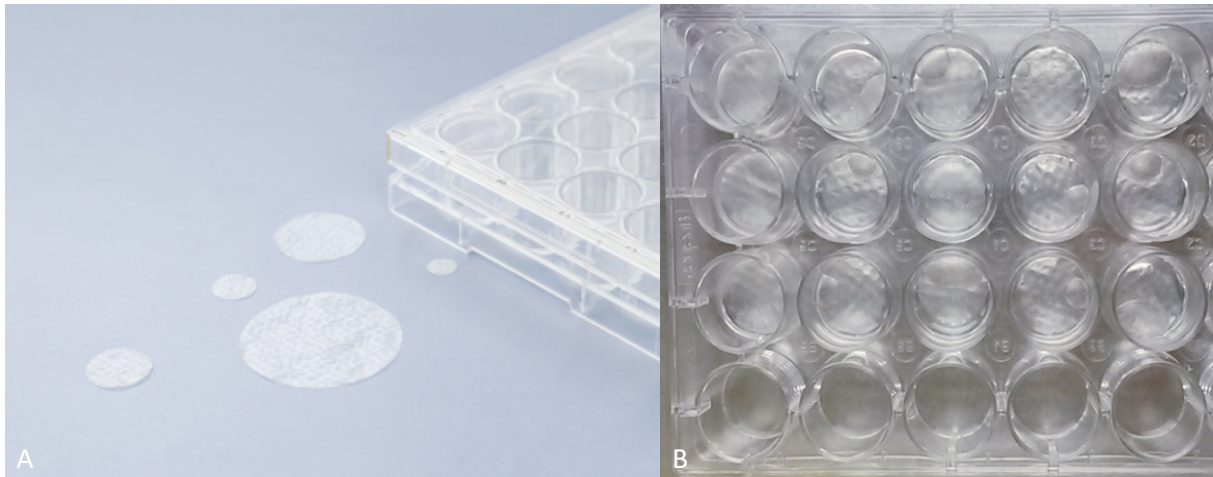


Figure 3: Picture A depicts several different sizes of Collagen Cell Carrier Membranes (CCC) on the left as well as CCCs in a 24-well tissue plate in B. (Illustration A was kindly provided by Viscofan-BioEngineering (67).

3.2. Easy Graft

Easy Graft, fabricated by the company GUIDOR, is a triphosphate (>99% tricalciumphosphate) granulate coated with a polylactide (glycolic acid and lactic acid). The granulate is linked together via a BioLinker® (N-methyl-2-pyrrolidone), liquid and water. This results in a sticky and pliable mass. As soon as the compound is added to body fluid or a pH neutral medium, it should harden within minutes, as the BioLinker® is flushed out of the porous scaffold (68), (69). In these experiments the 0.4 ml syringe was used, containing granules between 500 and 1000 μ m. Figure 2 shows a 0.4ml syringe containing only the dry granulate as it is supplied. The BioLinker® is packed in an extra container with a prefixed volume. Once the syringe is loaded with the BioLinker®, the two compounds can be integrated profoundly by moving either side of the syringe.



Figure 4: Easy Graft syringe: A prepackaged syringe containing 0.4ml dry granules.

3.3. Bone sialoprotein (BSP)

BSP, provided by Immundiagnostik AG, is produced by a Chinese Hamster Ovary cell line, which expresses the stable protein. The effect of this human recombinant protein was examined in a number of different experiments. The protein was used to coat Collagen Cell Carriers or the Triphosphate Granulate: Easy Graft.

3.4. Working Conditions

3.4.1. Laminar Air Flow

The laminar air flow ensured an aseptic environment for all the experiments. The materials were purchased pre-sterilized and were handled with sterile instruments. Other materials were autoclaved at 121°C for 20 min or heat-sterilized at 180°C for 2 hours.

3.5. Coating Procedures

To prove and identify the impact of additional BSP on the materials different coating techniques were used.

3.5.1. Preparing the CCC

Before seeding, each CCC has to be attached to the well bottom according to a protocol provided by the manufacturer. Each well was preloaded with PBS (pH 7.3/w/o $\text{Ca}^{2+}/\text{Mg}^{2+}$) and the CCC was laid on top of the liquid without submerging it. The volume was adapted to the diameter of the well, in this case 14 mm (24-well plate) matched with a volume of 250 μl .

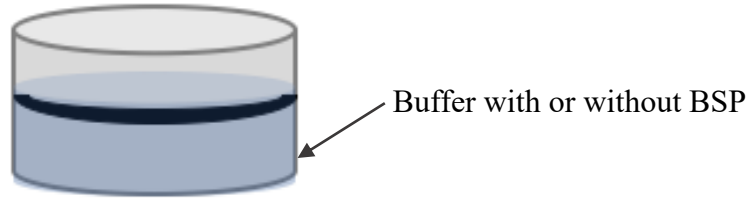


Figure 5: Well-draft: a single well containing PBS and a layer of CCC on top of the PBS. PBS is the Buffer utilized to equilibrate the membrane. Depending on the treatment it was mixed with BSP or left plain respectively.

The CCC was incubated on top of the PBS Volume for 30 min at room temperature. The remaining volume was aspirated ensuring the CCC to lie flat on the well bottom without any wrinkles or air enclosed below it. Afterwards the CCC was dried overnight under the laminar air flow hood, without the lid of the well plate. The last step before seeding could take place was the equilibration of the CCC for which 250 μ l of prewarmed medium (at 37°C) was added to each well and placed inside the incubator for 30 minutes. Finally, the medium was aspirated and replaced with the appropriate cells and medium.

3.5.2. Coating

Two different coating methods were applied, “BSP” and “BSP coat.”

Method 1: In the first coating method, 5 μ g of BSP were added to the PBS, which was added to the well plate before attachment, during the soaking process. Next, the CCC was placed on top of this liquid. After 30 min at room temperature the remaining PBS+BSP mixture was aspirated and the CCC was dried overnight to encourage adhesion onto the well floor.

Method 2: During the soaking process, the CCC was placed on top of only PBS, the liquid was aspirated after 30 minutes and the CCC was dried overnight to encourage membrane adhesion to the cell well. The CCC was coated after the drying process but before the equilibration step with prewarmed medium. The CCC was coated with 5 μ g of BSP in 100 μ l PBS, which was left to soak for one hour.

3.5.3. Coating Easy Graft

The granulate Easy Graft was stored and transported in a syringe with 0.4ml each at room temperature. In addition, the bio-linker was stored in an adjacent tube. The company does not specify the amount. The loose Easy Graft granules are transported in a syringe (see Figure 2). The bio-linker is added into the syringe and flushed back and forth within the syringe ensuring an even coating of all particles. This creates a moldable mass. To create even scaffolds two

approaches were tried. First, a 3D mold was created using PLA in a 3D printer, the second approached included flushing out the BioLinker® of the granules while they are still in the syringe to create a tough cylinder of Easy Graft. In the first approach the moldable Easy Graft with the BioLinker® was placed inside the PLA molds as seen in Fig. 4 A.

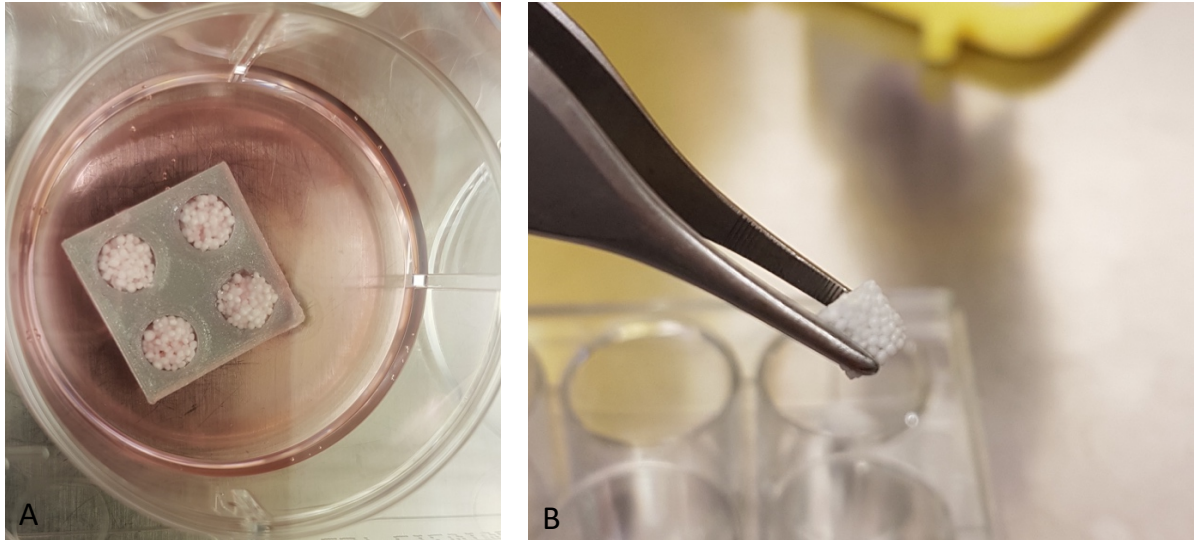


Figure 6: Easy Graft experiment: A shows a close up of a 24-well cell inside which the 3D PLA Mold containing Easy Graft is placed. B shows an image of Easy Graft cut into shape with a scalpel.

In order to remove the bio-linker and create a hard scaffold, the mold with the granules was placed in pH neutral medium (McCoy) to wash out the remaining bio-linker, to permit hardening and creating a permanent shape. This was to ensure the scaffold to harden completely and to be then removed from the mold. Thus, creating a cylinder, the size of 5 mm x 2 mm. Easy Graft did not harden completely inside the molds after 24 hours and therefore the hardening process was extended first to 48 hours then up to seven days. Still Easy Graft was not able to harden completely and upon taking the scaffold out of the mold was flaky and mostly fell apart.

The second method (Figure 4 B) was to create a hard scaffold, which was then cut to size. Therefore, the bio-linker had to be removed while Easy Graft was still inside the syringe.

The pliable mass was not removed from the syringe but was rinsed again with PBS, which washed out the BioLinker®, creating a hard cylinder of 2.4cm. This was then cut by hand into 3mm scaffolds, using a feather scalpel. The coating of BSP was done by placing 5µg of BSP solved in 14.3 µl of PBS and letting this incubate at -4°C overnight.

3.6. Cells

Four different cell lines were used throughout this work:

hOB: Primary human Osteoblasts, which originate from mesenchymal stem cells and are an experimental model to study bone growth.

These cells were isolated according to the protocol described in (70, 71), as well as a precise description in (72). The human probes were gathered during hip or knee joint replacement surgeries performed at the Universitätsmedizin Mainz. All patients of which residual bone material was used, signed a written consent form. The examination and further processing of the material was approved by the ethics committee of the Landesärztekammer Rheinland-Pfalz, in compliance with the Declaration of Helsinki and the ICH Guidelines for GCP.

After the bone fragments were gathered and rinsed with PBS, they were treated with collagenase type I for 45 minutes at 37°C, to carry out collagenase digestion. Afterwards the probes were rinsed in PBS several times and placed in 6-well plates with the medium suggested in the protocols, DMEM/F-12, which was supplemented with 10% FCS as well as 100U/ml penicillin, 100 µg/ml streptomycin, 100 µg/ml ascorbate, 59 µg/ml glycerolphosphate and 10 nM dexamethasone. The fragments were kept in an incubator at (5% CO₂, 37°C) to obtain outgrowth of human osteoblasts from the isolated bone fragments. The medium was changed twice a week. At the third passage of cells the cells were evaluated for the osteoblastic phenotype and could be used for experiments.

MG-63 and SaOS-2 cells: Two osteosarcoma cell lines, which have a faster growth rate and grow in a higher density compared to human osteoblasts (73). Since these cells are derived from a tumor cell-line, they provide a more homogeneous population (74). they behave similar to osteoblasts and are therefore considered osteoblast like cells. These cell-lines do not reflect the entire range of osteoblastic phenotypes (75, 76). These two cell lines were provided by ATCC, Manassas, USA.

HUVEC: Human umbilical vein endothelia cells were used to include vascularization as a factor into the experiments. These were provided by PromoCell GmbH, Heidelberg, Germany.

The appropriate medium of each cell line is found in the Appendix.

3.6.1. Cell passaging

The cultivation of cells required a passaging process in order to not overcrowd the cell culture flasks. When the cells had reached a density between 75 and 90% of the flask, they were sub-

cultivated. This process included washing the cells with PBS and detaching the cells with Accutase® (77) (at 37°C). Accutase® is a detachment enzyme isolated from crabs. The proteolytic and collagenolytic enzyme allowed a mild detachment without compromising most of the surface proteins. This enzyme solution is stored at 4°C and was activated by placing the flask on a 37°C hot plate, causing the cells to curl up and freely move within the flask. After 2 to 3 minutes, the flask with the cell culture was placed underneath a light microscope to verify, that all cells have detached from the flask bottom. Subsequently, medium containing FCS was added to inactivate the protease and the cells were centrifuged (1.400 rpm, 5min) and reseeded in a smaller fraction. The medium corresponding to each cell line are listed in Table 1.

3.6.2. Preservation (freezing of cells)

The cell suspension was centrifuged at 1.400 rpm for 5 minutes. The resulting cell pellet was resuspended in FCS containing 10% dimethyl sulfoxide (DMSO). DMSO is required for stabilizing the cell structure during the freezing process. Afterwards, cryo-tubes were loaded with the suspension and placed into a cryobox. To ensure a slow and less damaging freezing process the box was stored at – 80°C for one day and then moved into a N₂-tank at -196°C.

3.6.3. Cell counting

For cell counting a cell suspension is required. Cells were kept in a 37.5°C incubator with 5%CO₂ and grown in cell culture flasks of different sizes, with their respective media. To break the adhesion between the cells and the flask surface, the cultures were washed with PBS (Phosphate Buffered Saline) and treated with Accutase®. This cell suspension was then mixed 1:2 with Trypan blue solution (0.4%) to ensure that only viable cells were counted. The “Trypan blue dye exclusion method” (78) is based on the principle that intact membranes of living cells do not take up the dye and therefore stay white. Unlike dead cells, which are permeated by the dye and change color and are therefore not counted. Ten microliters of this mixture were pipetted onto a cell counting slide and placed within the LUNA Automated Cell Counter for counting.

3.6.4. Fluorescence Microscopy

To visualize cell growth and cell density both light microscopy and fluorescence microscopy (EVOS) were used. Through various wavelengths different colors such as green for GFP can be made visible. The excitation wavelength was at 470/422nm and the emission wavelength in nm 510/42, red: 530nm /593nm and blue 360nm/447nm respectively.

3.7. Colour and Cell Labeling

3.7.1. Hoechst cell staining

The Hoechst dye binds to DNA and is used as a staining method to identify cell nuclei. After diluting the staining solution in a ratio of 1:250, the Hoechst stain was added to prewashed cells and incubated for 10 minutes. The blue fluorescent color was detected by a fluorescence microscope (excited with UV light within the range of 340/380nm) (79).

3.7.2. Immunofluorescence

Immunofluorescence was used on HUVEC cells, which were seeded into a 24-well tissue culture plate at 15.000 cells per well. After one day the steps illustrated below were followed to conduct the immunofluorescence experiments. The medium was aspirated from each well, after which each well was washed with 500 µl PBS. To fixate the cells, 3.7% PFA was added for 15 minutes. After removing the PFA, the cells were washed with PBS twice. The cells were permeabilized with 1% Triton-X100 for 7 minutes. This reaction was blocked with 0.5% BSA in PBS for 30 minutes. The first antibody was added, and the plate was placed at 4°C overnight to ensure maximal attachment. On the next day, after washing each well twice with PBS, the second antibody was added and incubated at room temperature for 2h isolated from any light source. The plate was washed twice with PBS before the Hoechst dye was added (see Hoechst staining). After two final washing steps with PBS the immunofluorescences were detected via fluorescence microscopy. The antibodies were diluted with PBS with 0.5% BSA and compared to a negative control.

Table 2: Antibody Dilution

Antibody	Description	Dilution
CD31 mouse ab9498	1 st Antibody	1:50, 1:100, 1:200
CD31 rabbit ab28364	1 st Antibody	1:100, 1:200
vWF mouse ab68545	1 st Antibody	1:100, 1:200
vWF rabbit ab6994	1 st Antibody	1.100, 1:200
VEGFA rabbit	1 st Antibody	1:50, 1:100, 1:200
Rabbit IgG A11008	2 nd Antibody	1:200
Mouse: Alexa: A11001	2 nd Antibody	1:200
Hoechst	Nucleus staining	1:250

3.7.3. AlamarBlue®

AlamarBlue® staining is a method to test the cell viability and receive a quantitative feedback about the cell health. It has been shown to be a reliable and rapid assessment of the growth and proliferation of the cells (80). The solution has been verified to not be toxic and therefore does not impact the cell growth. (81). If the cells are alive and metabolically active, they will convert the dye Resazurin (non-fluorescent) to Resorufin (fluorescent). The fluorescence intensity is proportional to the amount of living cells in the assay (81). For the assay, a 10% alamarBlue® solution was made with the respective cell medium. To ensure a consistent concentration one solution with sufficient volume was made at the beginning of the experiment and then stored in a light free container at 4°C. Out of every well, of every treatment group, 3 x 100 µl were analysed. The fluorescence intensity measurements were taken after four hours of exposure using the Glomax Multi Detection System blue kit (525nm extinction and 580–640 nm emission).

After the measurements were completed, the remaining volume was aspirated in total and replaced with 1 ml of fresh medium until the next measurement. The viability tests were performed three-days interval.

3.7.3.1. CCC

The membrane was coated as explained above in the coating method section (3.5.2.). The alamarBlue® assay was used to quantify the viability of cells. Four different cell lines were evaluated: hOB, SaOS-2, MG-63 and HUVECs. The experiment was repeated twice to ensure consistency. The alamarBlue® method was used on day 1, 4, and 7 after seeding. Because of their different growth rates, the cells were seeded with the following adjusted densities:

SaOS-2	15.000 cells
hOB	25.000 cells
HUVEC	25.000 cells
MG-63	10.000 cells

The cells were seeded in triplicates into 24-well plates with the following treatments: a positive control (PC), which were cells seeded on a flat-bottom well plate, designed for cell attachment from the company “Cellstar®,” (referred to as tissue plate). An untreated CCC attached on a 24 flat bottom tissue plate (CCC), a CCC coated with BSP according to method one (3.5.2) and CCC coating method 2, respectively. At day 1, 4 and 7, the entire medium of each well was aspirated and replaced with 500 µl alamarBlue® Medium (10% alamarBlue® solution and 90%

appropriate medium). After 4 hours of incubation at 37C incubator, three times 100 µl from each well were aspirated and pipetted into a 96-well plate. This plate was then placed into the Glomax-Multi Detection System to measure the fluorescence activity (filter with 525nm extinction and 580–640 nm emission)

3.7.3.2. Easy Graft

AlamarBlue® was used to quantify cell viability. For this, 20.000 SaOS-2 cells were seeded onto each scaffold in 200 µl of medium. The scaffolds were placed in a 96-well culture plates. As depicted in Figure7, each experiment consisted of one negative control without scaffolds or cells (NC), one control with just the scaffold (EG), the scaffolds treated with BSP (BSP) and one row of cells seeded without a scaffold on the same ultra-low attachment plate (Cells). A positive control (PC) with 20.000 cells was seeded onto a separate 96 flat-bottom cell culture plate from the company Cellstar®. Each condition was set up in duplicates at first and then five-fold during the repetition of the experiment. On day 1, 5 and 7, cell viability was measured with alamarBlue®. This was done in the same fashion as the CCC Assay (3.7.3.1.).

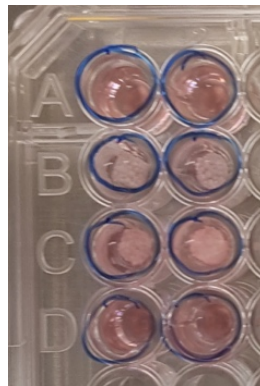


Figure 7: Experiment Easy Graft. NK: Negative control with no scaffold seen in row A, EG: scaffold without BSP seen in row B, BSP1: scaffold coated with 5µg BSP in row C. Cells seeded onto an ultra-low attachment plate without a scaffold (Cells).

3.7.3.3. Visualization of the Residue

During the alamarBlue® experiment with Easy Graft, the medium with the remaining, unattached cells had to be taken out of the 96-well at day one to be replaced with alamarBlue® to take the fluorescence measurement. This residue of the cells, which did not attach after 24 hours are seeded onto a flat-bottom 46- tissue plate. After another 24 hours, pictures were taken to visualize if any viable cells attached and how many cells were in the medium and did not attach to the scaffold originally.

3.7.4. Lightning Link

To mark and label BSP, the Lightning-Link Fluorescein Conjugation kit was used. This kit specifically targets amine groups and is therefore suitable to link Fluorescein to proteins. The kit contains the Lightning-Link mix, the LL-modifier reagent and the LL-quencher FD reagent. To label 125µg of BSP (concentration of BSP: 420µg/ml) 297,6 µl were combined with 29,8µl LL-modifier agent. (1 µl per 10 µl of the protein solution). This mixture was then directly pipette into the LL-Fluorescein vial and gently mixed through pipetting it up and down. After 4 hours, 29.8µl of quencher was added to stop the reaction. BSP was now linked with a fluorescent dye and stored at -4 °C. This Fluorescein-linked BSP was used to establish a standardized curve with 50µl increments of different concentrations. (10 µg, 7.5 µg, 5 µg, 2.5 µg, 1 µg, 0.5 µg, 0.25 µg) The fluorescence of each concentration value was measured three times at 498 nm. This was done using the blue kit of the Glomax at Ex 490 and EM 510-570. The linked protein was then used for the release experiment. This includes two Easy Graft scaffolds, coated overnight in 5µg linked- BSP. With 200 µl of PBS placed in cell culture at 37 °C in the dark. Over time, the released BSP in the medium was measured and the fluorescents were compared to the standard curve to backtrack the amount of protein released. Resulting in an estimate of BSP remaining inside the scaffold. The measurements were taken after 30 minutes, 1 hour, 2 hours, 4 hours and 24 hours.

3.7.5. Cytotoxicity

Cytotoxicity of the Easy Graft material was examined using the LDH-Glo assay from Promega. This assay utilizes LDH (lactate dehydrogenase) as a marker for cytotoxicity. If the integrity of the cell membranes is compromised, LDH will be released. This enzyme catalyzes the reaction from lactate to pyruvate, during which NAD is reduced to NADH. The provided reductase and the substrate for this reductase react with the created NADH to create a correspondent amount of luciferin. Ultra-Glo® Luciferase congruently converts Luciferin into a bioluminescent signal. This signal was measured and is an exact representation of the LDH and therefore the cytotoxicity in the sample.

For this 100ml of LDH storage buffer was created using:

- 20ml 1M Tris-HCl (pH7.3)
- 11.5ml Glycerol 87%
- 3.3ml Bovine serum albumin (BSA) 30%
- 65.2ml distilled water (aqua)

On day 1 (24h), 2 (48h) and 3 (72h), 10 μl of the medium of each 96-well was put into 990 μl LDH storing solution and placed at -20°C . For the evaluation and measurements, the samples had to be thawed and 50 μl of each sample was placed in a 96-well plate. To this 50 μl of LDH detection reagent was added in each well and let set for 60 minutes. The LDH Detection Reagent was created using the LDH Detection Enzyme mix from which 5 ml was added to 25 μl of reductase substrate. After 60 minutes the luminescence of each well was measured. Each well contained 100 μl (1:1 ratio 50 μl sample plus 50 μl LDH detection reagent). The cytotoxicity could then be deduced from the luminescence measured.

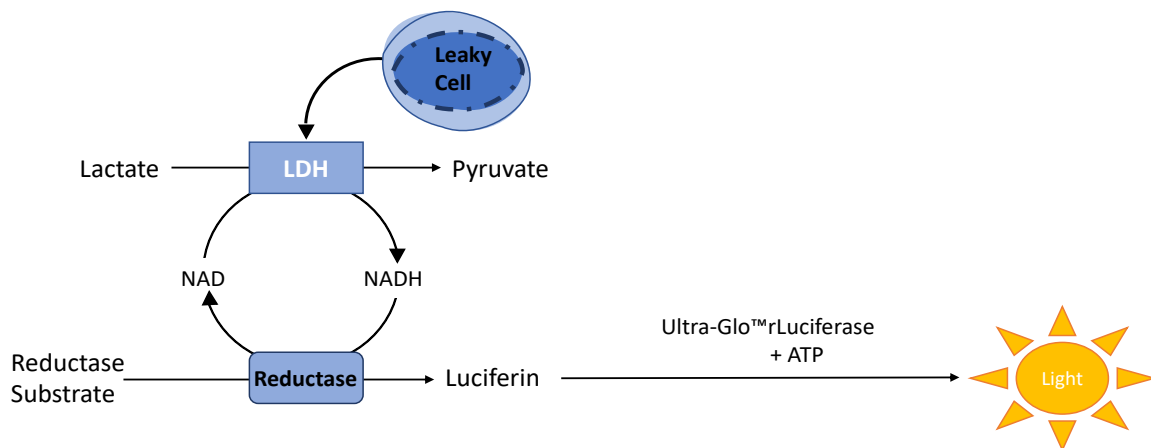


Figure 8: This image shows how cytotoxicity can be measured by monitoring luminescence. Whenever cells are destroyed LDH is released. This enzyme can catalyze lactate to pyruvate with the coenzyme NAD. NAD is created from NADH by the reductase activity from LDH-Glo. The amount of reductase that was used to reduce the substrate to Luciferin and create a measurable fluorescence is equivalent to the amount of LDH released by the cells.

The measurements contained six different groups. One was just medium with no cells, then there was a positive control of 200.000 cells on a 96-flat bottom tissue plate this is named “cells” in the graph. The treatment entitled negative control (NC) are 200.000 SaOS-2 cells seeded onto an ultra-low attachment plate. Then the levels of LDH were measured in wells with the scaffold (EG), as well as the scaffold treated with BSP.

3.7.6. BSP Release Measurement

To measure how much BSP was released from the scaffold and to draw conclusion of how much BSP is contained inside the scaffold after the coating procedure, a BSP release experiment was performed. For this a standardized curve of the fluorescence of lightning-link linked BSP was created at different concentrations. With threefold volumes of 50 μl the average fluorescence was measured at 10 μg BSP, 7.5 μg , 5.0 μg , 2.5 μg , 1.0 μg , 0.5 μg , 0,+25 μg respectively. Next, two Easy Graft scaffolds were coated with 5 μg of linked BSP. They were set overnight in the dark at -4°C . On the next morning, they were each placed in 200 μl PBS

inside a 96- well plate. For this, two scaffolds were used. After each time increment four 50 μ l measurements were taken adding to the entire volume (200 μ l) which was originally added to the scaffold. After the measurement the original volume was replaced with new medium. The fluorescence measurements were added to be able to deduce the amount of BSP inside the medium. Measurements were taken after 30 min, 1 h, 3 h, 5 h and 24 h.

3.8. Gene expression

In order to harvest enough cell material for a gene expression, collagen membranes (CCC) with a surface of 9.1 mm² were used with 150.000 SaOS-2 cells per CCC. These big CCCs were set up in 6- well plates in exactly the same fashion the 24-well assays were arranged. The set up contains two untreated CCCs, two CCCs soaked in 30 μ g BSP (Method number 1) and two CCCs coated with 30 μ g BSP (method number 2). After 4 days the cells were detached using Accutase®, centrifuged and stored at -80°C. The cells of the two membranes of one treatment, were merged for one cell pellet.

RNA isolation:

RNA isolation was achieved using the peqGOLD Micro Spin RNA Kit. The lysis process was combined with the QIASHredder Spin Column to obtain a maximal yield of RNA. To the cell material 300 μ l RNA lysis buffer was added into the QIA Shredder Column, which was subsequently centrifuged for 2 min at 13.000 rpm. Then, following the peqGOLD protocol, the cell extract was pipetted onto the DNA removing column and centrifuged at 10.000g for 1 min. The remaining filtrate was mixed with 200 μ l 70% Ethanol. Then the mixture was placed into the Perfect Bind MS RNA column and centrifuged at 10.000g for 1 min. The collection tube was replaced with a new collection tube. 500 μ l of washing buffer 1 was added into the Perfect Bind MS RNA column and was centrifuged at 10.000 g for 1 min. The excess medium, which had gathered in the collection tube was removed, without changing the collection tube.

The DNase step was completed with the Qiagen RNase free DNase. 10 μ l DNase stock solution (QIAGEN) was mixed with 70 μ l RDD buffer and pipetted directly onto the membrane of the Perfect bind MS RNA column. This was incubated for 15 minutes at room temperature. Then the column was placed onto a new collection tube and 400 μ l RNA Wash Buffer1 was added followed by an incubation for another 5 minutes. Subsequently the columns were centrifuged at 10.000 g for 5 minutes. The collection tube was exchanged for a new one. The washing step was repeated twice with 500 μ l washing buffer 2 at 10.000 g for 1 minute each

time. The collection tube had to be replaced by a new one for the next step in which the column was dried while being centrifuged for exactly 2 minutes at 10.000 g. The Perfect Bind MSRNA was then placed onto a new clean collection tube and 15 µl RNase free water was pipetted onto the column ensuring elution. The column was then centrifuged for 1 minute at 6.000 g (The RNA was stored at -80C)

The purity and concentration of each RNA sample was tested using 2 µl in a photometer. The 260/280 ratio was measured and was between 1.8 and 2.1.

cDNA Synthesis:

This was performed with the Thermocycler Peqstar 2X with the program for the M-MuLV-Rev. Tra:

<u>Thermocycler:</u>	<ol style="list-style-type: none"> 1. Heat Lid to 110°C 2. 5 minutes 65°C <hr style="width: 50%; margin-left: 0;"/> <ol style="list-style-type: none"> 3. 6 minutes 25°C 4. 1 h 42°C 5. 20 minutes 65°C 6. store at 4°C 	<p>Preparation 1 was placed into the thermocycler for Step 1 and 2. The lid was then manually opened after the 5 minutes of step 2 are completed to add preparation 2.</p>
----------------------	---	--

For each sample 1µg RNA had to be calculated and placed into the Thermocycler tubes. For example, if the concentration of the RNA sample was 0.200 µg/µl, 5µl of the RNA sample and 11 µl of RNase free water was added to the preparation, creating 11µl. The 2 µl of random primers and 2µl dNTP add to a final volume of 15 µl.

1.Preparation:
 2 µl Random Primers
 2 µl dNTP
 y µl RNA free water
 x µl RNA

 15 µl incl. RNase free water

2. Preparation:
 2 µl 10x MuLV RevTra-Buffer
 2 µl RNase free water
 1 µl M-MuLV Reverse Transcriptase (BioLabs. M0253S, 10,000U= 200,000U/ml)

After the entire program was finished, the cDNA synthesis was complete. The cDNA dilution for the quantitative polymerase chain reaction has to be adjusted accordingly to how much RNA material and therefore cDNA could be harvested. The usual ratio is 1:10 it can be changed to 1:5 if too little RNA was gained.

qPCR:

Expression of the following genes was tested: GAPDH, SP7, RUNX2, ALP, Col1, OPN and SPARC. For each gene a qPCR Mix had to be created out of the following ingredients:

- 4.8 µl RNase free water
- 0.1 µl reverse Primer
- 0.1 µl forward Primer
- 10 µl SyBr. Mix

In each well, the qPCR mix was placed and the 5µl of the respective sample was added. For each gene, an RNase free water control was included. The plate was then directly placed inside the X with the thermal cycling profile of Table 3.

Repetition	°C	min:sec
40x	95	02:00
	95	00:05
	60	00:25

Table 3: Thermal cycling profile of qPCR

The mRNA expression of the following genes was analyzed: Col1, OPN, ALP, SPARC, SP7 RUNX 2 with the Housekeeping gene GAPDH. Specific Information about the materials purchased, are found in the appendix.

The Gene expression could be determined and calculated with the $2^{-\Delta\Delta C_t}$ method (82).

3.8.1. Housekeeping Gene

GAPDH is a protein, mainly localised to the plasma membrane and the cytosol and has a variety of functions. But this is not why it is so often used in the analysis of mRNA and qPCRs. GAPDH is what is called a housekeeping gene, which means the expression level of GAPDH is rather uniform and thus often used to normalize the expression measured of other genes. GAPDH is one of the most commonly used housekeeping genes for a vast variety of tissues since so many cells produce it at constant levels and therefore serves as a guide during the investigation of other genes. In the quantitative measurements of mRNA GAPDH is used to control and understand the amount of RNA present. Therefore, the expression levels under investigation are put in relation to GAPDH to be correctly be interpreted with a uniform baseline (83).

3.9. Statistics

To analyze and verify experimental data, several statistical methods were used throughout this thesis using the software SPSS from IBM (Downloaded June 2020, Version 23). All the measurements were taken in triplicates except for the Easy Graft viability assay as the volume in the 96-well plate could only yield double measurements. All experiments were repeated at least two times. The data for each day of which the measurements were taken was examined for a normal distribution through a Shapiro-Wilk-Test as well as the descriptive analysis of a histogram. A one-way analysis of variance (ANOVA) was done to determine statistical differences between unrelated variables. Also, depending on the results of the Levene's test for equality of variances, the Tuckey or Games-Howell post hoc test were conducted to compare variables in pairs. Whenever the data proved to be not normally distributed, the Man-Whitney-U test was applied. When the data was normally distributed, which was determined through a Shapiro-Wilk test, a T-Test instead of a Man-Whitney-U test was conducted also with p defined as significant when below <0.05 . In some cases, data points had only a small number of cases ($n < 10$). In this case the data was considered nonparametric and Man-Whitney U and Kruskal Wallis test was conducted.

Whenever the p value is <0.05 the test is deemed as significant and labeled with a  in the graph.

Whenever a pairwise analysis was conducted with multiple pairs, such as different treatment groups on each day, the p value had to be adjusted to the number of pairs being tested. For example, if 4 pairs are being compared to each other, creating 6 comparisons, the p-value is divided by as many tests that were applied: $p(0,05)/6 = 0.0083$. This is to avoid false positive results.

4. Results

Two biomaterials were tested, Collagen Cell Carrier membranes (also called CCCs hereafter) and Easy Graft in combination with BSP for their behaviour and suitability in bone formation and their potential for future use in clinical treatment of bone fractures. In addition, benefits of both materials for the ossification when combining them with BSP were investigated.

4.1. Characterizing Cell Lines

4.1.1.1. Native pictures of the cell lines:

Two types of cell systems were used. Primary cells such as human umbilical vein endothelial cells (HUVECs) and human osteoblasts (hOBs), that can be maintained for a limited time in culture (Fig. 9 A, B). The second type of cells lines that were used are human osteosarcoma cell lines which were originally derived from a human cancer and are established, immortalized cells that can be propagated in culture without limitations, called SaOS-2 and MG-63 (Fig. 9, C, D). HUVECs and hOBs were directly retrieved from their original viable tissue and therefore feature donor specific phenotypes and growth characteristics. HUVECs as well as the hOBs grow in culture in a confluent monolayer and in both cases the cells present in polygonal shapes (Fig. 9 A, B). In contrast to HUVECs, hOBs have much larger and thinner extensions reaching out from their cell body, a typical feature of human osteoblasts. Osteosarcoma cell lines, such as SaOS-2 and MG-63, grow more rapidly in culture than the native cells, but still have osteogenic properties. They both have similar oval shapes (Fig. 9 C, D). These cells have been derived from a pathological tissue, an osteosarcoma, which is a malignant tumor of the bone. This is why they grow fast and stably and present as a homogenous population as seen in Fig. 9 C and D.

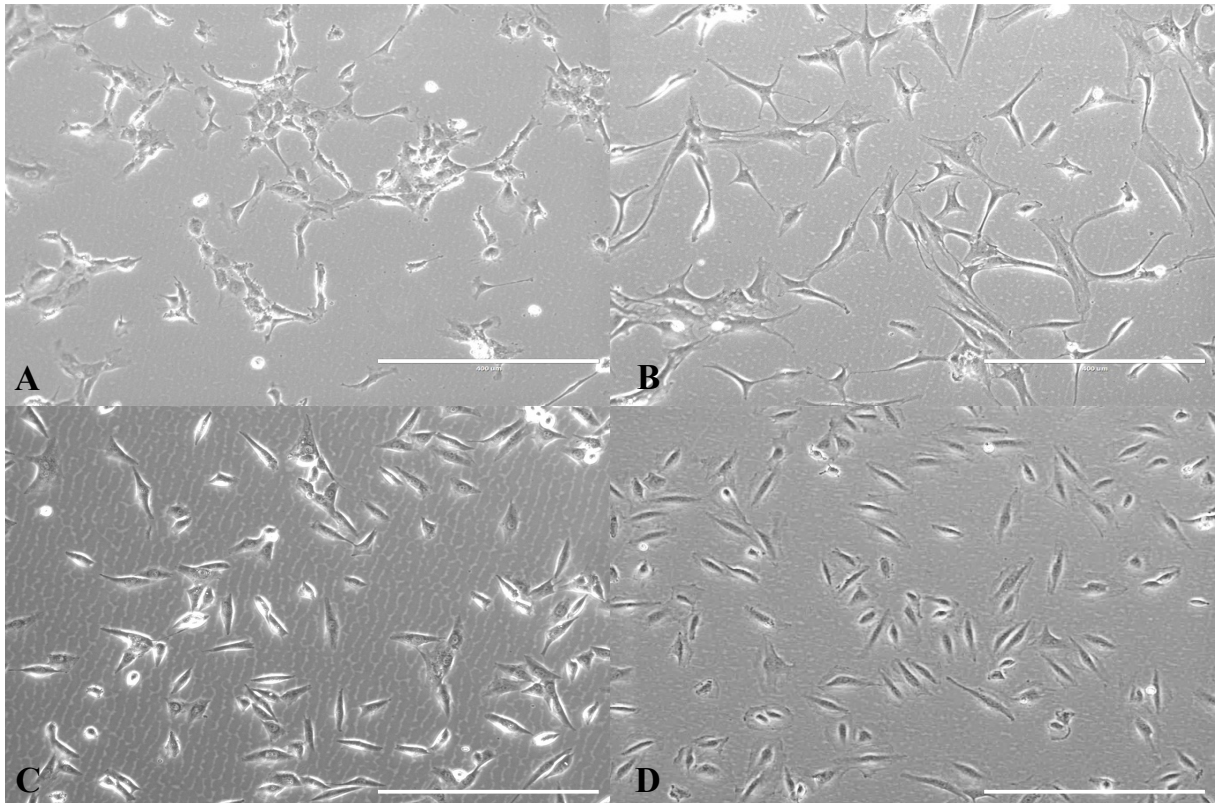


Figure 9: Photomicrograph of cultured cells from the following lines A: HUVECs B: hOBs C: MG-63 cells D: SaOS-2 cells, magnification is 10x. The scale bar indicates 400 μ m.

4.1.2. Immunofluorescence of the HUVECs cell line

Angiogenesis is an important step for initiation of bone growth. Therefore, it is essential to also consider endothelial growth when analyzing the environment of potential bone rehabilitation. In order to confirm that the HUVEC cells used here maintain their endothelial phenotype after multiple freeze thaw cycles and several cell passages (here up to 9 passages), immunofluorescent staining of HUVECs was performed. This was to demonstrate the expression of endothelial cell surface marker CD31, also known as Platelet Endothelial Cell Adhesion Molecule or PECAM-1 (84) and both the vascular endothelial growth factor A (VEGFA) and the von Willebrand factor (vWF).

4.1.2.1. CD31

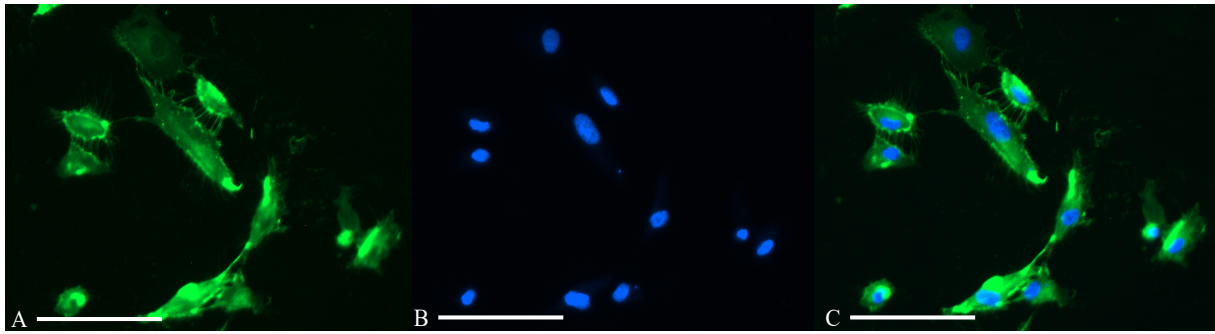


Figure 10: Immunofluorescence staining of HUVECs for the presence of CD31. A) immunofluorescence staining of CD31, B) Hoechst staining of the nucleus. C) Overlay of Hoechst and the CD31 staining. The scale bar indicates 100 μ m.

Fig. 10 shows the immunostaining in green of CD31 in panel A and in panel B the Hoechst staining of the nucleus in blue, as well as a combination of both pictures in an overlay in panel C. The staining demonstrates the presence of CD31 as a surface glycoprotein. It is expressed by many cells, especially in endothelial cells and HUVECs (85, 86). Therefore, its presence is an important indicator for endothelial cells. Yet CD31 on its own is not evidence enough to categorize these cells as endothelial cells (87).

4.1.2.2. VEGFA

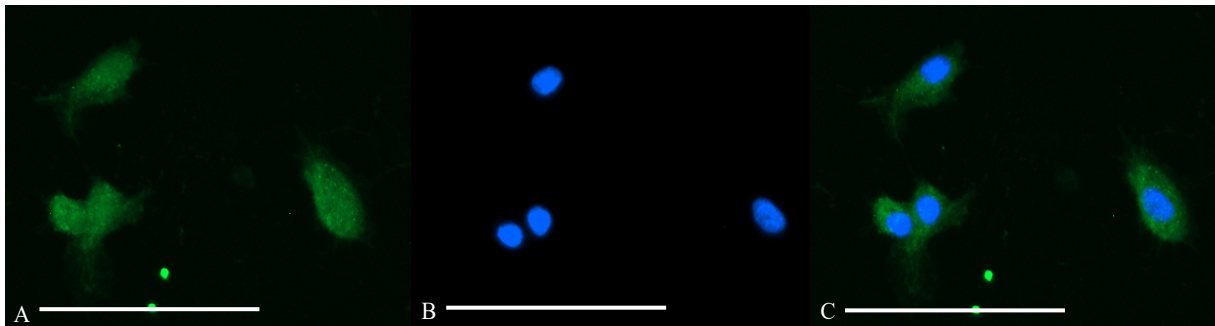


Figure 11: The image above shows an immunofluorescence staining of VEGFA in A, as well as a Hoechst staining of the nucleus in B and an overlay of Hoechst and the immunofluorescence in C. The scale bar indicates 100 μ m.

Fig. 11 shows an immunofluorescence staining for VEGFA. Panel A in Fig. 11 reveals that the growth factor VEGFA is present in the cytoplasm. The Hoechst staining in B outlines the nucleus, whereas the overlay of both staining in C presents the cells with both staining methods. The pictures in the panel above show the presence of VEGFA, supporting the endothelial phenotype of the HUVECs.

4.1.2.3. vWF

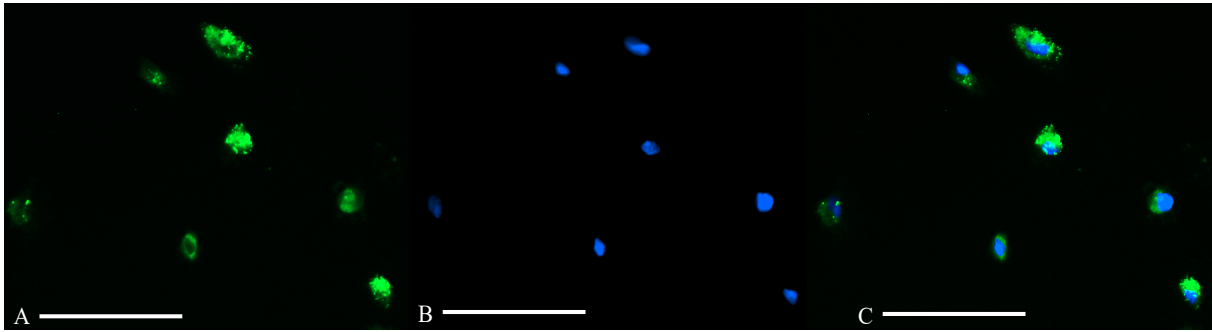


Figure 12: In this image, the immunofluorescence staining of vWF is shown in green in picture B and C. The Hoechst staining of the nucleus in blue is depicted in A. C is an overlay of Hoechst and the immunofluorescence. The white marker indicates 100µm.

Figure 12 shows an immunofluorescence staining of vWF. In A the green immunofluorescence indicates the presence of the von Willebrand factor, in B the blue nucleus of the HUVECs cells in the Hoechst staining. Panel C shows an overlay of the two pictures, combining both staining. Its presence is an indicator for an endothelial phenotype of the cells in question (86).

4.2. Collagen Cell Carrier Membranes (CCC)

Four reoccurring treatment groups were used in the experiments with the Collagen Cell Carrier, as seen in table 2. First, CCC, which is the plain Collagen Cell Carrier, second BSP, which is the CCC coated with BSP as described in 3.5.2. Method 1 and “BSP coat.”, which is the CCC coated using method number 2 and finally a positive control which consist in the same amount and kind of cell seeded onto a regular tissue plate to ensure normal growth.

The Collagen Cell Carrier needs to attach onto the bottom of a well in a 24-well plate, ideally an ultra-low attachment plate to test whether cells can adhere to this material and remain viable. In the following, the complications, and challenges of working with this material were examined.

Different Treatments of The Collagen Cell Carrier

Treatment Groups	CCC-Plain	CCC-BSP	CCC-BSP coat.	Positive Control
Treatment	No Addition of BSP	Coating Method 1: CCC was soaked with BSP for 30min, before the drying process overnight.	Coating Method 2: CCC was coated with BSP for 1 hour, prior to seeding.	No CCC, only cells on the well-plate

Table 4: List of Treatment Groups explaining the Treatment set-up.

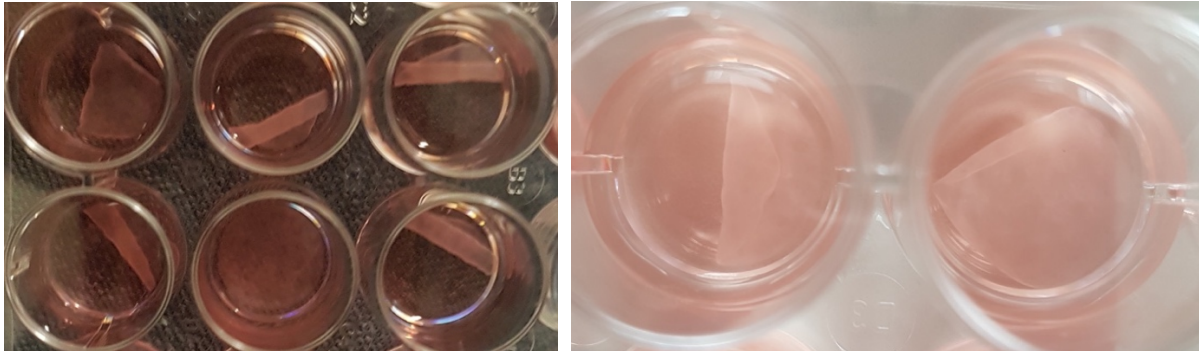


Figure 13: These images indicate the problems during the set-up of the CCC. The membranes would start to curl away from the tissue plate. On these membranes, no measurements were possible due to the curled-up structure of the membrane.

The Collagen Cell Carriers (CCCs) were treated according to the manufacturer's protocol. However, the attachment of the membranes to the well bottom did not occur in a consistent manner. The membrane detached and curled away from the flat bottom of a 24 well plate. Some membranes rolled up already within the first two days after seeding, others started to curl up within the first week. Initially, an attempt to attach the membranes in an ultra-low attachment plate was made. This was to make sure all cells, which were viable and were measured, were only those attached to the CCC and did not settle anywhere around the membrane. This was not possible as nearly all the membranes did not attach properly and rolled up as depicted in Figure 13. All the experiments were therefore performed in cell culture plates, leaving a small margin of livable tissue plate between the CCC and the edge of the 24 well, for cells to also attach. All membranes which were rolled up completely or where the edges were curled in a way that less than $\frac{3}{4}$ of the original area was shown, were discarded and not taken into account. This problem did not occur with the CCCs in the 6 well plate.

4.3. Cell Carrier Viability

To quantify if the Collagen Cell Carriers offer a suitable environment for bone formation and cell growth, and if BSP has an impact on this, the viability of four cell lines was measured using the alamarBlue® kit.

4.3.1.1. HOB

Viability Assay using alamarBlue® with Human Osteoblasts

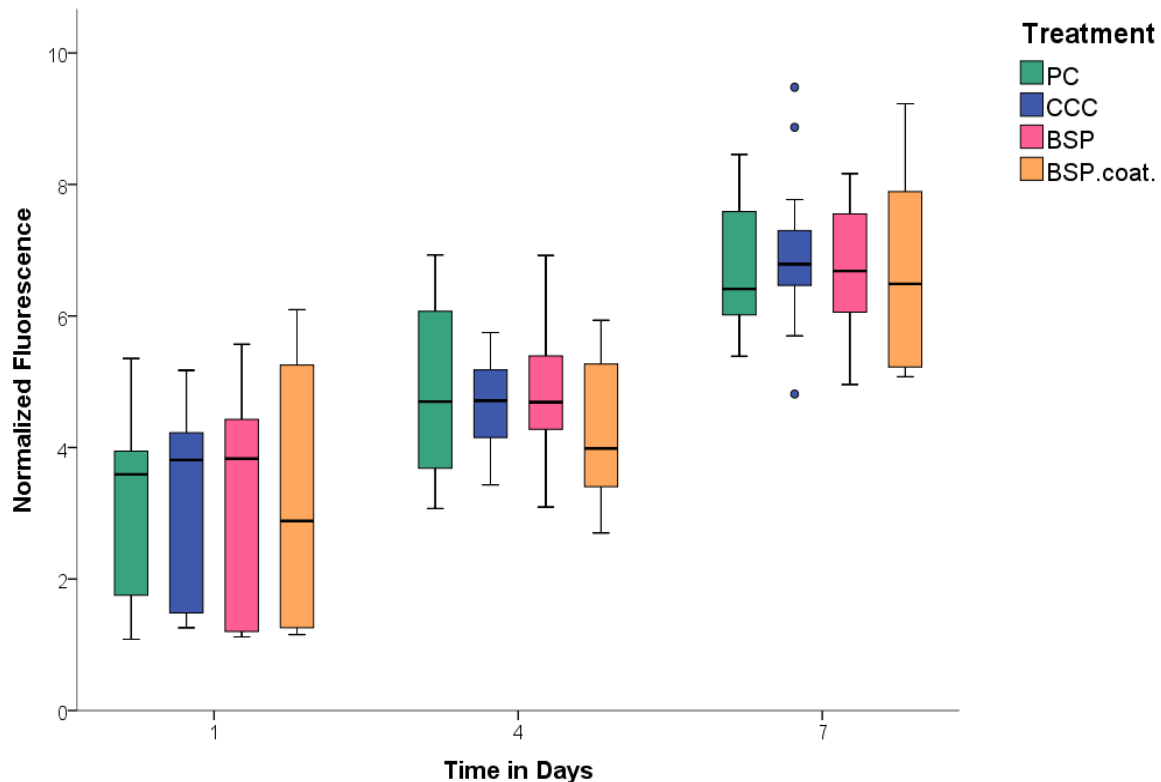


Figure 14: Testing the viability of human osteoblasts using alamarBlue®. Results are expressed as median and quartiles. Human osteoblasts were seeded onto Collagen Cell Carriers. The graph shows the results of four different treatments: a positive control, where human osteoblasts were seeded onto a regular tissue plate (PC, n=24), the Collagen Cell Carrier alone (CCC, n=21), the Collagen Cell Carrier coated with BSP, using method 1 (BSP, n=24), Collagen Cell Carrier coated with BSP using method 2 (BSP coat., n=18). The boxplot represents the fluorescence measurements taken on days 1, 4 and 7 which have been normalized over the negative control (only medium) of each day. A significant difference between two variables is marked with an \blacklozenge and a bracket connecting the two variables. (\blacklozenge $p < 0.008$). The scaling factor on the y-axis is 10000.

Fig. 14 shows the viability of human osteoblasts on the Collagen Cell Carriers over a period of seven days can be observed. Four different treatment groups are represented in the graph above: a positive control, where cells are seeded onto a plain tissue plate. The treatment CCC, which are cells seeded onto a plain Collagen Cell Carrier, BSP, which refers to the CCC coated with method 1 and BSP coat., which refers to coating method 2. The fluorescence measured using alamarBlue® kit directly indicates the viability of the cells, as only viable cells are able to turn the alamarBlue® dye into a fluorescent marker. Over the course of seven days, the fluorescence and therefore the viability of the different groups increased continually, indicating continuous cell growth. The data were normalized by subtracting the average fluorescence of only the medium from each data point of each day, respectively. The number of replicates (n) varies due to difficulties described in 4.2. The comparison of the data on day 1 did not account for any significant differences in all variables measured. At day 4 the data revealed a compelling

difference in the average of the treatment groups BSP against BSP-coat. ($p= 0.03$). This difference accounts for a mean difference of 6826.02 this can also be expressed in percentage as the cells with the treatment BSP have a 22% higher viability than these with the treatment BSP coat. on day 4 of the experiment. However, at day 7 there was no statistically significant difference between the different groups. Nevertheless, the medians of all the groups CCC, BSP and BSP coat is higher than the positive control, with CCC having the highest overall median. Overall, the data suggest that there might be a growth benefit for human osteoblasts when placed on the Collagen Cell Carrier, but the impact of BSP on the growth has to be further analyzed.

4.3.1.2. MG-63

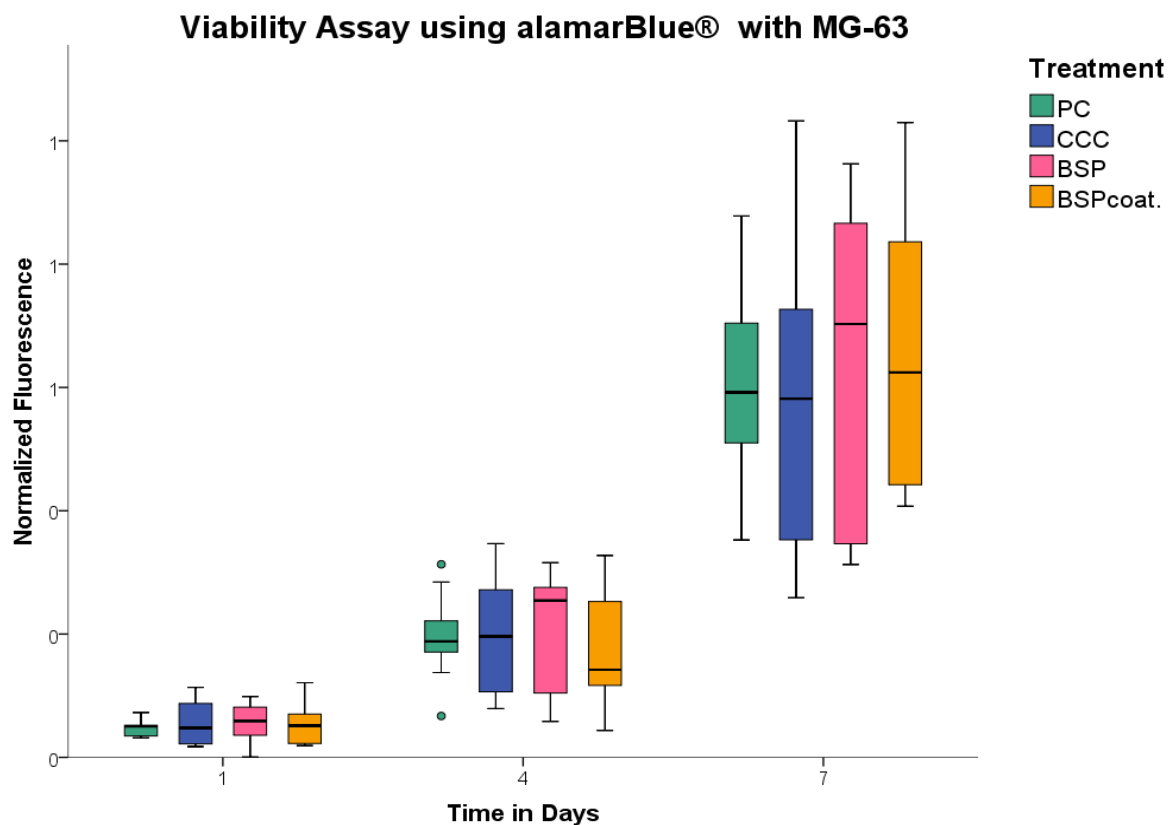


Figure 15: MG-63 viability assay using alamarBlue® over a seven-day period. Results are expressed as median and quartiles. MG-63 cells were seeded onto Collagen Cell Carriers. The graph describes four different treatments: a positive control, where MG-63 were seeded onto a regular tissue plate (PC, n=18), the plain Collagen Cell Carrier (CCC, n=18), the Collagen Cell Carrier coated with BSP coating, method 1 (BSP, n=15), Collagen Cell Carrier coated with BSP using method 2 (BSP coat., n=18). The boxplot represents the fluorescence measurements taken on day 1, 4 and 7 which have been normalized according to the negative control (only medium) of each day. If a significant difference between two variables was detected it is marked with a \blacklozenge and a bracket connecting the two variables (\blacklozenge $p<0.008$). Scaling factor on the Y-axis is 100000.

The graph in Fig. 15 depicts the viability trend of MG-63 cells in different treatment groups over a seven-day period. Overall, the fluorescence increased over the entire time period, indicating growth in every treatment group. According to the fluorescence intensity, the viability of the cells under each treatment advanced at each day of the measurement. On day one, the fluorescence was very similar to each group in question and no differences could be detected. Even though overall all measurements are higher on day 4, and the treatment with BSP appeared to correlate with a higher average and median growth (Fig. 15), no significant differences were measured. Expressed in percentage, the average fluorescence of the treatment BSP indicated a 16% higher viability than the positive control, which was also 10% higher than the CCC. Measurements that were taken on day 7 also did not show any significant differences when treatments were compared, even though the median of BSP seemed higher than the median in all the other groups of that day, but due to the behaviour of the data points, the difference was not significant. It is thus possible that MG-63 cells tend to grow better when seeded onto the CCC treated with BSP than on the CCC alone, but additional tests will have to be done to ensure that this tendency is statistically significant.

4.3.1.3. SaOS-2

Due to the small sample size the analysis of this graph will be qualitative only, since no statistical analysis can be performed.

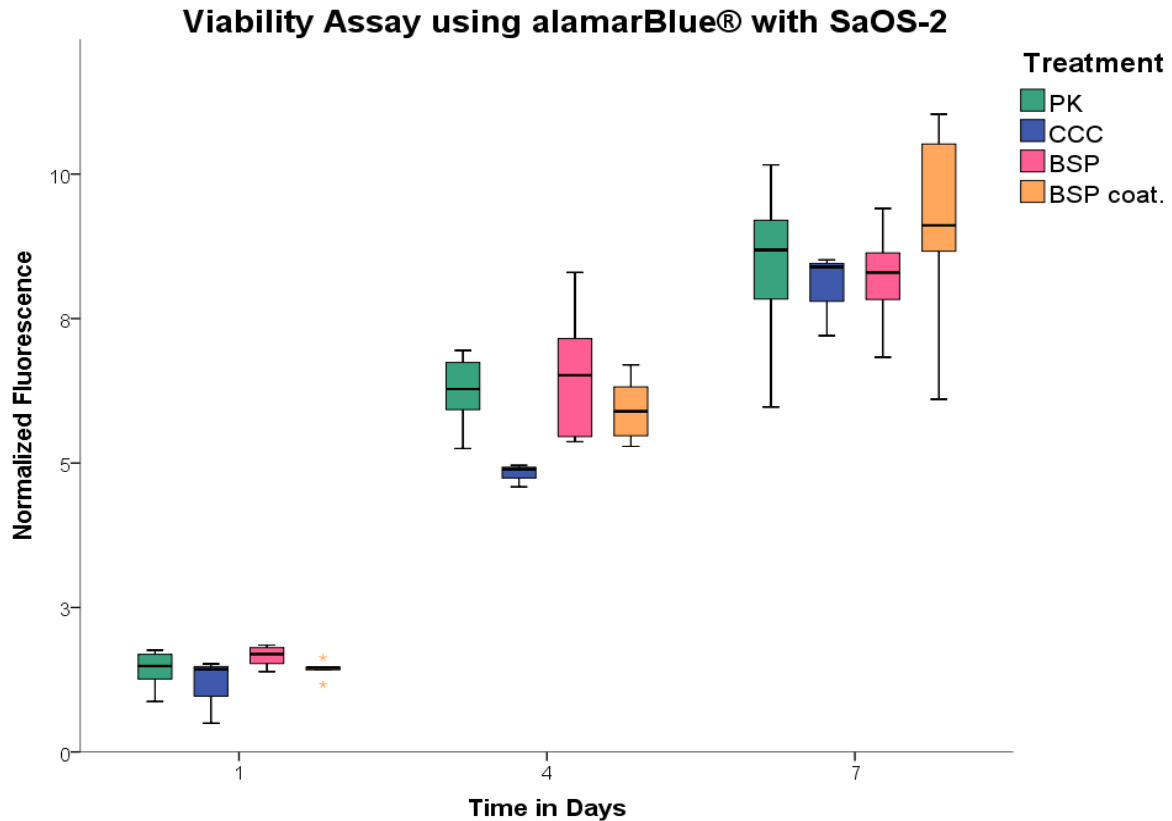


Figure 16: SaOS-2 viability assay using alamarBlue® over a seven-day period. Results are expressed as median and quartiles. SaOS-2 were seeded onto Collagen Cell Carriers. The graph describes four different treatments: a positive control (PC, n=9), the Collagen Cell Carrier (CCC, n=3), the Collagen Cell Carrier coated with BSP method 1 (BSP, n=6), Collagen Cell Carrier coated with BSP using method 2 (BSP coat., n=6). The boxplot represents the fluorescence measurements taken on day 1, 4 and 7 which have been normalized according to the negative control (only medium) of each day. Scaling factor on the Y-axis is 10000.

Fig.16 shows the viability of cells in the four different treatment groups (positive control, the CCC plain, BSP coating method 1 and BSP coat., which refers to coating method 2) over a period of seven days. There is an overall upward trend describing an increase in the fluorescence over the entire period of time, indicating an increase in viability in all treatment groups over this time. Whereas on day one the measurements were similarly leveled, on day four, the treatment group CCC lagged behind by a large gap. The fluorescence representing the viability of the positive control was 67% higher than the fluorescence of the CCC, on day four. The treatment BSP with its range of the data samples seemed to have the highest viability overall on that day. The gap between the CCC treatment and the other treatments disappeared by day seven, resulting in similar averages, except for BSP coat., which was clearly ahead of all the other treatment groups. Although this could indicate that BSP coat. is beneficial for SaOS-2 cells, a statistical significance is not yet reached, and more data will have to be collected to make a firm conclusion.

4.3.1.4. HUVECs

HUVECs are primary cells and therefore do not behave as uniformly as tumor cell lines and may also be more heterogeneous. To increase the validity of the data, the experiment with HUVECs was repeated twice with 4 membranes per treatment and repetition (n=24). Due to the complications described under 4.2, which consisted of CCC not attaching properly, some data points had to be removed. Additionally, the behaviour of the cells was different in experiment 1 compared to experiment 2. Hence, the results of both experiments had to be analysed in separate graphs to properly represent the data sets. This led to a lower number of data points, which is why these two graphs can only be evaluated in a qualitative manner, since any quantitative analysis could be misleading due to a low sample size.

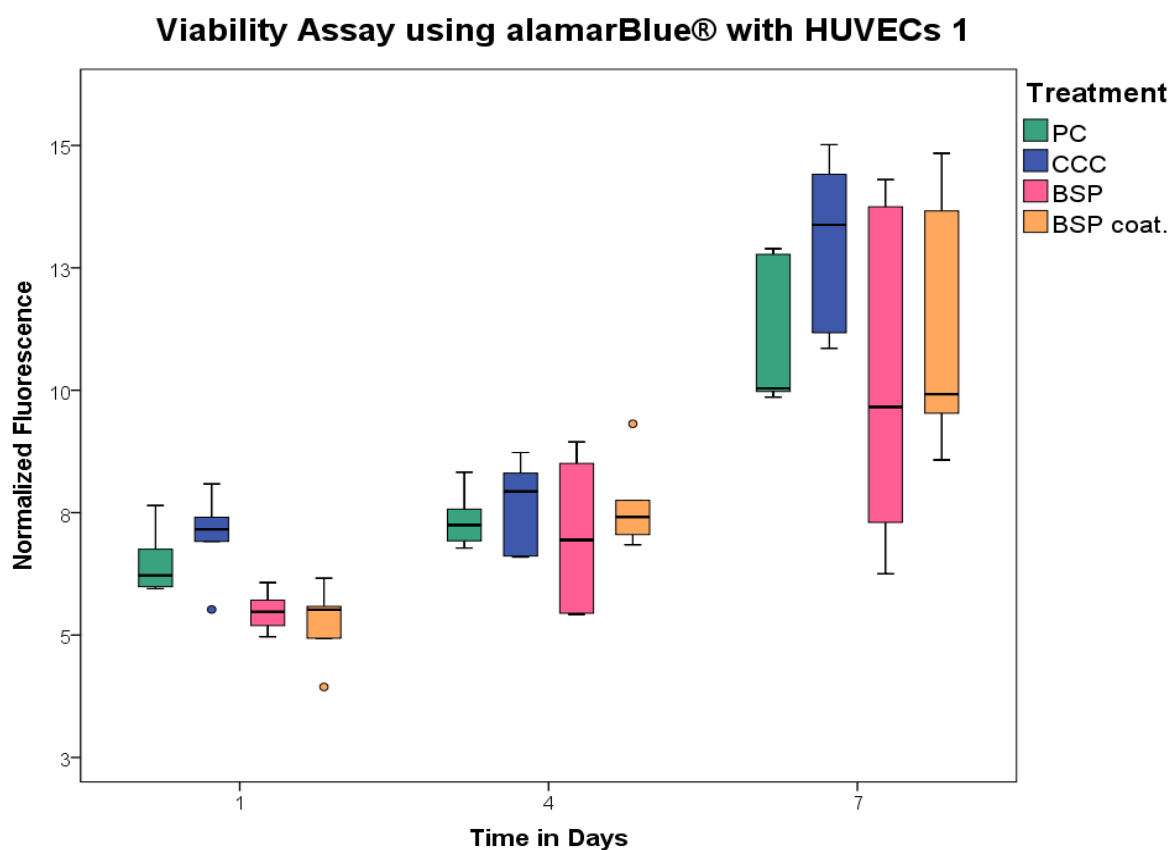


Figure 17: HUVEC viability assay number 1 using alamarBlue® over a seven-day period. Results are expressed as median and quartiles. HUVECs were seeded onto Collagen Cell Carriers. The graph describes four different Treatments: a positive control (PC, n=6), the Collagen Cell Carrier plain (CCC, n=6), the Collagen Cell Carrier coated with BSP method 1 (BSP, n=6), Collagen Cell Carrier coated with BSP using method 2 (BSP coat., n=6). The boxplot represents the fluorescence measurements taken on day 1,4 and 7, which have been normalized according to the negative control (only medium) of each day. Scaling factor on the Y-axis is 10000.

A 7-day viability assay was conducted on the Collagen Cell Carrier and an overall upward trend was observed, which indicated consistent growth over the entire time period. The median of the

treatment with plain CCC, is highest on every day of which measurements were taken compared to the other treatment groups (Fig.17). The treatments with BSP had a lower overall viability on day one but caught up and displayed a similar median fluorescence than the positive control. Overall, these two groups, BSP and BSP coat. have a higher variability in the samples than the positive control and the CCC, which makes it difficult to observe a definitive trend. The data point however to the possibility that a treatment of the cells with plain CCC is more beneficial compared to the positive controls and the BSP treated protocols.

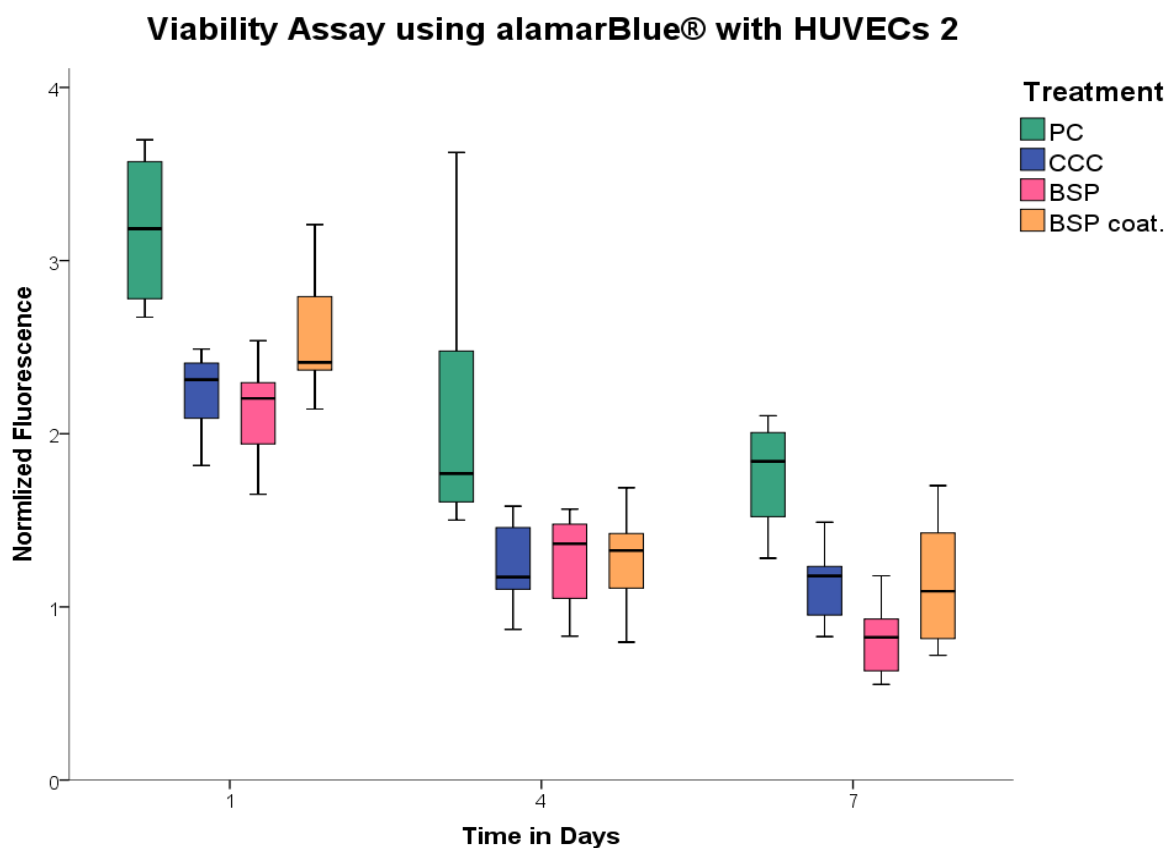


Figure 18: HUVEC viability assay number 1 using alamarBlue® over a seven-day period. Results are expressed as median and quartiles. HUVECs were seeded onto Collagen Cell Carriers. The graph describes four different Treatments: a positive control, where HUVECs were seeded onto a tissue plate (PC, n=9), the Collagen Cell Carrier plain (CCC, n=9), the Collagen Cell Carrier coated with BSP method 1 (BSP, n=9), Collagen Cell Carrier coated with BSP using method 2 (BSP coat., n=9). The boxplot represents the fluorescence measurements taken on day 1, 4 and 7 which have been normalized according to the negative control (only medium) of each day. Scaling factor on the Y-axis is 10000.

The experiment with the second isolate of HUVECs showed a downward trend in viability, including the positive control (Fig.18), suggesting that even under normal conditions this isolate of HUVECs cells did not thrive and grow and therefore the viability decreased. There are still viable cells since the measurements of only the medium has been subtracted and the fluorescence is still clearly higher than zero (Fig.18). Nevertheless, these cells had trouble attaching and growing even when no new biomaterial or BSP coating was used. Noticeably in

the positive control where cells seeded onto a plain tissue plate, had the most fluorescence on each measurement day. The average viability on day 4 from the positive control was around 20% higher compared to all other treatment groups. On day 7 this advantage was still at 20%, even 30% when compared to the treatment of BSP, when comparing the median fluorescence.

4.3.2. CCC Gene Expression

In the following section, the results of the impact of BSP on the CCC on gene expression in SaOS-2 cells are presented. The cells were seeded onto CCC in various treatments and after four days the cells were detached and analyzed via a qPCR. The control was the CCC without BSP.

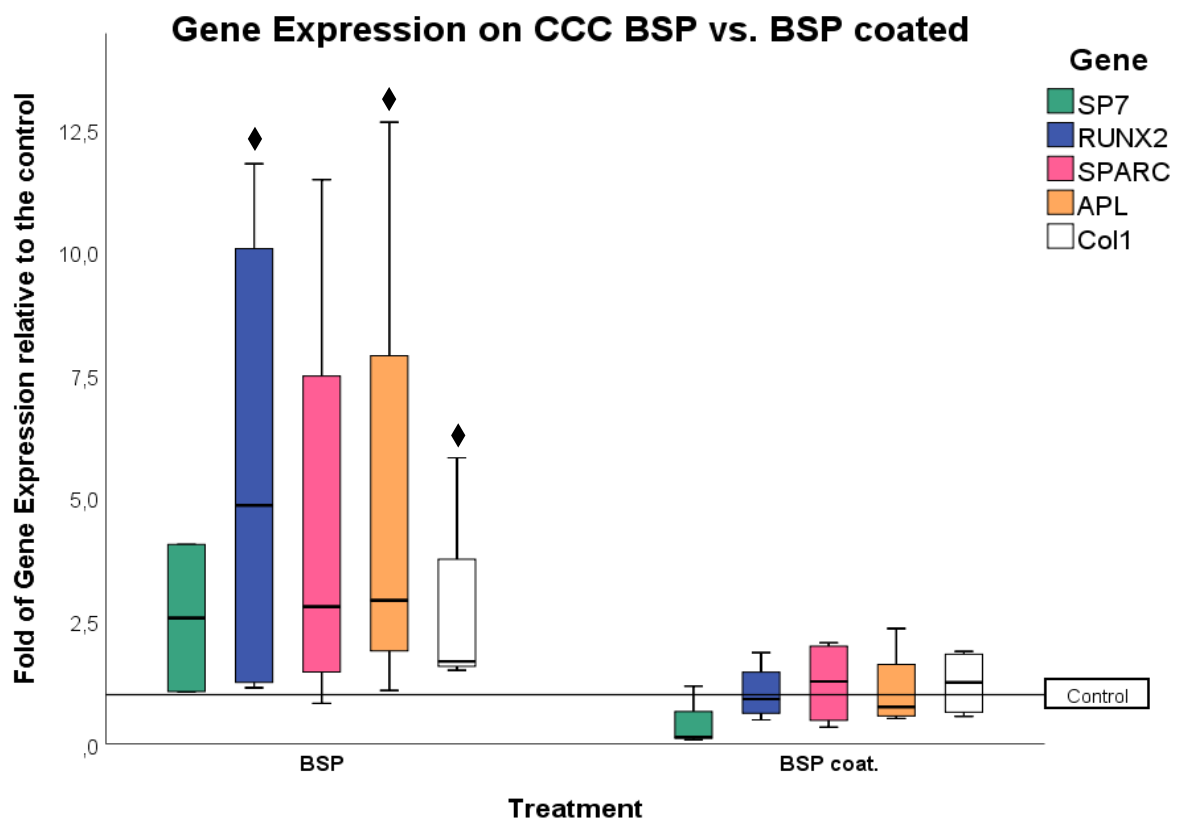


Figure 19: SaOS-2 cells seeded onto CCCs to analyze the effect of BSP on the gene fold increase of SP7, RUNX2, SPARC, ALP and Collagen1 over the control. The control is untreated cells on an untreated CCC. The graph shows gene expressions of all the genes as mentioned above in two different environments, depicted on the X-axis: the gene expression of the cells on a CCC treated with BSP, coating method1 (BSP, n=4) and the gene expression of the cells on a CCC treated with BSP coating method 2 (BSP coat, n=4). The control is SaOS-2 cells seeded onto plain CCCs (without BSP), for which the level of gene expression was set to 1. Results are shown with medians and quartiles. If a significant difference between the expressing gene and the control was detected it is marked with a \blacklozenge (\blacklozenge p<0.05).

150.000 SaOS-2 cells were seeded onto the CCCs with the indicated BSP treatment. After four days, quantitative real-time PCR was performed to evaluate the effect of BSP on these cells

while they were in contact with the CCC. For evaluation, the expression rates were compared to untreated CCCs as the control, CCCs coated in BSP using method number 1 (BSP) and CCCs coated with BSP with method number 2 (BSP coat.). The gene expression levels of *SP7*, *RUNX2*, *SPARC*, *ALP*, *OPN* and *Collagen1* were analyzed. *OPN* is not shown in the graph above as in all experiments, expression levels were not readily detected. None of the genes tested showed a significantly altered expression level under the conditions of BSP coat (method 2) versus plain CCC. *SP7* mRNA expression was not significantly increased in either treatment or in comparison to the control. *ALP* showed a significant increase in comparison to BSP coat. and to the control (CCC) (Median of BSP ALP 2.92-fold expression). *RUNX2* had a significantly higher expression level compared to BSP coat. and CCC as well with a median of 4.85-fold. The expression of *Collagen 1* was also significantly higher with a median of 1.68-fold. Due to its variability *SPARC* did not show a significant difference in expression compared to the control even though the median expression was at 2.80-fold. These findings suggest that the treatment of BSP does create a significant difference in the expression levels of *RUNX2*, *ALP* and *Collagen 1* in SaOS-2 cells.

4.4. Easy Graft

The material called “Easy Graft”, which was used in the performed experiments, is advertised to harden within minutes, once in contact with bodily fluids. Figure 20 shows the set-up of a 3D mold with Easy Graft in combination with the BioLinker® in a pliable mass. This set up was then left to harden inside the medium over several days. The scaffold did not completely harden inside the plastic mold after 1, 2 or 7 days and the scaffold was still unstable, leaving the removal difficult during which most scaffolds fell apart. In this set up only two of the available three sides of the cylinder were in contact with medium, the top and the bottom. Whereas the mold shielded all of the circumference of the scaffold, the BioLinker® was not successfully washed out of the scaffold even after an extended period of time. None of the resulting scaffolds were uniform in size, they were brittle or fell apart completely.

Thus, a new procedure had to be created to form uniform scaffolds, comparable in size and form, as is described in the methods section under 3.5.3. Here, the BioLinker® was washed out before the biomaterial was cut to the desired size. The material did harden within minutes when the BioLinker® was forcefully washed out of the material and was surrounded by a similar fluid to those found in the human body. Any mold or guide which reduces the contact area created a hindrance in this process.



Figure 20: Left: Scaffold in PLA mold surrounded by medium. Right: scaffolds taken out of the PLA mold. Most scaffolds are completely broken or considerably damaged.

4.4.1. BSP coating and release experiment

To investigate the effect the coating of BSP has on Easy Graft, measurements were set up to test whether and how long the protein could adhere to the granules of the material. To measure attachment, BSP linked to the fluorescent dye the Fluorescein labeling kit from Lightning Link was used.

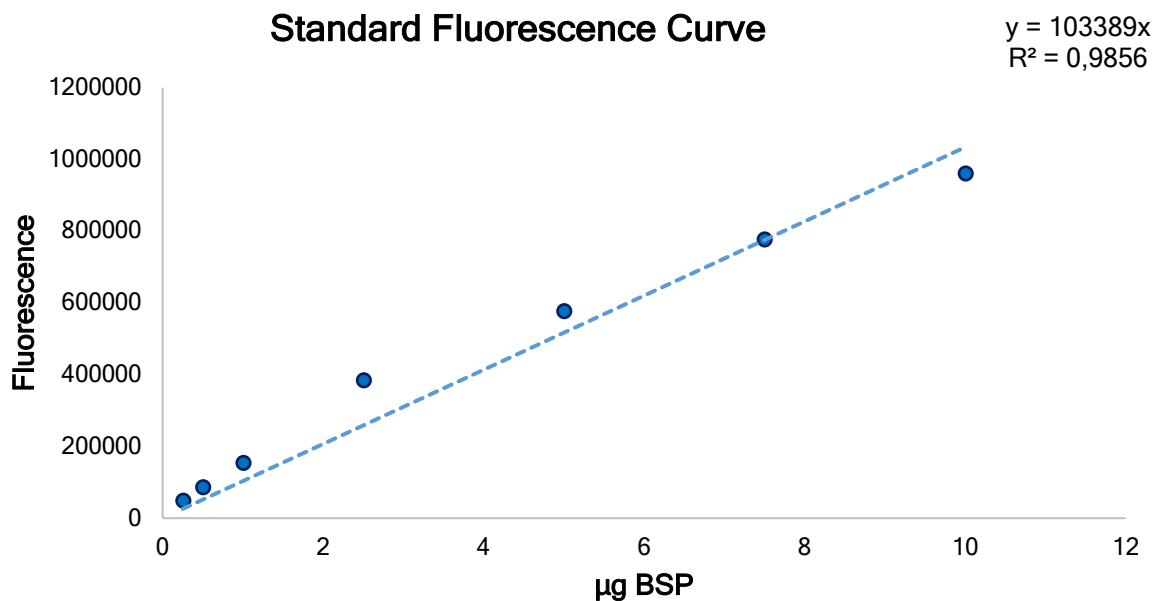


Figure 21: Standard fluorescence curve using Fluorescein-linked BSP. The graph depicts the amount of BSP in μg in correspondence to the fluorescence it generates. A linear regression was computed with the corresponding equation shown in the upper right corner as well as R^2 .

The measurements of the Fluorescein-linked BSP were portrayed in a scattered diagram into which a linear regression line was placed. This resulted in the regression formula: $y = 103389x$ with the coefficient of determination of 0.9856 (R^2). Through this curve the amount of fluorescence which was measured can be matched to the amount of BSP present in the sample.

Making it possible to backtrack the amount of BSP which is present through the measurement of fluorescence.

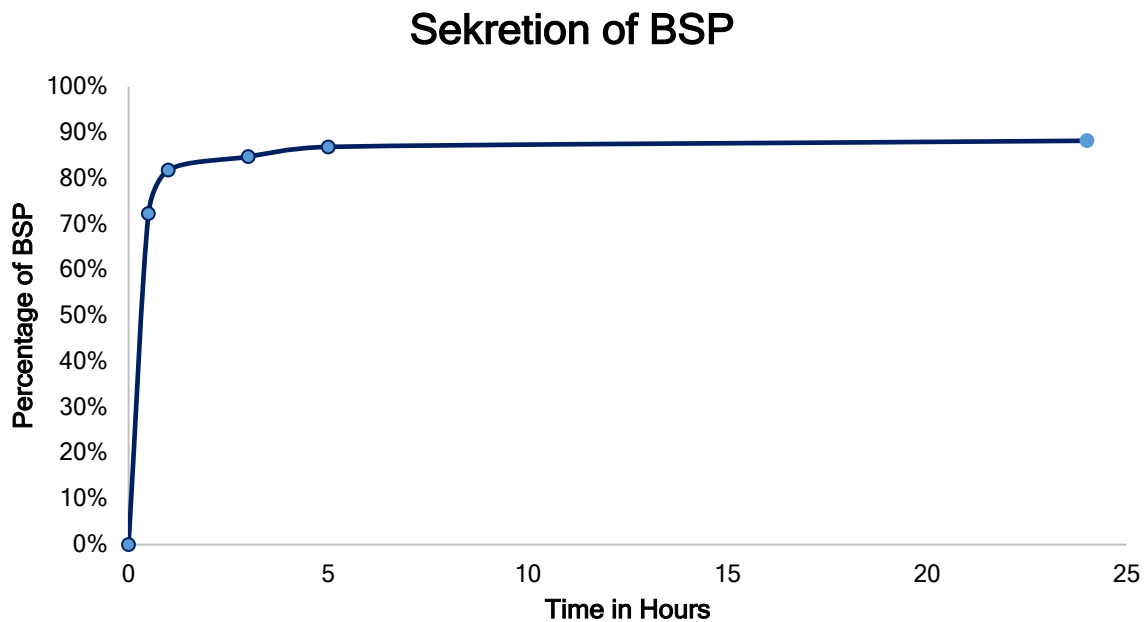


Figure 22: A scaffold of Easy Graft was coated with BSP. The amount of BSP released from the scaffold into its surrounding medium was measured via the fluorescence measured inside the medium for 24 hours. The amount of BSP found in the medium and therefore secreted from the scaffold is expressed in percentage.

The graph above describes the rate at which BSP was released from the scaffold into its surrounding medium. Therefore, at 0h, at the beginning, 0 percent which represented 5 μ g BSP was still inside the scaffold, and none had secreted outside of the scaffold. After 30 minutes, the medium taken of the scaffold contained a fluorescence of 373841.3. This represented 3.6 μ g BSP which was around 72.32 % of the BSP and indicated that already more than half of the BSP protein which was coated onto the scaffold was released into the surrounding medium after 30 minutes. The next measurement was taken at 1h and resulted in 0.48 μ g or 9.6% of BSP. After 3h and 5h the measurements resulted in 2.9% and 2.2% respectively. After 24h a combined protein amount of 4.4 μ g was released into the surrounding medium. This indicated that 0.59 μ g of BSP was still inside or attached to the scaffold after 24hours. Therefore, it can be concluded that after 24 hours around 11.8% of BSP was still inside or attached to the scaffold.

4.4.2. AlamarBlue® Viability Easy Graft

To test the viability of osteosarcoma cells on the biomaterial Easy Graft, five treatment groups were created: a positive control where SaOS-2 cells were seeded onto a regular tissue plate

(PC), one treatment group where the SaOS-2 cells were seeded onto an Easy Graft scaffold in an ultra-low attachment plate to make sure all viable cells are on the scaffold (EG) and one group with a scaffold which had been coated in BSP (BSP). To validate the data points another treatment group (cells only) was created, comparing the behavior on cells without a scaffold on the ultra-low attachment plate. The viability on the biomaterial was investigated as well as the behavior of BSP in interaction with Easy Graft.

4.4.2.1. Visualization

The images depicted in Figure 23 were taken from the residue medium and cells after the seeding onto Easy Graft had taken place. This was done to see how many cells had attached to Easy Graft material after 24 hours and whether the remaining cells were still viable and could potentially reattach and grow on regular tissue plates. To do this, the residue, the cells and the medium were reseeded onto a regular tissue plate after 24 hours. After an additional 24 hours, the images below were taken:

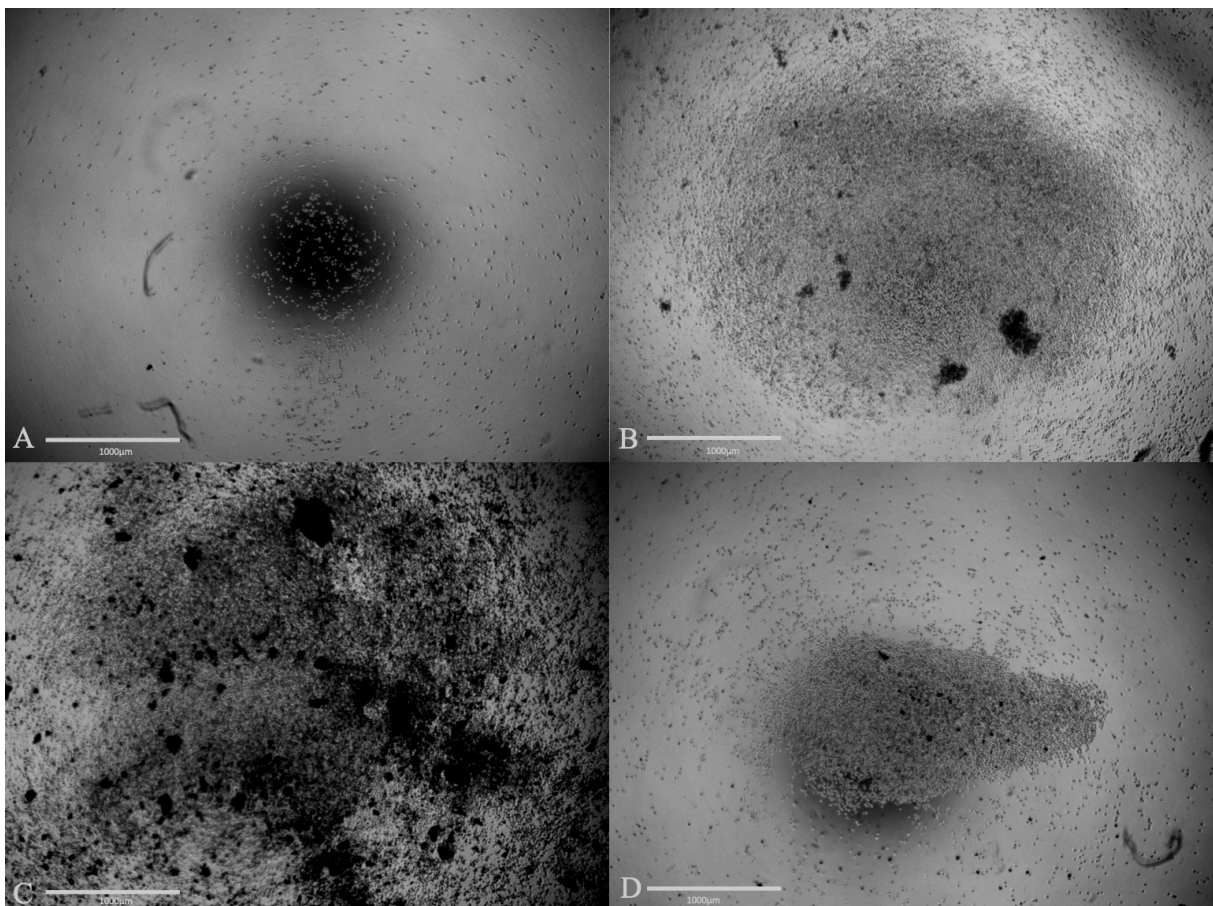


Figure 23: : Attachment of cells to Easy Graft. A) Residue of the PC: medium and cells 24hours after seeding onto a 96-well tissue plate. B) Residue of medium and cells 24hours after seeding onto an ultra-low attachment plate without a scaffold. C) Residue of medium and cells 24hours after seeding onto a scaffold with BSP, D) Residue of medium and cells 24hours after seeding onto a scaffold without BSP. The white scale bar indicates 1000µm.

Figure 23 shows images of medium and the containing cells, which did not attach to the easy graft scaffold after 24 hours. That medium, cell and debris mixture was transferred onto a 46-well plate and left with new medium for 24hours to see if any cells would reattach. In Fig. 23. A) there are very few cells and no debris visible. It can be assumed that none of these cells were vital as none of them had attached to the well bottom. This is demonstrated by the roundness of the cells. If attachment had taken place, the cells would appear polygonal and stretched out. Overall, very few cells are visible suggesting that most of the cells had attached in the initial seeding on the tissue plate. This was expected since picture A) is of the positive control where cells were seeded onto a plate with the ideal environment for attachment and growth. In panel B, the cells which were taken out of the 96-well ultra-low attachment plate are depicted. Here again, no viable cells which had attached are visible, but a much larger number of cells was present than in the experiment depicted in Fig.23A. This was expected, since cells are not able to attach to an ultra-low attachment plate, therefore serving as a negative control for attachment. Panels C and D in Fig.23 shows pictures of medium which had been taken from a 96-well ultra-low attachment plate with a scaffold. C was treated with BSP and D was just a plain scaffold. The image C in Figure 23 shows a high number of cells as well as detritus, which is not found at this level under the conditions depicted in Figure 23B or C. This suggests the treatment with BSP lead to more detritus into the surrounding medium than without BSP. Especially since the condition where the scaffold was untreated showed fewer cells but also fewer detritus which most likely are particles of the Easy Graft scaffold. In pictures B and C, a large number of dead cells were seen without any viable cells, this suggests cells could not attach well to the scaffold, therefore falling back into the surrounding medium. The most cells are seen in picture B, which could indicate that even though cells did not attach well to the Easy Graft scaffold, they did attach at some rate, since the negative control shows more cells overall. This points to a possible interaction between the cells and the Easy Graft material when it is previously treated with BSP.

Viability Assay using AlamarBlue on Easy Graft

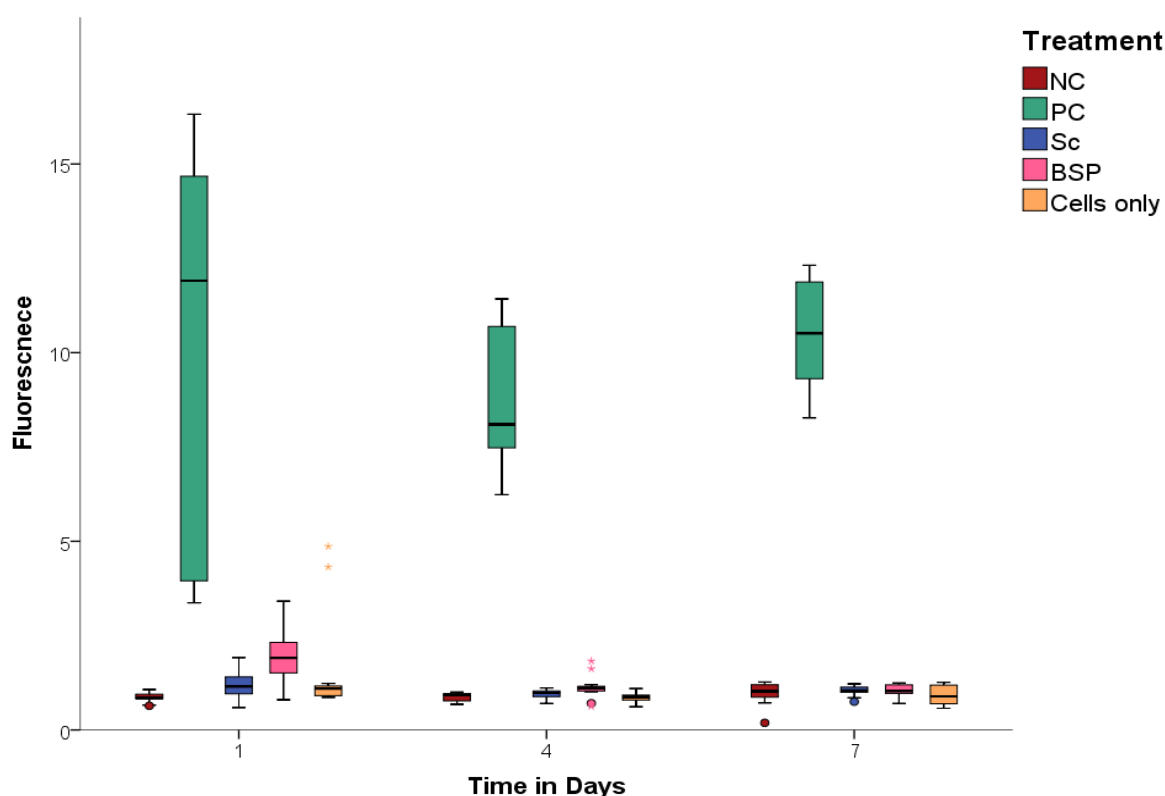


Figure 24: SaOS-2 viability assay using alamarBlue® over a seven-day period. Results are expressed as median and quartiles. SaOS-2 were seeded onto scaffolds of Easy Graft. The graph depicts five treatment groups: a positive control (PC, n=14), the Easy Graft scaffold (Sc, n=14), the Easy Graft scaffold coated with BSP (BSP, n=14), cells on the ultra-low attachment plate (Cells only n=14) and a negative control which is only medium (NK=14). The boxplot represents the fluorescence measurements taken on day 1, 4 and 7. A significant difference between two variables is not marked with a ♦ to ensure easy visualization (♦ p<0.008). Scaling factor on the Y-axis is 10000.

Next, the viability of SaOS-2 cells on Easy Graft using the alamarBlue® method was tested. Here, the positive control showed a large viability in data points on day 1. Generally, an upward trend from day 4 to day 7 was observed for the condition of the positive control, indicating an increase in cell viability. However, all other treatments resulted in viability data around the area of the negative control which was the fluorescence of the medium only. The data points could not be normalized with the medium as many treatments were so similar to the fluorescence of the negative control, that their data points would not have been visible on the graph. The difference between the positive control and all the treatment groups of each day were significant (p<0.008). They were not marked to ensure a concise visualization of the graph. For an easier depiction of the data, a graph without the positive control is shown in 4.4.1.3. These findings indicated Easy Graft on its own does not provide an environment suitable for the SaOS-2 cells to thrive on.

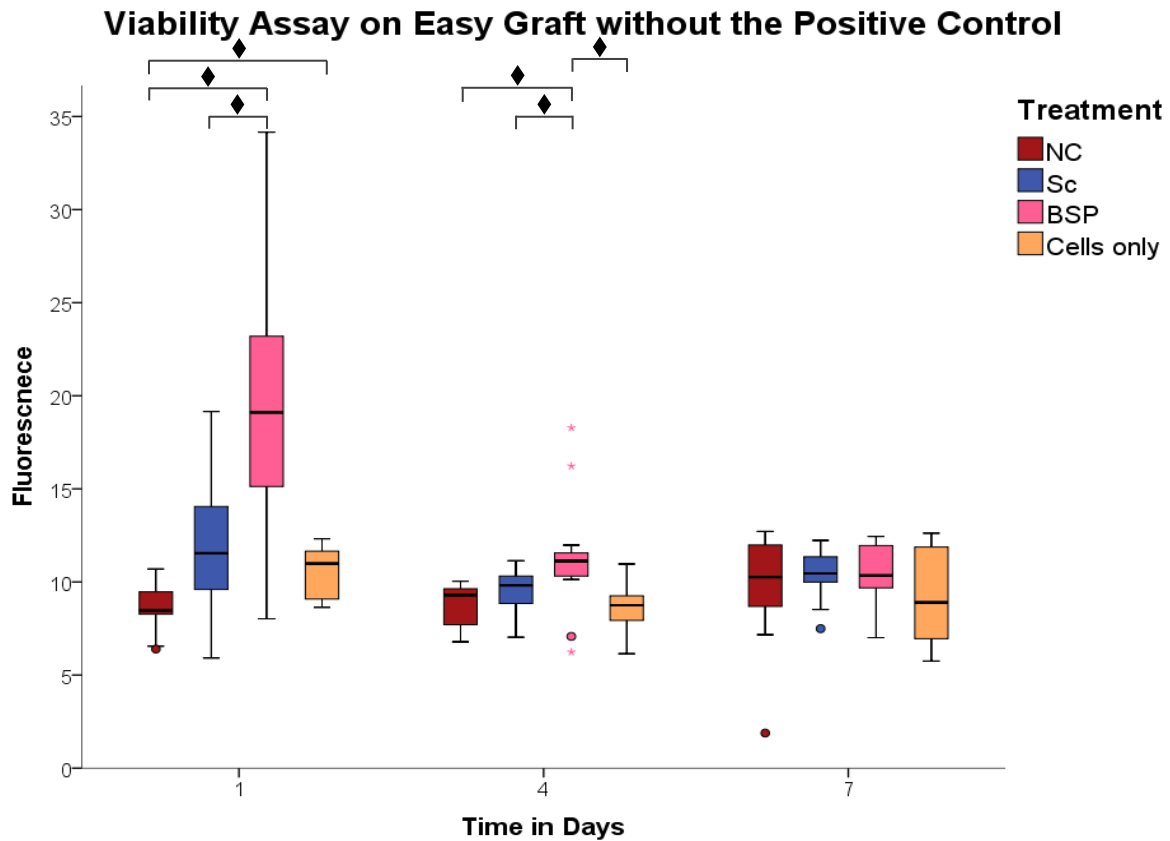


Figure 25: SaOS-2 viability assay using alamarBlue® over a seven-day period without the data obtained with the positive control. Results are expressed as median and quartiles. SaOS-2 were seeded onto scaffolds of Easy Graft. The graph depicts four treatment groups: The Easy Graft scaffold (Sc, n=14), the Easy Graft scaffold coated with BSP (BSP, n=14), cells on the ultra-low attachment plate (Cells only n=12) and a negative control which is only medium (NK=14). The boxplot represents the fluorescence measurements taken on day 1,4 and 7. A significant difference between two variables is marked with a ◆ (◆ p<0.008). Scaling factor on the Y-axis is 1000.

Since the signal obtained from the treatment group, positive control, were much higher than any other treatment group a separate graph was created to perform a better analysis of the remaining groups. The graph in Fig. 25 shows the four conditions Easy Graft as a scaffold with and without BSP, an ultra-low attachment plate seeded with cells, as well as a negative control, which includes only medium and no viable cells. Overall, there was no increase of the fluorescence over the seven days period of the assay suggesting that this assay with Easy Graft is not compatible with improved cell viability. This conclusion is justified by the fact that on day 7, no significant differences between the measurements were detectable. This includes the negative control, which is only medium. However, on day 1, the scaffold with BSP showed a significantly higher fluorescence when compared to the plain scaffold. On this day there were also significant differences between the negative control and the groups BSP and the negative control and Cells only. On day 4, the difference between the scaffold with BSP and the treatment group with the plain scaffold is still significant. The treatment group with BSP also

showed a significantly higher fluorescence than the negative control and the group only cells on day four. However, on day 7 no more significant differences in viability within the groups were detectable. This suggests that in a short term, BSP coated Easy Graft provides superior conditions for cell growth than the Easy Graft scaffold alone, but that this effect cannot be maintained over longer periods of time.

These findings indicated that cells were more viable when adjoined with Easy Graft with BSP coating than without BSP, suggesting that BSP coating could be beneficial for cells in a clinical setting.

4.4.3. Easy Graft Cytotoxicity

In the following experiment the level of LDH was measured using the LDH-Glo kit, which provides a luminescence readout directly correlating with the level of LDH (lactate dehydrogenase) released from a dead cell. LDH release is a measure for cytotoxicity, because it is only released from a cell once it is damaged. LDH catalyzes the oxidation of lactate by reducing NAD^+ to NADH, which is used to generate a bioluminescence signal through a luciferase reaction. The correlation of a high luminescence to a high level of LDH and therefore a high cytotoxicity can be made.

Luminescence of LDH over 3 Days

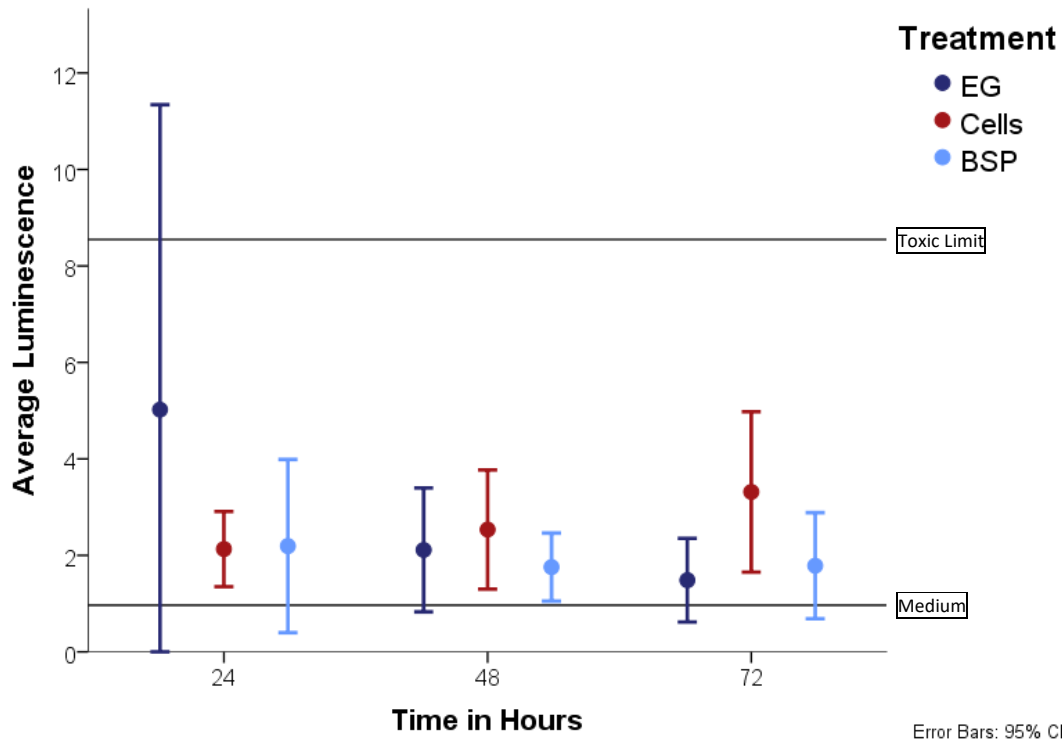


Figure 26: The cytotoxicity of Easy Graft and Easy Graft in combination with BSP was measured over 72 hours. The toxicity limit was measured using SaOS-2 cells seeded on an ultra-low attachment plate (n=6). The positive control (Cells, n=6) are SaOS-2 cells seeded on a tissue plate (drawn in red). The other treatment groups are Easy Graft plain (EG, n=6) and the scaffold coated with BSP (BSP, n=6). The scaling factor of the luminescence was 10^6 .

The graph in Figure 26 depicts the luminescence over 72 hours was measured using the LDH-Glo kit. The cytotoxic threshold marked as the toxic limit, was defined as the amount of luminescence measured when cells were seeded onto an ultra-low attachment plate, which can be defined as a non-viable environment, since cells cannot attach and therefore die within the first 24 hours. Therefore, any material or environment which is less viable for the osteosarcoma cells than the ultra-low attachment plate was considered toxic in this experiment. The lower limit is defined as LDH levels which were found in the medium without any cells. The averages of all measurements were below the toxic limit and above the luminescence of the medium indicating that Easy Graft with or without BSP is not a cytotoxic environment. However, it can be observed that at 24 hours, the standard deviation of the measurements with Easy Graft protruded into the toxicity range. This was not observed with the BSP treatment, which consists also of an Easy Graft scaffold with the addition of BSP. It could therefore be proposed that the addition of BSP leads to a better cell adhesion and better living environment for the cells, leading to lower cell death. The red markers represent the measurements that were taken of a

96-flat well tissue plate, which is the regular growing environment for these cells. The upward trend of this line was expected since the flat bottom of this well is very small and with a starting point of 20.000 cells, the bottom of the well becomes rapidly overcrowded. Overcrowding can lead to stress on the cells and cell death. This could explain the visible rise of luminescence and therefore LDH at hours 48 and 72. This environment, of an untreated tissue plate, is by definition non-toxic even though it had the highest LDH measurements after 72 hours.

In the wells where the SaOS-2 cells were seeded onto the Easy Graft scaffold, this crowding should be eliminated due to the 3D porous structure of the scaffold, which offers a larger surface area for the cells to attach to. After 72 hours, the lowest LDH measurements are of the treatment groups seeded onto a scaffold of Easy Graft with or without BSP, leading to the conclusion that this material is a nontoxic environment for osteosarcoma cells as it does not lead to a high rate of cell death within the first 72 hours.

5. Discussion

The aim of this thesis was to investigate the potential of Collagen Cell Carrier and Easy Graft as new biomaterials in the field of orthopedics in large bone defects and to specifically evaluate the additional effect of the protein BSP on bone and endothelial growth, when coated onto those biomaterials.

5.1. Cell Lines

There are several advantages to using a variety of cell lines. Each of the cell-lines present another important aspect in the modeling of bone growth. Human osteoblasts are an excellent model for human bone, as they are directly derived from a specific donor. Yet due to this they only represent the phenotype of this specific donor. They are limit in their yield and growth and differentiate and change over time and passage number (88). At the same time, they have a high value in analyzing clinical effects, since they are not malignantly transformed or immortalized and therefore represent a more native state than the osteosarcoma cell lines that already have accumulated a number of oncogenic mutations to overcome growth limitations.

HUVECs represent the aspect of vascularization in these experiments, which is directly linked to the success of bone formation. This primary cell line is also more susceptible to contamination, has a slower growth rate and is difficult to cultivate, compared to tumor cell-lines. Yet, it is a vital aspect of bone growth, as bone can only grow with adjacent vascularization (25).

Tumor cell lines such as SaOS-2 and MG-63 are less likely to be contaminated with other cell types; a particular danger when using primary cells directly derived from human tissue that may contain a mixture of cells. They provide a more homogeneous population (74) and are therefore an important model in the study of bone growth. Both of these cell lines behave similar to osteoblasts and are therefore considered osteoblast-like cells, even though they do not reflect the entire range of osteoblastic phenotypes (75, 76, 88).

SaOS-2 represent a more mature osteoblast phenotype, whereas MG-63 represent an immature osteoblast phenotype (89). Even though both cell lines have lots of similarities to primary human osteoblasts, they still offer some limitations such as the expression profile of integrins as well as certain proteins, proliferation kinetics and osteoid production (88, 90). MG-63 seems to have a similar integrin subunits and could be used for models such as adhesions of human osteoblasts, whereas the SaOS-2cells seem to be favorable to study the expression of osteoblast

specific proteins (89). The expression of a number of growth factors, their receptors as well as bone matrix associated proteins are very similar between SaOS-2, MG-63 cells and primary human osteoblasts (91), which confirmed that both MG-63 and SaOS-2 are useful model systems for *in vitro* bone modeling, but this also demonstrates the limitations of osteosarcoma cell lines. Therefore, a variety of cell lines were used in the experiments to evaluate different aspects of bone formation.

5.2. Collagen Cell Carrier – Viability Assay of Bone Cell Lines

The CCC is a membrane of collagen 1 fibrils which could potentially be used in orthopedics to close or cover a defect after it has been filled with a biomaterial such as Easy Graft. During the set-up of the experiments, the main difficulty was the attachment of the membrane to certain surfaces. It was not possible to attach the CCC onto the Ultra Low Attachment Plate (ULAP), even after priming it according to the manufacturer's instructions. Even on flat well tissue-plates, the membrane curled up partially. No data collected on membranes, which rolled up irrespective of the time were included in the analysis of the results. The membrane rolled up at inconsistent times, such as the first hours of application or after the first day. The observation, that the CCC membrane did not attach to the flat bottom of an ULAP can be concluded from the modification of this type of surface, which does not only inhibit cellular attachment, but also minimizes enzyme activation and protein adsorption (92). These unfavorable conditions cause the collagen to roll up and detach. Therefore, the experiment was set up with flat bottom tissue wells, which leave a margin around the membrane for cells to attach and grow as well. Culture well plates are also suggested in the protocol of use by the manufacturer although the interaction between the collagen and the well plate is not further explained.

5.2.1. Viability Assay of Primary Human Osteoblasts (hOBs)

To determine whether and how BSP can improve the viability of human osteoblasts on the CCC membranes, a viability assay with alamarBlue® was conducted. These cells demonstrated an important indicator for the human bone microenvironment *in vitro* in these experiments. What is most notable in the viability assay of the human osteoblasts (hOBs) cells is that at day 4 the “BSP” treatment group is noticeably more advanced in growth than the “BSP coat.” treatment group. Even though this difference has shrunk by day 7 it does indicate the difference these two coating methods have on the viability of hOBs on the CCCs. The method to let the dry CCC soak in a PBS/BSP combination and letting this set for 24 hours shows a

higher impact on the viability of human osteoblasts. This is also reflected by the findings of the gene expression analysis done with SaOS-2 cells. These support the observation, that the treatment group “BSP” has a superior effect on the expression levels of osteogenic markers, versus the treatment group “BSP coat.” It could therefore be proposed, that letting the soaked membrane set overnight bonds BSP in a superior way to the collagen fibrils, leading to a higher impact of the protein on the viability of cells. This is further analysed in paragraph 5.3.3. Overall, primary human osteoblasts seem to benefit from the CCC as a seeding environment with or without BSP. The median viability on day seven of the positive control on the tissue plate is lower than all the other treatment groups which were all seeded onto a CCC. However, this effect is too small to be statistically significant. This could be due to the time frame of seven days, as primary cells proliferate slower than established cell lines that were originally derived from tumor tissue, like SaOS-2 cells (88). It would be interesting if this effect, the superiority of the CCC as a seeding environment, could be replicated and amplified in during an experimental set up longer than seven days or *in vivo*. It shows however that human osteoblasts thrive on collagen. In this context, it is important to note, that data from the calvarial rat model indicated in previous experiments, that collagen alone does not lead to bone induction in the cranium, but requires the addition of BSP to be effective (93).

5.2.2. Viability of Cells from the Bone Osteosarcoma cell line MG-63

Although cells of the human osteoblast like MG-63 cell line are in many ways similar to human osteoblasts, they proliferate much faster, therefore possibly showing effects that cannot be observed with the primary human osteoblasts in the same time frame (88). In this assay no statistically, significant effect was measured in the viability of the different treatment groups, but there are trends which can be observed. The treatment group “BSP” has the highest median of fluorescence as of day four continuing into day seven. Here, the same coating method as in the previous experiment with hOBs seem to show an advantage in the viability of osteosarcoma cells. This illustrates the superiority of the coating method, where BSP is set to bind with the collagen overnight unlike when BSP is added onto the CCC shortly before seeding in method number two (See paragraph 5.3.3.). This indicates, that BSP might be beneficial for growth of MG-63 cells on biomaterial, here CCC membranes, within the first week of cultivating. It has been reported, that the MG-63 cell line is representative for human osteoblasts in the analysis of interaction with collagen 1 (94). This would also fall in line with the data provided by O’Toole et al who have shown that BSP coated implants are osteoinductive in the rat calvarial model (95) as well as Wang et. al who states that collagen1 with BSP but not alone

advances the mineral deposition in the calvarial defect (93). Since these studies were *in vivo* the positive effect of BSP on bone growth in combination with collagen 1, is most likely bigger due to factors which could not be recreated through the set-up of this experiment, such as the inflammatory response, bone regeneration of the rat, mechanical stress on the implant and the variety of growth factors and invasion of cells. These positive indicators for bone viability on this biomaterial *in vitro* are important to enhance the material and its coating, for an ideal set up *in vivo* in later experiments.

5.2.3. Viability Assay of cell line SaOS-2

A positive effect on the growth of SaOS-2 cells seeded on a collagen membrane or 3D collagen matrix was reported already back in 1992 (96). Overall, the SaOS-2 cell line grows evenly and steadily over the course of seven days on CCC, as portrayed in the viability assay. The one treatment group clearly lagging behind in the viability measurements, is the plain CCC, as it produces a much lower fluorescence by day four. It must be noted that this observation could be a consequence of the low repetition (n=3) since this treatment does catch up to the other treatments in the fluorescence measurements by day 7. The overall low repetition was due to the difficulties in the beginning of the set-up of the experiments as the membranes would not attach and started to curl up by day seven. Any measurements taken in a membrane which would later on curl up were discarded. Yet it has been reported that cell lines MG-63 as well as SaOS-2 in culture have a similar expression profile of cytokines and growth factors as human osteoblasts (91), and show a similar behaviour *in vitro* as human osteoblasts. Therefore, it is likely that these cell lines model the behaviour for primary human osteoblasts and the similar viability data obtained for hOBs and MG-63 cells in this study are consistent with this contention. Since this experiment was repeated with other cell line as well, the overall trend analysis was clear and therefore this set up was not repeated many more times. Another consistent trend with the viability assay of the cell line MG-63 is the advanced median viability of the treatment group BSP by day four. This trend cannot be deemed statistically significant, due to the low repetition, but in context with the findings of the cell line MG-63, it suggests the benefit of the coating of BSP with CCC within the first few days after seeding.

5.3. HUVECs

5.3.1. Validation of HUVECs as the cellular model

Successful bone formation requires a blood supply and is therefore vital for the bone formation and bone growth on biomaterials. HUVECs as an endothelial cell line were used as

a vascular model system, to test the viability of endothelial cells on the CCCs. To validate whether HUVECs are the right choice as a vascular model, a verification of the presence of proteins typical for endothelial cells was of critical importance. Immunofluorescence data obtained from HUVEC cells clearly showed expression of these typical markers, for instance the endothelial specific surface protein CD31, vascular endothelial growth factor A (VEGFA) and von Willebrand factor (vWF). CD31 is a surface glycoprotein, which is expressed in HUVECs but also present in other cells, such as monocytes, macrophages and platelets (85, 87). VEGFA is short for vascular endothelial growth factor A, which is an important mediator of angiogenesis. It is part of the angioblast differentiation process and increases vascular permeability, which is vital during angiogenesis for plasma proteins to migrate to the site of angiogenesis (97). The interaction of osteoblasts and chondrocytes takes place in part through their expression of VEGF, which helps these cells to promote the invasion of blood vessels (28). Due to its various roles during vascularization, it can be considered a marker of endothelial cells. The von Willebrand factor (vWF) is essential in the process of primary blood coagulation (98). It is a multimeric glycoprotein, which is found in platelets and endothelial cells. Through its expression and ability to enhance adhesion the formation of thrombi is made possible. Therefore, its presence is indispensable in HUVECs and another indicator, that the phenotype of the cells used in the experiments described here, is in agreement with an endothelial phenotype (86, 99).

Although the immunofluorescence result represents a good validation of the endothelial phenotype, the staining provided a qualitative result and did not allow a quantification of the expression of these endothelial markers. The results however provided a good indication that the phenotype of these HUVECs cells was not altered substantially during the cell passages and can therefore be considered to be representative for endothelial cells.

5.3.2. Viability Assay of HUVEC cell line

The main limitation for a correct assessment of the viability of HUVECs was their different growth rate in different replications of the assay. Instead of only evaluating one or the other it is important to analyse both sets of data points, to avoid any bias or false conclusions. HUVECs are derived from immune-privileged fetal tissue, the umbilical vein and are thus much more susceptible to different environmental effects, culture conditions and cell density, than cell cultures derived from a tumor cell line (100). Even though the conditions were close to the same in the replication of the assay, the different stages of the experiment such as the thawing process, medium change, replating and splitting can affect their growth. HUVECs, grow in

monolayer and after they have reached confluence build what is called the cobblestone phase (101). However, this phase could not be reached in the time frame chosen for this experiment and since this experiment did not include imaging of the cells on the CCC, it is unknown if the cells were confluent by the end of the experiment. Since in the second assay performed, their overall viability was lower than in the first assay and growth was not continuous, a direct comparison of the data obtained from both assays remained difficult. The decreasing viability in the second assay, displayed in all treatment groups no matter if the cells were seeded on the CCC or on a perfectly coated tissue plate. This supports the notion that these cells had difficulties to grow, no matter the environment and does not lead to the conclusion that collagen is not ideal for this cell line.

Nevertheless, the first assay did show overall growth, with the most successful treatment being the plain CCC. Endothelial cells can interact with other cells but also adhere to extracellular matrix components through several surface glycoproteins such as the receptors of the integrin family. Integrins can bind to numerous extracellular matrix proteins such as vitronectin or proteolyzed collagen. Among these, the $\alpha_v\beta_3$ Integrin is important since it not only stimulates angiogenesis but can also bind to the RGD motif of BSP (102). During angiogenesis it is known that endothelial cells express $\alpha_v\beta_3$ receptors and it has been demonstrated that it is through the $\alpha_v\beta_3$ integrin that BSP mediates HUVEC attachment and migration and therefore might be a stimulator of angiogenesis (49). However, here it was observed that the treatment group without BSP, i.e., plain collagen 1 fibrils lead to the highest viability of HUVECs in this assay. The measurement of the fluorescence after the use of alamarBlue® on the plain CCCs, reflects that this treatment had a higher viability than any other treatment group. Collagen 1 is known to influence the behaviour of endothelial cells. This was shown back in 1991 by Jackson and Jenkins, who added collagen 1 to HUVECs (103). They reported that collagen 1 acts as a stimulus for endothelial cells for vascular tube formation. Collagen has several repeats of RGD sequences which are also found in BSP, which were suspected to be cause for this effect. Nevertheless it was shown that this RGD motif alone does not lead to tube formation (104), but also, does not inhibit it (102). This suggests that other mechanisms triggered by the interaction between BSP and HUVECs also contribute to the effect of collagen to HUVEC growth. The addition of BSP was proposed to enhance the viability of HUVECs on collagen fibers. However, this could not be verified in the time frame, which was chosen for this experiment. The lack of a broader experimental set up calls for further analysis of HUVECs on collagen membranes such as CCC with or without BSP. Since the CCCs can be obtained in different sizes one future possibility would be to try a similar set up

for a longer period of time to test if the viability or growth of HUVECs would benefit from contact with the treated material over a longer period of time. It would be beneficial to include the aspect of imaging in future experimental set up to analyse if the HUVECs grow into a confluent monolayer, since this is the necessary precursor for vascularization.

5.4. BSP Coating Stability on the CCC

In the process of evaluating whether BSP has an effect on gene expression of SaOS-2 cells within the first four days of seeding onto a CCC, there were two coating methods which were analyzed, and termed: “BSP” and “BSP coat.” The main difference was that in the “BSP” method, the membrane was soaked with the protein and then left to dry overnight at room temperature. Whereas “BSP coat.”, was a coating process where the protein was left on the membrane for 60 minutes prior to seeding. The “BSP” treatment had a significant effect on SaOS-2 cells in the expression levels of some osteogenic markers. This is supported by the analysis of the viability assay which showed some compelling evidence in the primary human osteoblasts assay as well as the MG-63 assay. In both assays the method BSP showed a superior mean viability on day four. This represents an important finding, which is relevant for the future use of the CCC material but also bears information about the stability of the protein BSP itself: the method where BSP was left overnight at room temperature apparently did not lead to the degradation of the protein. It was still stable and able to influence the cells seeded on the membrane. It is known, that BSP has a specific binding site for collagen, it is plausible that the method “BSP” of soaking the dry membrane with BSP/PBS, cause BSP to properly link to collagen and therefore attach higher amounts of BSP to the collagen. The method of placing a diluted solution on the membrane after it had been treated according to protocol and then seeding the cells onto it, does not seem to result in the same attachment of BSP. This is especially important for a potential clinical application, as it promises a material which can be used to deliver growth factors, as well as a protein, which holds its stability at room temperature over 24 hours. In the experiment described here the BSP treated CCC membrane was only stored at room temperature for 24 hours, but it is not unlikely that this protein would stay stable for even longer periods of time, when linked to collagen at room temperature without any additional protection. Future experiments will have to be done to demonstrate and validate this. In the case of a clinical benefit through the coating of biomaterials and implants with BSP, it will be important to know that BSP does not degrade at room temperature and does most likely not need a synthetic optimization for it to link to collagen. This is supported by the review of Krueger et al, who states that the strong link of BSP to collagen present this combination as an

ideal candidate for scaffolds (105). Other studies support the coupling of BSP and collagen as well, since they bind together with a strong affinity still leaving the HA-nucleating regions free for other interactions and increasing nucleation potency (106). Whereas it has also been stated that it is the collagen binding peptide of BSP which leads to osteoblastic differentiation (107). The interaction of BSP with collagen is therefore an important interface in the analysis of the CCC as a biomaterial. Overall, it can be stated that linking BSP to collagen overnight lead to a superior effect in viability as well as the expression in some osteogenic markers. This supports the hypothesis, that the CCC is a suitable carrier for BSP, on which the protein is stable and active for a time frame of at least 24 hours.

5.5. Gene Expression

In these experiments the expression levels of certain genes were examined. SaOS-2 cells were seeded onto Collagen Cell Carrier membranes (CCC) with two different BSP coating methods as well as the plain CCC as the control, to analyze the expression levels of *ALP*, *Coll*, *SP7*, *RUNX2*, *SPARC* and *OPN*. SaOS-2 cells were used since they are widely recognized to model human bone cell behavior. Even though there are differences in the expression of cytokine receptors and other phenotypic behavior, osteosarcoma cell lines, such as this one, have a useful and widely accepted role in the molecular analysis of genes associated with osteoblast function (91). They are considered “osteoblast-like” cells and proliferate at a faster rate than primary human osteoblasts (88) and thus yield enough cells within four days to obtain sufficient quantities of RNA for an accurate qPCR. The genes, that were selected to be measured in this experiment, *ALP*, *Coll*, *SP7*, *RUNX2*, and *OPN*, are considered osteogenic markers, which are often used to verify bone formation. For example these markers were used in experiments that tested whether BMP-2 and -7 can have a positive effect on bone formation and therefore clinical value as growth factors to enhance human fracture healing (108). In current clinical practice, BMP-2 and -7 are approved for the applications in specific indications such as the acute defect in the tibia for BMP-2 and non-unions in the tibia for BMP-7 (55).

The expression levels of *RUNX2*, *ALP* and *Coll* mRNA did rise significantly in SaOS-2 when they were seeded on the CCCs treated with BSP compared to CCC without BSP, and when harvested on day 4. This was in agreement with the data reviewed by Krueger et al. indicating that previous studies had measured the rise of markers from osteoblast differentiation as early as four days after BSP is combined with collagen (105). It is thus likely that this increase in expression levels of *RUNX2*, *ALP* and *Coll* in SaOS-2 cells grown on CCC

membranes coated with BSP reflects a positive effect of BSP on bone growth when coupled to the right material.

5.5.1. Collagen 1 and ALP as Markers of Ossification

Collagen 1 is considered a marker in the process of ossification since it is vital in the first steps of bone formation. During osteoblastogenesis multipotent mesenchymal cells start to differentiate into the osteoblast lineage afterwards these cell types start to proliferate and producing proteins such as fibronectin and type1 collagen (109). During this phase genes such as *Coll1* are upregulated (110). Then, osteoblasts start to cluster and form layers. Through the production of non-collagenous and collagen proteins, such as collagen 1 the extracellular matrix is built. The upregulation of *ALP* in Osteoblast is induced through the proteins of the extracellular matrix such as different collagens and fibronectin (110-113). As mineralization starts, alkaline phosphatase (ALP) is present in high levels in osteoblasts (112). Therefore, the finding that both, *COL1* and *ALP* mRNA expression rises in SaOS-2 cells seeded on CCCs with BSP suggests that bone formation takes place and that this is driven by the presence of BSP. It is important to take into account that SaOS-2 cell line has a mature osteoblast phenotype and therefore generally has high levels of ALP activity (88, 89). Since the expression levels here are set in reference to SaOS-2 on collagen membranes, *ALP* expression levels are still significantly higher with BSP than without, but it would be interesting to verify this effect with an immature osteoblast phenotype.

5.5.2. Interaction of RUNX2 and SP7 with BSP

RUNX2 as well as *SP7/Osterix* are both vital for the osteoblast differentiation and it has been reported that deleting either one or both leads to failure of ossification (32, 114). Yet in this experiment, where expression levels in SaOS-2 on a CCC with BSP compared to no BSP were analyzed, only the *RUNX2* gene was observed to rise significantly in expression, whereas the median of the expression levels of the *SP7* gene remained similar to the control. The increase of *RUNX2* mRNA expression following exposure to BSP was expected since it had also been observed in other studies (72, 115). It should be noted, that Gordon et al. not only demonstrated the rise of the expression level of *RUNX 2* but also of *SP7*, which is in contrast to the data presented here (115). It is known that *RUNX2* is part of the many transcription factors orchestrating the differentiation from mesenchymal stem cells into osteoblast progenitors and further to immature osteoblasts. In this process, *RUNX2* is part of the initial step from mesenchymal stem cells to osteoprogenitor cells, but for these cells to become

immature osteoblasts, SP7 has to be present as well and RUNX2 and SP7 have to physically interact to regulate the expression of target genes (116). The expression of *RUNX2* itself in osteoblasts is regulated by enhancers, which are activated through the enhanceosome made of many transcription factors especially DLX5/6 and MEF2 but also SP7 (32). RUNX2 is present in many stages of bone formation and is also an inhibitor of the process that turns mature osteoblasts into osteocytes, whereas BSP itself is produced by differentiated osteoblasts (51). It is thus interesting to note, that BSP in the experimental setting used here only induced expression of RUNX2 but not SP7 since an effective skeletogenesis requires both of these proteins. It is therefore possible that BSP leads to a higher expression of RUNX2 in SaOS-2 cells, because they represent mature osteoblasts which react to RUNX2 alone by halting their differentiating into osteocytes, a process where SP7 is not required. The interaction of SP7 and RUNX2 takes place in an earlier stage of differentiation, when mesenchymal stem cells turn into osteoprogenitor cells and it is likely that SaOS-2 cells do not represent this earlier differentiation stage. It would thus be interesting to test whether BSP treatment would lead to a higher expression of *SP7* as well as *RUNX2* in mesenchymal cells or other bone marrow derived precursors of osteoblasts. In this context, the finding that SP7 targets BSP directly in osteoblasts and actually can activate BSP expression would be directly relevant (117), because this could indicate that the interaction of SP7 and RUNX2 leads to osteoblast differentiation, which then produces BSP, which in turn leads to higher levels of RUNX2 that inhibits further differentiation into osteocytes. Approaches to raise the expression of SP7 have been made in human mesenchymal stem cells with BMP 6 (118) and BMP2 (119). Future experiments should therefore also investigate whether a combination of several growth factors can both raise the expression of *RUNX2* as well as *SP7* at the same time. It is plausible that this would lead to higher osteoblastic growth and bone formation.

5.5.3. Expression Levels of SPARC

The expression level of *SPARC* is not significantly higher than the control, with a median of 2.5-fold, compared to the control without BSP. Yet it is important to discuss the aspect BSP might have on *SPARC*, since *SPARC* plays an important role in bone remodeling and *SPARC* null mice have a lower bone formation as well as bone resorption (120). SPARC can interact with collagen 1 directly and it has been suggested that SPARC plays an important role for the assembly of collagen itself (121). It is therefore associated with deposition of collagen in forming the extracellular matrix (ECM) (122). It is plausible to assume that when osteoblasts produce high amounts of Col1 and ALP, SPARC will also coincide in time as they

are all part of the bone formation process responsible for the building of the ECM. It can therefore be assumed that even though BSP does not seem to have a direct impact on SPARC in the set-up of this experiment, if bone formation is induced it would rise at a later point in time. In future experiments it should be verified if the expression level of *SPARC* does not rise at all or if the point at which the level of *SPARC* rises was not captured by the set-up of this experiment. In the study of Graf et al., the coating of BSP on the implant material TICER®, a mix of titanium oxide and hydroxyapatite ceramic, showed an increased expression of SPARC in the visualization of immunocytochemistry after five days (123). This study was done with maxillary bone cells. Since this immunocytochemistry was a visualization and not quantified, it is not possible to directly compare the impact of BSP on these two materials. Nevertheless, in both studies there is a rise of SPARC: In Graf et al., the protein is visualized and in this study the expression of the mRNA rose, yet not to a statistically significant level. The discrepancy, that the expression level was not significantly higher in the experiments here, could be due to the number of measurements or the short time frame. In future experiments this should be further analyzed.

5.5.4. Osteoblast Differentiation and OPN

As osteoblasts differentiate, they acquire the expression of certain markers for example BSP and osteopontin (OPN) (124). Here, levels of OPN were too low to be measured, even in the control of CCCs without BSP. OPN a phosphorylated sialoprotein, which also possesses an RGD motif, has been shown to inhibit *in vitro* mineralization with hydroxyapatite (125). OPN is found in osteoclasts as well as in osteoblasts and osteocytes (37, 38, 42). It is in correlation with high bone turnover and active osteoblasts (121). The importance of RUNX2 as a regulator of bone formation was already discussed above but is another important mediator here as well. RUNX2 interacts with a range of other proteins to regulate gene expression during bone turnover. It regulates the expression of, but not limited to, bone sialoprotein as well as osteopontin (126). Thus, it could be concluded that the expression levels of *OPN* should rise in the presence of such high *RUNX2* expression. But it has also been shown that BSP *-/-* mice produce high levels of *OPN* (127). It can be proposed that the presence of BSP leads to low levels of OPN. Yet this does not explain why the SaOS-2 seeded onto the plain CCC membrane also express diminishingly low levels of *OPN*. It also does not align with the data presented by Baranowski et al., who analyzed the gene expression of human osteoblasts on titanium when functionalized with BSP (128). Even though *OPN* did not rise significantly, they were able to register elevated expression levels. In a study where bone marrow cells were seeded onto a

collagen 1 matrix, the expression of *OPN* gene rose over time as well (129). Yet, in that study the time frame were weeks and the data here was taken on day four after seeding. The response of the expression rate of *OPN* in osteosarcoma cells to BSP, as well as the expression rates of *OPN* genes when cells are seeded onto collagen needs to be further investigated.

When comparing other studies with similar approaches similarities as well as differences could be found. The gene expression of human osteoblasts on titanium with and without BSP was measured by Baranowski et al., who also observed a significant rise in the expression level of *RUNX2*, just like it was measured here, but a significantly lower *ALP* expression level (128). As well as a relatively higher expression level of *OPN*. This effect was no longer visible by day 7. Another study analyzed the gene expression from human osteoblasts on calcium phosphate scaffolds after fourteen days (130). Here *ALP* as well as *SPARC* showed a downregulation whereas *OPN* and *RUNX2* were nearly unchanged in their expression rate. This difference is most likely due to the point in time when measurements were taken, as well as the seeding environment of calcium phosphate. Also, this experiment was done with primary bone marrow cells whereas the experiments performed here used SaOS-2 cells an established cancer cell line. Still, the genes that were induced to be expressed at higher levels by BSP in SaOS-2 cells are involved in the mineralization of tissue, indicating the validity of the approach to use an established cell line, albeit the limitations present.

Through previous studies it has already been shown that collagen type 1 by itself can induce osteoblastic differentiation (129) as well as increase mineralization (113). If this could be enhanced by the combination of BSP to the material prior to seeding it with cells, this material would offer an enormous potential for clinical application in orthopedics. Future *in vivo* and *in vitro* studies, would have to focus on this as well as optimize the combination of BSP and collagen type 1.

Overall, the two variables: time and type of cell line, should be examined in greater depth. It was already discussed how SaOS-2, as a mature phenotype, could have an impact on the expression levels of osteogenic markers. To understand how BSP impacts these expression rates, experiments need to be repeated with a less differentiated phenotype, such as mesenchymal or bone marrow cells. For example, a study has shown that when bone marrow cells are seeded onto a collagen type 1 matrix, they demonstrate osteoblastic behavior faster than the bone marrow cells on a conventional culture dish. Further, the activity of *ALP* and calcium deposition was increased solely by seeding osteoblasts on collagen type 1 matrix, but

this effect only is clearly visible after three weeks (131). Therefore, the timeline of future experiments needs to be extended, as four days only gives limited insight to regulation of osteogenic markers.

5.6. Easy Graft

To analyze the value and use of Easy Graft as a Biomaterial, four general criteria, defined in the chapter 2.4 “biomaterials”, are to be considered. Biocompatibility, chemical inertness and stability, sound engineering design and economic viability. Easy Graft is a material originally invented and approved for the field of dental surgery and periodontics. There, it was designed to be a place holder for jawbone defects, for example in alveolar ridge preservation after tooth extraction (132) or a socket preservation (133). It can be molded and placed inside any individual defect, bone or cavity and will harden as a porous scaffold. Easy Graft was made with the intention to stabilize the cavity and to be used in aesthetic restorations, bridging of defects and for osteoconduction. For these purposes, the scaffold needs to harden quickly to stabilize the cavity and possibly provide a suitable environment for a tooth prosthetic. Depending on the size of the defect, the material will be resorbed and replaced with bone inside the mandibula, which can take up to a year (134). It has been reported by the manufacturer that this material will completely dissolve during a time frame of 5 to 15 months (133). Since Easy Graft is a porous scaffold, blood and cells can flow through it and create bone within and around it, slowly replacing it during this process. Its porous structure leads to a higher osteoconduction, since it enables bone to grow into the scaffold (54). The material has already been approved for clinical use and can be considered biocompatible, since it can be sterilized and is pharmacologically inert.

The β - Tricalcium phosphate (β -TCP) granules, which are the main component of Easy Graft, do not elicit an inflammatory response, are non-toxic and had been proposed for bone grafting already in 1977 (135) and for bone repair and reconstruction later on (2,3). It should be noted however that the replacement of β -TCP by bone does not occur in a fully equitable way. A number of studies reported that less bone volume is produced compared to the volume of β -TCP that is reabsorbed. It has therefore been suggested that to combine β -TCP in clinical use with other less resorbable bone graft substitutes or to use it as an expander in autologous bone grafts (136).

5.6.1. Cell viability on Easy Graft

In the use in periodontics, Easy Graft is surrounded and implanted in oral mucosa and surrounded by highly vascularized tissue. This is a completely different environment than when implanted into or adjacent to bone, since oral mucosa contains an abundance of cells and growth factors. These are not present in the same amount in bones and therefore bone provides a problematic environment for cell growth. This is one of the reasons the viability of cells on Easy graft during implantation of the maxillary cannot be directly translated to the field of orthopedics. During the viability assay used in this thesis, cells were placed on top of the scaffold in the well without movement. This means the cells which do not directly attach onto the scaffold sink to the bottom of the well. Here they can still attach to the bottom of the 3D Granules of Easy Graft, but since the set-up lacks movement in the medium, there is no circulation of the cells. In a biological setting, such as an implantation, blood would flow around the scaffold and supply a new set of cells and growth factors, until more and more cells attach over time and start to grow. For an ideal biomaterial adhesion of cells should be as high as possible. The experiment did not provide the simulation of blood flow; however, the medium was enhanced with fetal calf serum and thus the lack of growth factors should not have been the problem of attachment. Even though the set-up of the viability assay had some limitations, the low rate of growth and adhesion to the scaffold is not explained. If this material proved an ideal environment for SaOS-2 cells to grow, the lack of movement would not have decreased or even abolished this effect. It is important to note that this indicates that this material is not ideally made for the adhesion growth of osteosarcoma cells and therefore human osteoblast would most likely have trouble attaching and growing as well. This is supported through the data depicted in 4.4.1, which show, large amounts of dead cells, which did not attach to the Easy Graft scaffold. This indicates the surface of Easy Graft is not ideal for attachment. It even suggests, that BSP did not help, but exacerbated this effect, since the pictures from this treatment demonstrate even larger amounts of nonattached and dead cells in the well. This however is disputed by the observation of the cytotoxicity assay. This assay, which measured the LDH and therefore the amount of leaky cells during a three day assay, shows that the measurements of pure Easy Graft within the first 24 hours, has a standard deviation reaching well into the toxic area. This was not seen with the scaffold coated with BSP. It could be proposed that the cells had difficulties attaching and surviving on pure Easy Graft, and this was reduced with the addition of BSP, therefore leading to fewer cell deaths in the treatment of BSP and lower levels of LDH measured. This is coherent with the data presented by Hilbig et al, who had found that BSP promoted attachment on their implants in question (137). The

interaction of BSP needs to be further analyzed, with emphasis on the coating procedure of BSP and its effect on adhesion of cells onto Easy Graft. The interaction of BSP and Easy Graft should be improved in further experiments through processes like physisorption, which has proven to work with calcium phosphate cement scaffolds (72) as well as titanium scaffolds (128) in the past.

The Easy Graft is a β -TCP where granules are coated with a PLGA-polymer (polylactic-co-glycolic acid) and when in contact with the BioLinker[®], this coating provides the elasticity which enables the material to mold into any required form. The experiments in this thesis, i.e. the viability assay, as well as the data on the residual cells, could not produce a positive effect on cell growth or cell adhesion on the granules with this coating. Thus, the function of the scaffold, porous structure as well as a poly (lactide-co-glycoside) coating, was not critical to the growth of osteosarcoma cells. Now it could be postulated that the attachment as well as the growth of these cells would benefit of the presence of the BioLinker[®], which was washed out prior to seeding in the set-up of this experiment. Since the manufacturer proclaims himself that the BioLinker[®] will be flushed out *in vivo* within the first three hours of implantation, this refutes this postulation and shows, that the BioLinker[®] is not meant to help cell growth or cell adhesion.

To analyze if BSP could be beneficial for bone formation, it was used as a treatment group in the viability assay. In 4.4.1. the assay was performed with Easy Graft scaffolds and the osteosarcoma cell line SaOS-2, since this cell line is suitable to model human bone formation, but the cells proliferate much faster than primary human bone cells. This viability assay clearly showed that very few, next to no cells, attach and survive on the Easy Graft scaffold in this setting. It has already been demonstrated that in calvaria rat models, that poly (lactide-co-glycoside) coated β -tricalcium phosphate (Easy Graft) is osteoconductive and enhances bone formation in critically large defects. This aspect of osteoconduction is mainly attributed to the materials adaptability and porosity, creating scaffolds with macropores of 500 and 1000 μm , and therefore complying with the architecture needed for sound osteoconduction (54). The stabilization and bridging effect Easy Graft has on the bone, leads to an elevated rate of bone formation, but only after 6 weeks in the calvarial model (138). Yet this success could not be verified through the assays in this thesis, mainly because this material did not show any osteoinductive properties and therefore on its own is not a viable environment for cells such as osteosarcoma cells. However, the addition of BSP on the Easy Graft scaffold had a significant effect on the viability of SaOS-2 cells within the first 24 hours as well as after four days of the experiment. Even though all treatments end on similar low viabilities by day seven, on day one

the viability of the the cells seeded onto the scaffold with BSP was significantly higher than the viability of the cells seeded on the plain scaffold. This effect stays significant on day four. Therefore, it is important to notice the drawbacks of the set-up of this experiment. It would be interesting to see if the addition of BSP would help to enhance bone growth and calcium deposition when implanted *in vivo* or if the attachment of the cells onto the scaffold were to be improved, if the effect of BSP were more drastic. At this point it can only be concluded that Easy Graft is useful in the stabilization of fractures and that this material still needs further adjustments to create an environment acceptable for a good habitation of bone cells.

5.6.2. Easy Graft cytotoxicity

Although the SaOS-2 cells did not seem to live and thrive on this material, the cytotoxicity test nevertheless support the notion that Easy Graft can be considered as non-toxic, even if the testing environment was set up under *in vitro* and not under *in vivo* conditions. Though the standard deviation of the plain Easy Graft scaffold does reach above the limit of cytotoxicity, this is as previously discussed most likely due to the lack of proficient adhesion of the cells on this biomaterial. For the cytotoxicity assay, an LDH-Glo kit was used with a measuring volume of 10 μ l. This is important as this volume is very small and therefore prone for measuring mistakes. Yet the toxicity limit in this experiment was also defined by the data collected during this experiment and it is therefore conceivable that the low LDH values detected with Easy Graft represent a true absence of toxicity. This is supported by the finding that even with 10 μ l of volume, high amounts of LDH could be detected in the control that dictates the upper limit. It is thus unlikely that the manipulation of small volumes has affected the assay and the Easy Graft material can be considered nontoxic.

5.6.3. Chemically Inertia and Stability

It is very important when considering this material for clinical use, that it can only harden as fast as advertised when the bodily fluids surrounding the scaffold are in movement and are in contact with the largest surface of the scaffold as possible. The idea behind this process is the mechanism of washing out the bio-linker thereby hardening and creating a stable form. This is a significant factor to note, since biomaterials, that are needed in orthopedics should provide a solution for multifracture and trauma repair in combination with osteosynthesis. It could be postulated that Easy Graft in the combination with plates, screws and prosthetics will be compromised in the hardening process, as was shown when the scaffolds were left to harden in the PLA (poly lactic acid) mold (see Fig. 20). If this material were to be

applied in the field of orthopedics, it would be critical that it can harden fast and thorough enough to stabilize fractures. This would not work when Easy Graft is used in combination with osteosynthesis measures and would even be difficult on its own as fractures are often surrounded by hematomas, stagnant blood, and swelling. It is a completely different set up than the molds and cavities which have thus far been the environment of implantation, which provide a safe haven for Easy Graft in periodontics. Within the limitations of my experimental set up, it is difficult to prove that osteosynthesis, such as plates would be unable to be paired with Easy Graft and is therefore an aspect to be considered in further *in vivo* experiments. The way the scaffolds were formed in my second attempt included the hardened substance to be cut into size by hand which leaves a margin for error in the formation and weight of the scaffold. However, since the results of the cell viability assays did not differ significantly from each other, this error could be considered negligible

5.6.4. Sound Engineering Design

The third criterium relates to the design of the biomaterial and has already been partly discussed when describing the manufacturing of the scaffold. Part of the engineering design is also the possibility of coating this material. In 4.4.1 the procedure of coating Easy Graft with BSP was addressed. The measurements clearly showed an early release of BSP into its surrounding medium within the first 3 hours. Similarly to the release of the BioLinker®, for which *in vivo* experiments showed a release of 90% in the first 3 hours (68), BSP was almost fully solved out of the scaffold within the first 3 hours as well. Through every movement in the medium, more BSP is released into the surroundings. Therefore, the setup of the experiment, where at every measuring point the entire medium was taken out with a pipette to measure the amount of BSP leaked, was not an ideal set-up. The movement of draining the medium and replacing it with PBS most likely increased the flushing out of BSP. It is thus conceivable that BSP cannot attach properly to the calcium phosphate granules of Easy Graft, most likely due to the poly lactide coating. Nevertheless, the experiments of 4.4.1 show that after 24 hours only around 12% of the initial amount of BSP is still attached to or surrounding the Easy Graft scaffold. In future experiments the bond between Easy Graft and the protein BSP needs to be elevated to be able to evaluate the effect of BSP. Even though the coating procedure is compromised, the viability assay indicates, that BSP did improve the viability of SaOS-2 cells significantly within the first day. This shows that an initial boost can have a substantial impact on the cells and still shows the value if the initial addition of BSP. In future experiments it should be evaluated if a higher affinity of BSP to the scaffold leads to a higher measurable

effect of BSP on the viability of cells. Baranowski et. al showed that when calcium phosphate scaffolds were placed inside a calvarial defect model, the sheer presence of the scaffold whether with BSP or without lead to a higher bone volume as well as thickness (139). This is most likely attributed to the fact that bridging the defect with a porous scaffold allows cells to flow through it and leads to a better bone regeneration. This can be attributed to the positive effects of osteoconductivity as well as putting mechanical as well as sheer pressure on the area. This effect would most likely be recreated with Easy Graft *in vivo*, but above that the material has not shown any other beneficial properties in these experiments.

5.6.5. Economic Aspects

If Easy Graft was to be considered in a clinical setting at a larger scale, economic consideration would become important. Such an assessment is difficult, as the comparison has to be drawn to the autologous bone graft made from the iliac crest of a patient. Here the costs of the operation, as well as prolonged hospital stay, and possible complications have to be taken into consideration. Depending on the source, one syringe of 0.4 ml Easy Graft costs around 100 -115 Euro. If the growth rate and the advantages of Easy Graft were the same, as the autologous bone graft, this could be considered a far superior solution. This is because its yield is not limited, no second defect to harvest the material needs to be made and it could possibly be combined with autologous bone graft. There are many draw backs of autologous bone grafts such as limited availability of healthy bone, secondary surgery costs, harvest site morbidity and long-term pain issues. Since this material does not offer the same advantages of osteoinduction, as an autologous graft out of the iliac crest with stem cells and osteogenic enhancement, a direct comparison remains problematic.

6. Conclusion

6.1. Collagen Cell Carrier in Clinical Use

The experiments in this study were able to show a positive trend in the impact of BSP on the viability of different cell lines seeded on CCCs. This trend, though not statistically significant, was replicated with MG-63 as well as SaOS-2 and showed a superior viability of the treatment BSP on day four of the assay. The hOB assay revealed the treatment group BSP as a superior method of coating, with a higher viability than the other coating method of BSP onto the CCC. Since this trend subsides by day seven, future experiments are still needed to evaluate and expand on this effect. Another important advantage of the CCC as a biomaterial is the possibility of its combination with growth factors or other proteins. This study was able to show that the CCC functions well with the combination of growth factors such as BSP, as it presents itself as an ideal coating surface for growth factors. BSP was able to attach and stay stable over 24 hours to the CCC to then interact with the seeded cells on the CCC. It could be considered a reliable vehicle for the direct delivery of such proteins and growth factors to the site of implantations. The CCC could therefore be used as a coated occlusion material, whenever autologous bone grafts are executed, as well as in combinations with prosthetics and implants.

6.2. Easy Graft in Clinical Use

This study is one of the first studies to evaluate Easy Graft as a new solution for multifragmented bone repair or repairing fractures of critical size. Unfortunately, this study also indicates that this material would only provide an osteoconduction through the bridging of the defect, without any further advantages of bone cell viability. The coating of the material does not seem to help establish a suitable environment for bone cells to adhere or grow properly. It has been shown that the bridging of defects alone does lead to faster bone formation in the calvarial model (139). Yet this characteristic can be attributed to any biomaterial which can be fit to size and help to stabilize the fracture with a degree of porosity and does not emerge Easy Graft as a new and improved management of bone fractures. The coating strategies of this material should be explored and improved such as physisorption, to elevate the material in its osteoinduction.

6.3. Advances with BSP

In this study it was observed that BSP does lead to elevated osteogenic markers of ALP, RUNX2 and Col1 in SaOS-2 cells grown on CCCs and continually shows advances in cell viability within the first four days. Yet on its own it is questionable if BSP will lead to the improved bone healing properties, since it did not lead to a significantly higher viability in either hOB, MG-63, SaOS-2 or HUVEC cell lines during these *in vitro* assay after seven days. In future experiments it would be interesting to combine BSP with other growth factors for a broader increase in osteogenic markers and stronger and longer improvements in cell viability and cell proliferation. Combinations with growth factors of the bone morphogenetic family seem to be promising and should be further evaluated.

7. Bibliography

1. Skripitz R, Roth A, Peters KM, Zimmermann G, Goost H, Randau T, et al. Supportive Methoden zur Knochenheilung. In: Peters KM, König DP, Roth A, editors. Fortbildung Osteologie 4. Berlin, Heidelberg: Springer Berlin Heidelberg; 2018. p. 33-69.
2. Rottensteiner U. Knochen-Tissue-Engineering im Critical Sized Femurdefektmodell der Ratte nach Bestrahlung. Gießen: Universitätsbibliothek; 2016.
3. Boulefour W, Juignet L, Bouet G, Granito RN, Vanden-Bossche A, Laroche N, et al. The role of the SIBLING, Bone Sialoprotein in skeletal biology — Contribution of mouse experimental genetics. *Matrix Biology*. 2016;52-54:60-77.
4. Xu L, Zhang Z, Sun X, Wang J, Xu W, Shi L, et al. Glycosylation status of bone sialoprotein and its role in mineralization. *Experimental Cell Research*. 2017;360(2):413-20.
5. Lowe JS, Anderson PG. Chapter 13 - Musculoskeletal System. In: Lowe JS, Anderson PG, editors. *Stevens & Lowe's Human Histology (Fourth Edition) (Fourth Edition)*. Philadelphia: Mosby; 2015. p. 239-62.
6. Shipman P, Walker A, Bichell D. *The Human Skeleton*: Harvard University Press; 2013.
7. Baron R. *Anatomy and Ultrastructure of Bone – Histogenesis, Growth and Remodeling*: MDTtext.com, Inc., South Dartmouth (MA); 2000 2000.
8. White TD, Folkens PA. Chapter 4 - BONE BIOLOGY & VARIATION. In: White TD, Folkens PA, editors. *The Human Bone Manual*. San Diego: Academic Press; 2005. p. 31-48.
9. and SW, Wagner HD. THE MATERIAL BONE: Structure-Mechanical Function Relations. *Annual Review of Materials Science*. 1998;28(1):271-98.
10. Mistry AS, Mikos AG. Tissue Engineering Strategies for Bone Regeneration. In: Yannas IV, editor. *Regenerative Medicine II: Clinical and Preclinical Applications*. Berlin, Heidelberg: Springer Berlin Heidelberg; 2005. p. 1-22.
11. McKee MD, Cole WG. Chapter 2 - Bone Matrix and Mineralization. In: Glorieux FH, Pettifor JM, Jüppner H, editors. *Pediatric Bone (Second Edition)*. San Diego: Academic Press; 2012. p. 9-37.
12. J. Gordon Betts TJC, Kelly A. Young CSU, Long Beach, James A. Wise HU, Eddie Johnson COCC, Brandon Poe STCC, Dean H. Kruse PCC, et al. *Anatomy and Physiology*: OpenStax is licensed under Creative Commons Attribution License v4.0; Apr 25, 2013. Available from: <https://openstax.org/details/books/anatomy-and-physiology>.
13. Capulli M, Paone R, Rucci N. Osteoblast and osteocyte: Games without frontiers. *Archives of Biochemistry and Biophysics*. 2014;561:3-12.
14. Stock SR. The Mineral-Collagen Interface in Bone. *Calcif Tissue Int*. 2015;97(3):262-80.
15. Boskey AL. Noncollagenous matrix proteins and their role in mineralization. *Bone and Mineral*. 1989;6(2):111-23.
16. Wolf G. Function of the Bone Protein Osteocalcin: Definitive Evidence. *Nutrition Reviews*. 1996;54(10):332-3.
17. Viguet-Carrin S, Garnero P, Delmas P. The role of collagen in bone strength. *Osteoporosis international*. 2006;17(3):319-36.

18. Olszta MJ, Cheng X, Jee SS, Kumar R, Kim Y-Y, Kaufman MJ, et al. Bone structure and formation: A new perspective. *Materials Science and Engineering: R: Reports*. 2007;58(3-5):77-116.
19. Florencio-Silva R, Sasso GRdS, Sasso-Cerri E, Sim, #xf5, es MJ, et al. *Biology of Bone Tissue: Structure, Function, and Factors That Influence Bone Cells*. *BioMed Research International*. 2015;2015:17.
20. Sambrook P. 5 - BONE STRUCTURE AND FUNCTION IN NORMAL AND DISEASE STATES. In: Sambrook P, Schrieber L, Taylor T, Ellis AM, editors. *The Musculoskeletal System (Second Edition)*: Churchill Livingstone; 2010. p. 61-76.
21. Fratzl P, Weinkamer R. Hierarchical Structure and Repair of Bone: Deformation, Remodelling, Healing. In: van der Zwaag S, editor. *Self Healing Materials: An Alternative Approach to 20 Centuries of Materials Science*. Dordrecht: Springer Netherlands; 2007. p. 323-35.
22. Teitelbaum SL. Bone resorption by osteoclasts. *Science*. 2000;289(5484):1504-8.
23. Miller SC, Jee WSS. The bone lining cell: A distinct phenotype? *Calcif Tissue Int*. 1987;41(1):1-5.
24. Franz-Odenaal TA. Induction and patterning of intramembranous bone. *Front Biosci*. 2011;16:2734-46.
25. Long F, Ornitz DM. Development of the endochondral skeleton. *Cold Spring Harbor perspectives in biology*. 2013;5(1):a008334.
26. Reddi AH. *Cell Biology and Biochemistry of Endochondral Bone Development. Collagen and Related Research*. 1981;1(2):209-26.
27. Marsell R, Einhorn TA. The role of endogenous bone morphogenetic proteins in normal skeletal repair. *Injury*. 2009;40:S4-S7.
28. Marsell R, Einhorn TA. The biology of fracture healing. *Injury*. 2011;42(6):551-5.
29. Tuvo G, Mora R, Galli GB. Treatment of Noninfected Nonunions: Normotrophic Nonunions. In: Mora R, editor. *Nonunion of the Long Bones: Diagnosis and treatment with compression-distraction techniques*. Milano: Springer Milan; 2006. p. 173-6.
30. Komori T. Runx2, A multifunctional transcription factor in skeletal development. *Journal of Cellular Biochemistry*. 2002;87(1):1-8.
31. Komori T. Regulation of bone development and maintenance by Runx2. *Front biosci*. 2008;13(13):898.
32. Komori T. Runx2, an inducer of osteoblast and chondrocyte differentiation. *Histochemistry and cell biology*. 2018;149(4):313-23.
33. Kaback LA, Soung DY, Naik A, Smith N, Schwarz EM, O'Keefe RJ, et al. Osterix/Sp7 regulates mesenchymal stem cell mediated endochondral ossification. *Journal of Cellular Physiology*. 2008;214(1):173-82.
34. Komori T. Signaling networks in RUNX2-dependent bone development. *Journal of Cellular Biochemistry*. 2011;112(3):750-5.
35. Nishio Y, Dong Y, Paris M, O'Keefe RJ, Schwarz EM, Drissi H. Runx2-mediated regulation of the zinc finger Osterix/Sp7 gene. *Gene*. 2006;372:62-70.
36. Sweetwyne MT, Brekken RA, Workman G, Bradshaw AD, Carbon J, Siadak AW, et al. Functional analysis of the matricellular protein SPARC with novel monoclonal antibodies. *Journal of Histochemistry & Cytochemistry*. 2004;52(6):723-33.
37. Alford AI, Hankenson KD. Matricellular proteins: Extracellular modulators of bone development, remodeling, and regeneration. *Bone*. 2006;38(6):749-57.

38. Holland P, Harper SJ, McVey JH, Hogan B. In vivo expression of mRNA for the Ca⁺⁺-binding protein SPARC (osteonectin) revealed by in situ hybridization. *The Journal of cell biology*. 1987;105(1):473-82.
39. Delany AM, Hankenson KD. Thrombospondin-2 and SPARC/osteonectin are critical regulators of bone remodeling. *Journal of cell communication and signaling*. 2009;3(3-4):227-38.
40. Ribeiro N, Sousa SR, Brekken RA, Monteiro FJ. Role of SPARC in Bone Remodeling and Cancer-Related Bone Metastasis. *Journal of Cellular Biochemistry*. 2014;115(1):17-26.
41. Denhardt DT, Noda M. Osteopontin expression and function: role in bone remodeling. *Journal of Cellular Biochemistry*. 1998;72(S30–31):92-102.
42. Sodek J, Ganss B, McKee MD. Osteopontin. *Critical Reviews in Oral Biology & Medicine*. 2000;11(3):279-303.
43. Chellaiah MA, Kizer N, Biswas R, Alvarez U, Strauss-Schoenberger J, Rifas L, et al. Osteopontin deficiency produces osteoclast dysfunction due to reduced CD44 surface expression. *Molecular biology of the cell*. 2003;14(1):173-89.
44. Malaval L, Wade-Gu  ye NM, Boudiffa M, Fei J, Zirngibl R, Chen F, et al. Bone sialoprotein plays a functional role in bone formation and osteoclastogenesis. *J Exp Med*. 2008;205(5):1145-53.
45. Christenson RH. Biochemical markers of bone metabolism: an overview. *Clinical biochemistry*. 1997;30(8):573-93.
46. Harris NL, Rattray KR, Tye CE, Underhill TM, Somerman MJ, D'Errico JA, et al. Functional analysis of bone sialoprotein: identification of the hydroxyapatite-nucleating and cell-binding domains by recombinant peptide expression and site-directed mutagenesis. *Bone*. 2000;27(6):795-802.
47. Hunter GK, Goldberg HA. Nucleation of hydroxyapatite by bone sialoprotein. *Proceedings of the National Academy of Sciences*. 1993;90(18):8562.
48. Raynal C, Delmas PD, Chenu C. Bone sialoprotein stimulates in vitro bone resorption. *Endocrinology*. 1996;137(6):2347-54.
49. Bellahcene A, Bonjean K, Fohr B, Fedarko NS, Robey FA, Young MF, et al. Bone sialoprotein mediates human endothelial cell attachment and migration and promotes angiogenesis. *Circulation research*. 2000;86(8):885-91.
50. Hodivala-Dilke KM, Reynolds AR, Reynolds LE. Integrins in angiogenesis: multitasking molecules in a balancing act. *Cell and tissue research*. 2003;314(1):131-44.
51. George A, Veis A. Phosphorylated Proteins and Control over Apatite Nucleation, Crystal Growth, and Inhibition. *Chemical Reviews*. 2008;108(11):4670-93.
52. Addison WN, Azari F, S  rensen ES, Kaartinen MT, McKee MD. Pyrophosphate inhibits mineralization of osteoblast cultures by binding to mineral, up-regulating osteopontin, and inhibiting alkaline phosphatase activity. *Journal of Biological Chemistry*. 2007;282(21):15872-83.
53. Park J, Lakes RS. *Biomaterials: an introduction*: Springer Science & Business Media; 2007.
54. Denry I, Kuhn LT. Design and characterization of calcium phosphate ceramic scaffolds for bone tissue engineering. *Dental Materials*. 2016;32(1):43-53.
55. Blokhuis TJ, Arts JJC. Bioactive and osteoinductive bone graft substitutes: Definitions, facts and myths. *Injury*. 2011;42:S26-S9.
56. Albrektsson T, Johansson C. Osteoinduction, osteoconduction and osseointegration. *European Spine Journal*. 2001;10(2):S96-S101.

57. Kang Y, Kim S, Fahrenholtz M, Khademhosseini A, Yang Y. Osteogenic and angiogenic potentials of monocultured and co-cultured human-bone-marrow-derived mesenchymal stem cells and human-umbilical-vein endothelial cells on three-dimensional porous beta-tricalcium phosphate scaffold. *Acta Biomaterialia*. 2013;9(1):4906-15.
58. Janicki P, Schmidmaier G. What should be the characteristics of the ideal bone graft substitute? Combining scaffolds with growth factors and/or stem cells. *Injury*. 2011;42:S77-S81.
59. Demers C, Hamdy CR, Corsi K, Chellat F, Tabrizian M, Yahia LH. Natural coral exoskeleton as a bone graft substitute: a review. *Bio-medical materials and engineering*. 2002;12(1):15-35.
60. Parikh S. Bone graft substitutes: past, present, future. *Journal of postgraduate medicine*. 2002;48(2):142.
61. Chattopadhyay S, Raines RT. Collagen-based biomaterials for wound healing. *Biopolymers*. 2014;101(8):821-33.
62. Miyata T, Taira T, Noishiki Y. Collagen engineering for biomaterial use. *Clinical Materials*. 1992;9(3):139-48.
63. Zimmermann G, Moghaddam A. Allograft bone matrix versus synthetic bone graft substitutes. *Injury*. 2011;42:S16-S21.
64. C. Chow L. Next generation calcium phosphate-based biomaterials. *Dental Materials Journal*. 2009;28(1):1-10.
65. Biase PD, Capanna R. Clinical applications of BMPs. *Injury*. 2005;36(3, Supplement):S43-S6.
66. BioEngineering V. Collagen Cell Carrier 2017 [Available from: <https://www.viscofan-bioengineering.com/collagen-products/research-grade/collagen-cell-carrier>].
67. BioEngineering V. Collagen Cell Carrier (CCC) 2017 [cited 2020 10/16]. Available from: <https://www.viscofan-bioengineering.com/collagen-products/research-grade/collagen-cell-carrier>.
68. Guidor SS. GUIDOR Easy-Graft 2018 [Available from: https://www.guidor.com/de_de/easy-graft.html].
69. Guidor SS. Giodor Easy Graft FAQa 2018 [Available from: https://www.guidor.com/de_de/faq].
70. Hofmann A, Ritz U, Hessmann M, Schmid C, Tresch A, Rompe J, et al. Cell viability, osteoblast differentiation, and gene expression are altered in human osteoblasts from hypertrophic fracture non-unions. *Bone*. 2008;42(5):894-906.
71. Hofmann A, Ritz U, Verrier S, Eglin D, Alini M, Fuchs S, et al. The effect of human osteoblasts on proliferation and neo-vessel formation of human umbilical vein endothelial cells in a long-term 3D co-culture on polyurethane scaffolds. *Biomaterials*. 2008;29(31):4217-26.
72. Klein A. Functionalisation of biomaterials with bone sialoprotein for joint and bone replacement: Universitätsbibliothek Mainz; 2018.
73. Pautke C, Schieker M, Tischer T, Kolk A, Neth P, Mutschler W, et al. Characterization of osteosarcoma cell lines MG-63, Saos-2 and U-2 OS in comparison to human osteoblasts. *Anticancer Res*. 2004;24(6):3743-8.
74. Boskey AL, Roy R. Cell culture systems for studies of bone and tooth mineralization. *Chemical reviews*. 2008;108(11):4716-33.
75. Czekanska E, Stoddart M, Richards R, Hayes J. In search of an osteoblast cell model for in vitro research. *Eur Cell Mater*. 2012;24(4):1-17.
76. Kartsogiannis V, Ng KW. Cell lines and primary cell cultures in the study of bone cell biology. *Molecular and cellular endocrinology*. 2004;228(1-2):79-102.

77. Sigma-Aldrich. Product Information Accutase Solution 2019 [Available from: <https://www.sigmaaldrich.com/content/dam/sigma-aldrich/docs/Sigma/Datasheet/6/a6964dat.pdf>].
78. Strober W. Trypan blue exclusion test of cell viability. *Curr Protoc Immunol*. 2001;Appendix 3:Appendix 3B.
79. Sigma-Aldrich. MERCK DAPI 2019 [Available from: https://www.sigmaaldrich.com/catalog/product/roche/10236276001?lang=de®ion=DE&qclid=CjwKCAjw-7LrBRB6EiwAhh1yX7vVbcRXAYHzuYEuvD8b-E1_S3ZxR834sV-gl_fiqe3fSJaf5AkInhoC7ggQAvD_BwE].
80. Thermo Fisher Scientific. alamarBlue Cell Viability Reagent o.J. [Available from: <https://www.thermofisher.com/order/catalog/product/DAL1025>].
81. Scientific TF. alamarBlue HS and alamarBlue Assays for Cell Viability [Available from: https://www.thermofisher.com/de/de/home/life-science/cell-analysis/fluorescence-microplate-assays/microplate-assays-cell-viability/alarblue-assay-cell-viability.html?ef_id=Cj0KCQjw84XtBRDWARIsAAU1aM0CMVP9B6KJkGHK56yeiPs0k6csfmgYzYIZH1JP4Z7pCmgYxh-HiYwaAhD9EALw_wcB:G:s&s_kwid=AL!3652!3!355223665570!p!!q!!alar%20blue&qclid=Cj0KCQjw84XtBRDWARIsAAU1aM0CMVP9B6KJkGHK56yeiPs0k6csfmgYzYIZH1JP4Z7pCmgYxh-HiYwaAhD9EALw_wcB].
82. Livak KJ, Schmittgen TD. Analysis of relative gene expression data using real-time quantitative PCR and the 2- $\Delta\Delta$ CT method. *methods*. 2001;25(4):402-8.
83. Barber RD, Harmer DW, Coleman RA, Clark BJ. GAPDH as a housekeeping gene: analysis of GAPDH mRNA expression in a panel of 72 human tissues. *Physiological Genomics*. 2005;21(3):389-95.
84. DeLisser HM, Newman PJ, Albelda SM. Molecular and functional aspects of PECAM-1/CD31. *Immunology today*. 1994;15(10):490-5.
85. Simmons DL, Walker C, Power C, Pigott R. Molecular cloning of CD31, a putative intercellular adhesion molecule closely related to carcinoembryonic antigen. *J Exp Med*. 1990;171(6):2147-52.
86. Müller AM, Hermanns MI, Skrzynski C, Nesslinger M, Müller K-M, Kirkpatrick CJ. Expression of the endothelial markers PECAM-1, vWf, and CD34 in vivo and in vitro. *Experimental and molecular pathology*. 2002;72(3):221-9.
87. Pusztaszeri MP, Seelentag W, Bosman FT. Immunohistochemical expression of endothelial markers CD31, CD34, von Willebrand factor, and Fli-1 in normal human tissues. *Journal of Histochemistry & Cytochemistry*. 2006;54(4):385-95.
88. Rodan SB, Imai Y, Thiede MA, Wesolowski G, Thompson D, Bar-Shavit Z, et al. Characterization of a human osteosarcoma cell line (Saos-2) with osteoblastic properties. *Cancer research*. 1987;47(18):4961-6.
89. Czekanska E, Stoddart M, Richards R, Hayes J. IN SEARCH OF AN OSTEOBLAST CELL MODEL FOR IN VITRO RESEARCH.
90. Declercq H, Van den Vreken N, De Maeyer E, Verbeeck R, Schacht E, De Ridder L, et al. Isolation, proliferation and differentiation of osteoblastic cells to study cell/biomaterial interactions: comparison of different isolation techniques and source. *Biomaterials*. 2004;25(5):757-68.
91. Bilbe G, Roberts E, Birch M, Evans DB. PCR phenotyping of cytokines, growth factors and their receptors and bone matrix proteins in human osteoblast-like cell lines. *Bone*. 1996;19(5):437-45.
92. Merck KGaA. Corning® Costar® Ultra-Low Attachment Multiple Well Plate 2020 [Available from: <https://www.sigmaaldrich.com/catalog/product/sigma/clc3473?lang=de®ion=DE>].

93. Wang J, Zhou H-Y, Salih E, Xu L, Wunderlich L, Gu X, et al. Site-Specific In Vivo Calcification and Osteogenesis Stimulated by Bone Sialoprotein. *Calcif Tissue Int.* 2006;79(3):179-89.
94. Clover J, Gowen M. Are MG-63 and HOS TE85 human osteosarcoma cell lines representative models of the osteoblastic phenotype? *Bone.* 1994;15(6):585-91.
95. O'Toole GC, Salih E, Gallagher C, FitzPatrick D, O'Higgins N, O'Rourke SK. Bone sialoprotein-coated femoral implants are osteoinductive but mechanically compromised. *Journal of Orthopaedic Research.* 2004;22(3):641-6.
96. Masi L, Franchi A, Santucci M, Danielli D, Arganini L, Giannone V, et al. Adhesion, growth, and matrix production by osteoblasts on collagen substrata. *Calcif Tissue Int.* 1992;51(3):202-12.
97. Carmeliet P. Mechanisms of angiogenesis and arteriogenesis. *Nature Medicine.* 2000;6(4):389-95.
98. Furie B, Furie BC. The molecular basis of blood coagulation. *Cell.* 1988;53(4):505-18.
99. Turner NA, Nolasco L, Ruggeri ZM, Moake JL. Endothelial cell ADAMTS-13 and VWF: production, release, and VWF string cleavage. *Blood, The Journal of the American Society of Hematology.* 2009;114(24):5102-11.
100. Heiss M, Hellström M, Kalén M, May T, Weber H, Hecker M, et al. Endothelial cell spheroids as a versatile tool to study angiogenesis in vitro. *The FASEB Journal.* 2015;29(7):3076-84.
101. Smeets EF, von Asmuth EJ, van der Linden CJ, Leeuwenberg JF, Buurman WA. A comparison of substrates for human umbilical vein endothelial cell culture. *Biotechnic & histochemistry.* 1992;67(4):241-50.
102. Buerkle M, Pahernik S, Sutter A, Jonczyk A, Messmer K, Dellian M. Inhibition of the alpha-v integrins with a cyclic RGD peptide impairs angiogenesis, growth and metastasis of solid tumours in vivo. *British journal of cancer.* 2002;86(5):788-95.
103. Jackson CJ, Jenkins KL. Type I collagen fibrils promote rapid vascular tube formation upon contact with the apical side of cultured endothelium. *Experimental Cell Research.* 1991;192(1):319-23.
104. Jackson CJ, Knop A, Giles I, Jenkins K, Schrieber L. VLA-2 mediates the interaction of collagen with endothelium during in vitro vascular tube formation. *Cell Biology International.* 1994;18(9):859-68.
105. Kruger TE, Miller AH, Wang J. Collagen Scaffolds in Bone Sialoprotein-Mediated Bone Regeneration. *The Scientific World Journal.* 2013;2013:812718.
106. Baht GS, Hunter GK, Goldberg HA. Bone sialoprotein-collagen interaction promotes hydroxyapatite nucleation. *Matrix Biology.* 2008;27(7):600-8.
107. Choi YJ, Lee JY, Chung CP, Park YJ. Enhanced osteogenesis by collagen-binding peptide from bone sialoprotein in vitro and in vivo. *Journal of Biomedical Materials Research Part A.* 2013;101(2):547-54.
108. Sakano S, Murata Y, Miura T, Iwata H, Sato K, Matsui N, et al. Collagen and alkaline phosphatase gene expression during bone morphogenetic protein (BMP)-induced cartilage and bone differentiation. *Clin Orthop Relat Res.* 1993(292):337-44.
109. Jensen ED, Gopalakrishnan R, Westendorf JJ. Regulation of gene expression in osteoblasts. *Biofactors.* 2010;36(1):25-32.
110. Javed A, Chen H, Ghori FY. Genetic and Transcriptional Control of Bone Formation. *Oral and maxillofacial surgery clinics of North America.* 2010;22(3):283.
111. Clarke B. Normal Bone Anatomy and Physiology. *Clinical Journal of the American Society of Nephrology.* 2008;3(Supplement 3):S131.

112. Lian JB, Stein GS. Development of the osteoblast phenotype: molecular mechanisms mediating osteoblast growth and differentiation. *Iowa Orthop J*. 1995;15:118-40.
113. Mathews S, Bhone R, Gupta PK, Totey S. Extracellular matrix protein mediated regulation of the osteoblast differentiation of bone marrow derived human mesenchymal stem cells. *Differentiation*. 2012;84(2):185-92.
114. Nakashima K, Zhou X, Kunkel G, Zhang Z, Deng JM, Behringer RR, et al. The novel zinc finger-containing transcription factor osterix is required for osteoblast differentiation and bone formation. *Cell*. 2002;108(1):17-29.
115. Gordon JAR, Tye CE, Sampaio AV, Underhill TM, Hunter GK, Goldberg HA. Bone sialoprotein expression enhances osteoblast differentiation and matrix mineralization in vitro. *Bone*. 2007;41(3):462-73.
116. Rashid H, Ma C, Chen H, Wang H, Hassan MQ, Sinha K, et al. Sp7 and Runx2 molecular complex synergistically regulate expression of target genes. *Connective tissue research*. 2014;55(sup1):83-7.
117. Yang Y, Huang Y, Zhang L, Zhang C. Transcriptional regulation of bone sialoprotein gene expression by Osx. *Biochemical and Biophysical Research Communications*. 2016;476(4):574-9.
118. Zhu F, Friedman MS, Luo W, Woolf P, Hankenson KD. The transcription factor osterix (SP7) regulates BMP6-induced human osteoblast differentiation. *Journal of Cellular Physiology*. 2012;227(6):2677-85.
119. Matsubara T, Kida K, Yamaguchi A, Hata K, Ichida F, Meguro H, et al. BMP2 Regulates Osterix through Msx2 and Runx2 during Osteoblast Differentiation. *Journal of Biological Chemistry*. 2008;283(43):29119-25.
120. Boskey AL, Moore DJ, Amling M, Canalis E, Delany AM. Infrared analysis of the mineral and matrix in bones of osteonectin-null mice and their wildtype controls. *Journal of Bone and Mineral Research*. 2003;18(6):1005-11.
121. Rosset EM, Bradshaw AD. SPARC/osteonectin in mineralized tissue. *Matrix Biology*. 2016;52-54:78-87.
122. Bradshaw AD. The role of SPARC in extracellular matrix assembly. *Journal of cell communication and signaling*. 2009;3(3-4):239.
123. Graf HL, Stoeva S, Armbruster FP, Neuhaus J, Hilbig H. Effect of bone sialoprotein and collagen coating on cell attachment to TICER® and pure titanium implant surfaces. *International Journal of Oral and Maxillofacial Surgery*. 2008;37(7):634-40.
124. Aubin JE, Liu F, Malaval L, Gupta AK. Osteoblast and chondroblast differentiation. *Bone*. 1995;17(2, Supplement 1):S77-S83.
125. HUNTER GK, KYLE CL, GOLDBERG HA. Modulation of crystal formation by bone phosphoproteins: structural specificity of the osteopontin-mediated inhibition of hydroxyapatite formation. *Biochem J*. 1994;300:723-8.
126. Otto F, Lübbert M, Stock M. Upstream and downstream targets of RUNX proteins. *Journal of Cellular Biochemistry*. 2003;89(1):9-18.
127. Granito Rn, Boulefour W, Sabido O, Lescale C, Thomas M, Aubin JE, et al. Absence of Bone Sialoprotein (BSP) Alters Profoundly Hematopoiesis and Upregulates Osteopontin. *Journal of Cellular Physiology*. 2015;230(6):1342-51.
128. Baranowski A, Klein A, Ritz U, Ackermann A, Anthonissen J, Kaufmann KB, et al. Surface Functionalization of Orthopedic Titanium Implants with Bone Sialoprotein. *PLoS One*. 2016;11(4):e0153978-e.
129. Mizuno M, Kuboki Y. Osteoblast-Related Gene Expression of Bone Marrow Cells during the Osteoblastic Differentiation Induced by Type I Collagen. *The Journal of Biochemistry*. 2001;129(1):133-8.

130. Klein A, Baranowski A, Ritz U, Götz H, Heinemann S, Mattyasovszky S, et al. Effect of bone sialoprotein coated three-dimensional printed calcium phosphate scaffolds on primary human osteoblasts. *Journal of Biomedical Materials Research Part B: Applied Biomaterials*. 2018;106(7):2565-75.
131. Mizuno M, Imai T, Fujisawa R, Tani H, Kuboki Y. Bone Sialoprotein (BSP) is a Crucial Factor for the Expression of Osteoblastic Phenotypes of Bone Marrow Cells Cultured on Type I Collagen Matrix. *Calcif Tissue Int*. 2000;66(5):388-96.
132. Saito H, Shiao HJ, Prasad H, Reynolds MA. Evaluation of a poly (lactic-co-glycolic) acid-coated β -tricalcium phosphate bone substitute for alveolar ridge preservation: case series. *Clinical advances in periodontics*. 2017;7(4):190-4.
133. Guidor S. GUIDOR Easy-Graft CLASSIC Alloplastic Bone Grafting System 2020 [Available from: <https://us-professional.gumbrand.com/guidor-products/guidorr-easy-grafr-classic-alloplastic-bone-grafting-system.html>].
134. Perkins DW, Angelini AA. Dear Reader. 2014.
135. Cameron H, Macnab I, Pilliar R. Evaluation of a biodegradable ceramic. *Journal of biomedical materials research*. 1977;11(2):179-86.
136. Moore WR, Graves SE, Bain GI. Synthetic bone graft substitutes. *ANZ journal of surgery*. 2001;71(6):354-61.
137. Hilbig H, Kirsten M, Rupiotta R, Graf H, Strasser S, Armbruster F. Implant surface coatings with bone sialoprotein, collagen, and fibronectin and their effects on cells derived from human maxillar bone. *European journal of medical research*. 2007;12(1):6.
138. Bizenjima T, Takeuchi T, Seshima F, Saito A. Effect of poly (lactide-co-glycolide)(PLGA)-coated beta-tricalcium phosphate on the healing of rat calvarial bone defects: a comparative study with pure-phase beta-tricalcium phosphate. *Clinical oral implants research*. 2016;27(11):1360-7.
139. Baranowski A, Klein A, Ritz U, Götz H, Mattyasovszky SG, Rommens PM, et al. Evaluation of bone sialoprotein coating of three-dimensional printed calcium phosphate scaffolds in a calvarial defect model in mice. *Materials*. 2018;11(11):2336.

8. Appendix

Cells and their appointed medium	
hoB	DMEM/F-12 + GlutaMax + FCS 10% + PS 1%
HUVEC	EBM-2 + suppl. (Hydrocortisone, hFGF, VEGF, R3-IGF, Ascorbid Acid, hEF, A-1000, Heparin) + FCS 5% + PS 1%
MG-63	MEM Earle's + FCS 10% + PS 1%
SaOS-2	Mc Coy's 5 α + FCS 5% + PS 1% + Glutamin

Materials

Substance/Machine	Provider
Accutase [®] solution	Sigma-Aldrich [®] , Steinheim, Germany
alamarBlue [®] stock solution	Life Technologies, Invitrogen [™] , Karlsruhe, Germany
Alizarin red S	Fluka -Chemie GmbH, Buchs, Switzerland
BSA, bovine serum albumin	PAA Laboratories GmbH, Pasching, Austria
BSP, Bone sialoprotein	Immundiagnostik AG, Bensheim, Germany
Collagen Cell Carrier	Viscofan Bio Engineering (Weinheim, Germany)
Cell counter, Luna [™] automated cell counter L10001	Logos Biosystems, Annandale, USA
Cell culture flasks, 25 cm ² / 75 cm ² / 175 cm ²	Greiner Bio-One GmbH, Frickenhausen, Germany
Dulbecco's modified Eagle medium (DMEM/ F-12) + GlutaMAX	Gibco [®] , Life Technologies, Grand Island, USA
Dulbecco's modified Eagle's medium/nutrient mixture F-12 Ham	Sigma-Aldrich [®] , Steinheim, Germany
DMSO, Dimethyl sulfoxide, HYBRI-MAX [®]	Sigma-Aldrich [®] , Ayshire, UK
dNTP Mix, 10 mM	Bioron GmbH, Ludwigshafen, Germany

Easy Graft	Sunstar GUIDOR [®] , Swiss
EBM-2, Endothelial basal medium-2	Lonza Group AG, Basel, Switzerland
Eppendorf Safe-Lock tubes, 0.5 ml / 1.5 ml / 2.0ml / 5.0ml	Eppendorf AG, Hamburg, Germany
EVOS [®] Digital Inverted Microscope	Life Technologies, Carlsbad, USA
FCS, Foetal calf serum	Biochrom AG, Berlin, Germany
Freezing container, Cryo 1C	NUNC International, Rochester, USA
Glomax [®] -Multi detection system	Promega, Madison, USA
Hoechst stain solution	Sigma-Aldrich [®] , Steinheim, Germany
Incubating mini shaker, 444-0274	VWR International, Radnor, USA
Incubator, HERAcell 240	Heraeus Holding, Hanau, Germany
Laminar airflow cabinet, NuAIRE TM Biological	NuAire, Plymouth, USA
Lighning-Link [®] Fluorescein Conjugation Kit	Innova Bioscience, Cambridge, UK
Luna TM cell counting slides	Biozym Scientific GmbH, Hessisch Oldendorf, Germany
Luna TM automated cell counter	Logos Biosystems, Annandale, USA
Microplates, 96-well, F-bottom	Greiner Bio-One GmbH, Frickenhausen, Germany
MEM with Earle's salts	Biochrom AG, Berlin, Germany
PBS: Dulbecco's Phosphate Buffered Saline	Sigma-Aldrich [®] , Steinheim, Germany
Penicillin/Streptomycin 10,000U/ml	Gibco [®] , Life technologies, Grand Island, USA
peqGOLD MicroSpin Total RNA Kit	PEQLAB Biotechnologie GmbH, Erlangen, Germany
PFA, Paraformaldehyde	Carl-Roth [®] GmbH, Karlsruhe, Germany
Pipettes COSTAR [®] , 5 ml / 10 ml / 25 ml	Corning Inc., Corning, USA
PowerUp TM SYBR [®] green master mix, 2x	Applied Biosystems, Austin, USA
PCR 8-well tube strips and caps	PEQLAB Biotechnologie GmbH, Erlangen, Germany
Qiagen RNeasy [®] Micro Kit	Qiagen GmbH, Hilden, Germany
QIAshredder	Qiagen GmbH, Hilden, Germany
qPCR SemiSkirted 96-well PCR plates	PEQLAB Biotechnologie GmbH, Erlangen, Germany
Quality pipette tips, 20 µl	Sarstedt AG, Nümbrecht, Germany
Random primers, 500 µg/ml, 20 µg	Promega, Madison, WI, USA
RNase free water	Qiagen GmbH, Hilden, Germany
RNase-free DNase Set	Qiagen GmbH, Hilden, Germany
Scalpel, disposable, No. 11	Feather [®] Safety Razor Co., Osaka, Japan
SYBR [®] green PCR master mix	Applied Biosystems, Austin, USA

Tissue culture plates, Cellstar®, 6-well / 24-well	Greiner Bio-One GmbH, Frickenhausen, Germany
Tips, 100 µl	Greiner Bio-One GmbH, Frickenhausen, Germany
Triton™ X-100	Sigma-Aldrich®, Steinheim, Germany
Trypan blue stain, 0,4%	Gibco®, Invitrogen™, Carlsbad, USA
Tubes, CELLSTAR®, 15 ml / 50 ml	Greiner Bio-One GmbH, Frickenhausen, Germany
ULAP, ultra-low-attachment plates, 24-well	Corning Inc., Corning, USA

Antibodies

Gene	from QuantiTect® primers	Specification	Sequence	Acc Nr.
ALP		QT00012957	fw: gtacaacaccaatgccagg rv: cagattcccagcgtccttg	NM000478
Col1		QT00037793	fw: gattccctggacctaagggtgc rv: agcctctccatctttgccagca	NM000088
OPN		QT01008798	fw: ggtcactgatttcccacgg rv: ctctctgcttccatgtgtg	NM001040058
RUNX2		QT00020517	fw: ctgtgggttactgtcatggcg rv: aggtagctactggggagga	NM001024630
SPARC		QT00018620	fw: agtggagttggatcggt rv: aacgagttctcagcctgtga	NM003118
SP7		QT00213514	fw: acaagcactaatgggctcct rv: ggggtgtcatgtccagaga	NM001173467
GAPDH			fw: cgaccactttgtcaagctca rv: aggggagattcagtggtg	M33197

Calculations

Summarized P-values of each experiment in question are stated below. The prerequisites and tests, which were completed prior to the non-parametric tests or t-tests are not shown.

hOB-Viability Assay

	Day 1	Day 4	Day 7
PC vs. CCC	0,813	0,592	0,669
PC vs. BSP	0,721	0,985	0,781
PC vs. BSP coat.	0,890	0,063	0,802
CCC vs. BSP	0,660	0,518	0,496
CCC vs. BSP coat.	0,989	0,056	0,577
BSP vs. BSP coat.	0,442	0,031	0,961

P-Values depending on the prerequisites for the tests were either determined through the Mann-Whitney U test or the T-Test.

MG-63 Viability Assay

	Day 1	Day 4	Day 7
PC vs. CCC	0,913	1,000	0,628
PC vs. BSP	0,274	0,580	0,656
PC vs. BSP coat.	0,815	0,462	0,963
CCC vs. BSP	0,682	0,901	0,682
CCC vs. BSP coat.	0,791	0,673	0,118
BSP vs. BSP coat.	0,556	0,509	0,486

P-Values depending on the prerequisites for the tests were either determined through the Mann-Whitney U test or the T-Test.

Gene Expression Assay

	BSP vs. Control	BSP coat. vs. Control
SP7	0,629	0,629
RUNX2	0,029	1,000
SPARC	0,343	1,000
APL	0,029	0,343
Col1	0,029	1,000
OPN	-	-

P-Values were determined through the Mann-Whitney U test.

EG Viability Assay

	Day 1	Day 4	Day 7
PC vs. NC	0,000	0,000	0,000
PC vs. Sc.	0,000	0,000	0,000
PC vs. BSP	0,000	0,000	0,000
PC vs. Cells only	0,000	0,000	0,000
NC vs. Sc	0,014	0,056	0,982
NC vs. BSP	0,000	0,001	0,874
NC vs. Cells only	0,000	0,454	0,329
Sc. vs. BSP	0,001	0,006	0,839
Sc. vs. Cells only	0,635	0,050	0,178
BSP vs. Cells only	0,035	0,001	0,137

P-Values depending on the prerequisites for the tests were either determined through the Mann-Whitney U test or the T-Test.